THE
PHYSICAL
SOCIETY

MEMOIRS

OF THE

COLLEGE OF SCIENCE

UNIVERSITY OF KYOTO

SERIES A

VOL. XXVIII No. 2

1956

KYOTO

MEMOIRS OF THE COLLEGE OF SCIENCE, University of Kyoto, Series A,
Vol. XXVIII, No. 2, Article 1, 1956

TIME VARIATION OF THE ATMOSPHERIC RADON-CONTENT NEAR THE GROUND SURFACE WITH RELATION TO SOME GEOPHYSICAL PHENOMENA

BY

Sigeru OKABE

(Received October 19, 1956)

ABSTRACT

The daily variation of atmospheric Radon-content near the surface of the ground was observed in Tottori for one year and the effect of wind direction, wind velocity, atmospheric pressure, atmospheric temperature, and rain fall on Radon-contents of atmosphere were investigated. And from these data, the influence of local earthquakes occurring in the vicinity of Tottori on the increase of atmospheric Radon-content is discussed in some detail and their correlation was fairly well ascertained.

1. Introduction

The discovery of radioactive substances in the atmosphere was made by Elster and Geitel (**1**), who gave a physical explanation by it for the weak conductivity of the air. After them, many measurements of radioactive substances in the atmosphere have been made at various places in the world. These investigations have made it clear that the chief radioactive substances in the atmosphere are Radon, Thoron and their decay products, and they have a close relationship with the meteorological elements and the position of observatory. The fact that the mean Radon-content in the atmosphere near the ground surface over the continents amounts to about $100\sim2000\times10^{-18}$ C cm^{-3} and over the oceans to about $1\sim2\times10^{-18}$ C cm^{-3}(**2**), shows that the origin of Radon is continental, and this suggests that the Radon-content in the atmosphere may have some relation with any geophysical phenomena originating from the change of state of the ground, for example, in case of the occurrence of earthquakes or the displacement of active faults. Taking meteorological and seismological factors into consideration, a series of measurements of the atmospheric Radon-content were made at the site of 2 m above the ground surface once a day for a period of one year from March, 1955 to February, 1956 at the play ground of Tottori University in Tottori. The details of the experiments and the results will be presented in the following.

2. Method of measurement

In measuring the radioactive elements in the atmosphere, Radon is preferably

adopted as the object of measurement, for it has a relatively long half-life, this condition being considered to be the most suitable in the present investigation for detecting any correlation between the time variation of atmospheric radioactivity and geophysical phenomena. There are three possible methods of measuring the radioactive elements in the atmosphere; one is in removing the emanations from the air by absorption and condensation, and measuring them in an ionization chamber, or only using an ionization chamber of large volume for measurement (e.g. 13~45 liters by Vancour (**3**)). Since the above-mentioned "enrichment method" is comparatively difficult for daily measurement, and also since, in the large ionization chamber method, only small part of the atmospheric Radon is measured, these methods were not employed. The second method utilizes the property of some radioactive decay products which carry a positive electrical charge. These products are deposited on negatively charged collectors, where their ionization effect can be examined. This technique is termed the "induction method". The experimental technique of the induction method is simpler than that of emanometry, but quantitatively less reliable. The third method consists in the deposition of radioactive matter from a given amount of air by point discharge, as suggested by Sella (**4**). The same method in a modernised arrangement was used recently by Wilkening (**5**). In these circumstances the "induction method" was preferably used for the present investigation after improving both the method and instrument so as to increase quantitative reliability.

(*a*) *Arrangement of the induction method*

According to Eckmann (**6**), the RaA atoms are positively charged immediately after their formation. Furthermore, the other by-products also carry, at least in part, electric charges. Consequently, if they did not soon lose a large part of their charge by interaction with the ions in the atmosphere, they would be collected on a negatively charged body. The general type of a practical technique for carrying out such measurements is that in which a wire is kept at a high negative electric potential, exposed for several hours, and then wound on a spool and examined in an ionization chamber. Concerning this method, Gerdien (**7**) and Bauer (**8**) tried some improvements and introduced the aspiration process for collection.

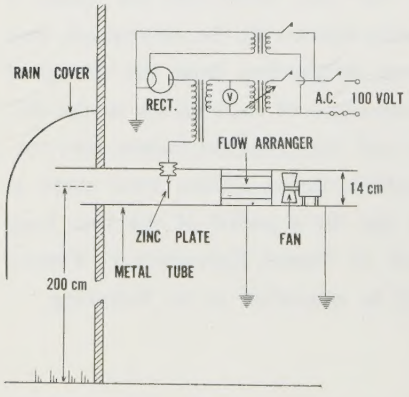

Fig. 1. Measuring arrangement.

In the present investigation the following induction method was adopted, its arrangement being shown in Fig. 1, and the practical technique is briefly described as follows: the aspiration tube is set at the height of 2 m above the

ground surface; the velocity of air aspiration is adjusted to 2 m/sec; a piece of metal plate of zinc ($4.5 \times 6\,cm^2$) is hung for 30 minutes in the aspirator tube, and it is kept at an electric negative potential of about 11 K.V. After the metal plate has acquired a certain amount of radioactivity, it is measured with a Lauritsen electrometer, the value of which is expressed as d.p.m. (scale-division per minute) and shows the mean value of change in scale-division per 10 minutes in the present observations. Both the velocity of air aspiration and the plate's electric negative voltage were so arranged as to gain the most favourable conditions for the present study, after numerous careful tests. By the above described arrangement, the weak point of the induction method (the uncertainty of measured air mass), is greatly mitigated, and it is certainly serviceable for the present study on time variation of air Radon. Since the Lauritsen electrometer (**9**) is well known, the description of its details will be omitted here.

(*b*) *Comparison with actual value*

It is said that the induction method supplies only relative values which, when obtained under similar working conditions, are more or less comparable with one another. However Eve (**10**) has obtained reliable quantitative results by exposing the collecting wire in a large closed vessel, 16 m^3 in volume, and compares the resultant activity with that obtained under the condition of a known quantity of Radon in the same vessel.

In the present case, a method was applied to get a reliable actual Radon-content. A known quantity of Radon, which has reached equilibrium with its decay products, is sent into the aspirator. It is measured by the above-described induction method, and the division of Lauritsen electrometer is compared with a known quantity of introduced Radon. Then from the result obtained, a division of 1.0 d.p.m. on the Lauritsen electrometer is approximately equal to 141×10^{-18} C cm^{-3}. But in this report, the content of Radon is generally shown by d.p.m. units except for special cases.

(*c*) *Decay of collected radioactive elements*

From the observation of the decay curve of induced decay products, collected elements can be analysed. The data of decay curves, which were obtained from prelimi-

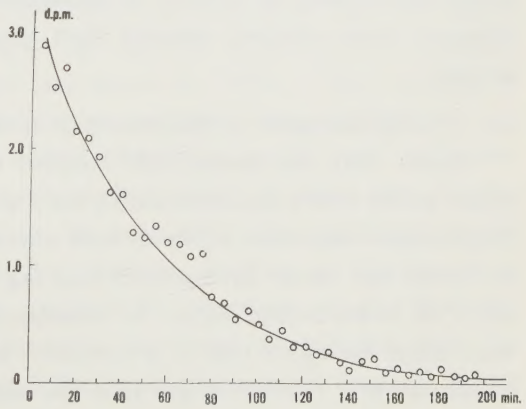

Fig. 2. Decay curve of Type I.

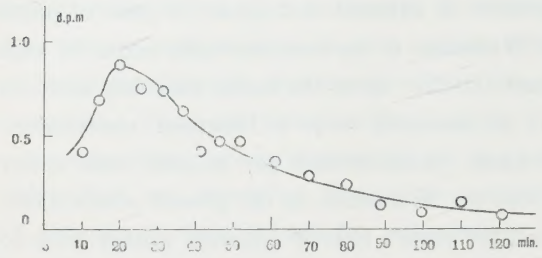

Fig. 3. Decay curve of Type II.

nary observations conducted at Tottori from December 1952 to January 1954, and Misasa (a place of radioactive hot springs) from September 1952 to June 1953, can be classified into two representative types, which are shown in Figs. 2 and 3. The analysis of a curve of the type as that in Fig. 2 by means of the ordinary procedure for examining the graph represented by means of a semilogarithm shows that the collected elements are RaA, RaB and RaC, while a curve of the type as in Fig. 3 shows that the same elements are contained, but in this case RaB and RaC have not reached a radioactive equilibrium with RaA. In conclusion, it has been made clear that the radioactive elements collected on the surface of a metal plate are only decay products of Radon.

The appearance percentage of the two types of curves mentioned above are respectively 10 : 1 at Tottori and 3 : 1 in Misasa. The high ratio of Misasa is considered to be attributable to its local characteristic of having many radioactive hot springs, each spring containing 100～300 mache Radon. In carrying out these observations, it was planned to measure the air Radon every noon in routine work and to denote the mean value of division of the first 10 minutes in the decay curve as the Radon value of that day.

3. Variation of the atmospheric Radon-content

The daily observation by the method described above was made during the one year period from March 1955 to February 1956 at the play ground in the Tottori University to study the relation of atmospheric Radon-content with the meteorological elements. Some relations obtained from these observations will be discussed in this section.

(a) Diurnal variation of Radon-content of the atmosphere

Becker (**11**) and Maćek (**12**) reported that the diurnal curves certainly show a single period with a maximum during the night and a minimum during the afternoon. Measurements conducted in Tottori show somewhat different results from those obtained by Becker and Maćek having some time lag, as shown in Fig. 4. In this figure, the curve of Radon-content seems to correspond to the diurnal variation of temperature, except during the time of a rain fall. Its reason is supposed to be that the rate of exhalation of radioactive gas from the soil is affected by the temperature, dryness of the soil, surface ground moisture, and wind force. In general the temperature has

a close relationship with the above-mentioned effects; for example, in the daytime there being no dew and the temperature being high, by the diffusion and suction effect of the wind upon the ground capillaries, Radon is brought into the atmosphere and transported to greater heights by vertical convection, and then the Radon-content in the lower air becomes small. And moreover, the Radon-content may be affected by a change in electric field, as Radon decay products carry positive charges. But in the present observation the measurement of electric field was not made, and its effect remained unsolved.

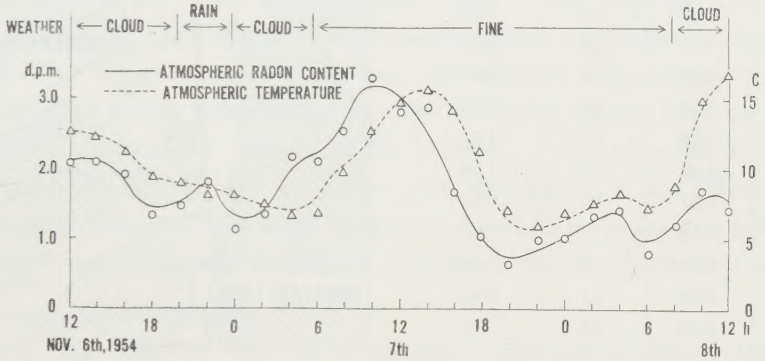

Fig. 4. Diurnal variation of atmospheric Radon-content observed at Tottori.

(b) Relations to direction of the wind

It is expected that the Radon-contents of the atmosphere become large in land wind and small in maritime wind, when they are measured at Tottori which is close to the Japan sea. In this section the relation between the direction of the wind and the mean value of Radon-content will be discussed. On such phenomena as the hysteresis of the wind, i.e. the classification of winds from Siberia or from Korea, or the effect of deep snow, for example, no consideration is given here. The data during the observation year classified according to the direction of wind are averaged for each direction and their "standard value" are shown in Table 1. The meaning of "standard value" is as follows: the reliability of each mean value of Table 1 is not equal, because the number of data of each wind direction is not the same and, moreover, there may be some uncertainty as to the wind direction. To avoid these defects, by giving the weight of accuracy of 1.0 for the mean value of a wind direction and weight of 0.5 for the both mean values for adjoining direction, a weighted mean value of three adjoining directions is assigned for "standard value". Thus the "standard value" is supposed to show smoother and more reliable data than the ordinary mean value, and be more suitable for future treatment, as shown in Fig. 5 which shows the mean and standard values for each wind direction. It is also to be

Table 1. Atmospheric Radon-content correlated with the wind directions.

Wind direction	Mean value (d.p.m.)	Number of data	Standard value (d.p.m.)
N	0.71	18	0.75
N N E	0.67	20	0.79
N E	1.11	40	1.06
E N E	1.38	14	1.19
E	0.92	6	1.17
E S E	1.46	14	1.44
S E	1.93	22	1.83
S S E	2.01	8	1.79
S	1.24	25	1.42
S S W	1.18	12	1.22
S W	1.29	9	1.14
W S W	0.81	20	0.91
W	0.73	15	0.67
W N W	0.41	5	0.54
N W	0.58	17	0.62
N N W	0.90	31	0.77

Remarks.

When direction of the wind observed at 9 and 12 o'clock differed so large from each other, these data are omitted here.

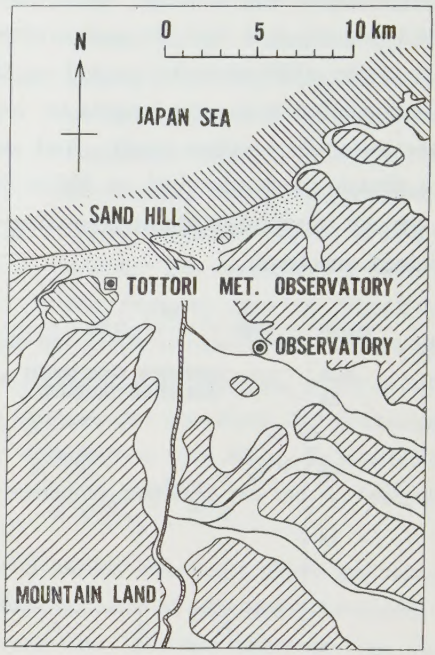

Fig. 6. Position of the Observatory and its surroundings.

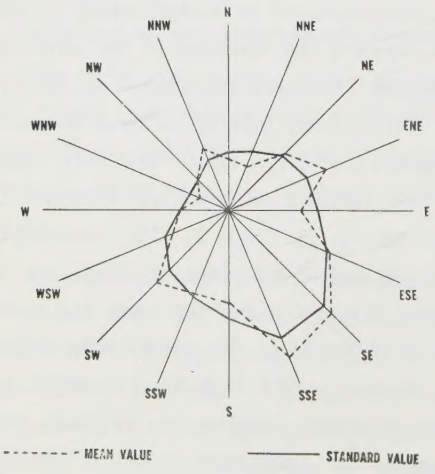

Fig. 5. Value of atmospheric Radon-content for each direction of wind at Tottori.

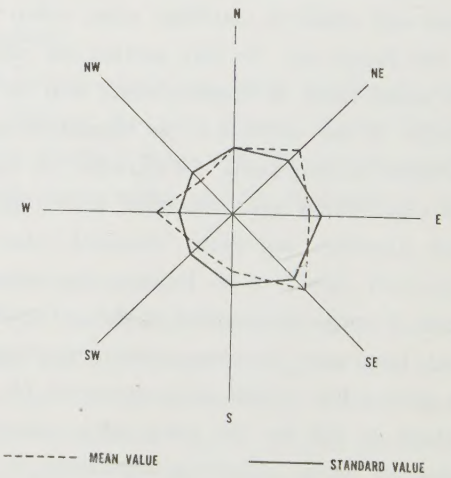

Fig. 7. Value of atmospheric Radon-content for each wind direction at Misasa.

remarked that the direction of the wind of that day was decided by referring to the data of wind direction observed at 9 and 12 o'clock in Tottori Meteorological Observatory and when direction of the wind at both times differed so greatly from each other, the latter was employed. For the convenience of reference the position of the observation station and the Tottori Meteorological Observatory, and their surroundings are shown in Fig. 6. The value assigned for the north-west wind representing air masses of maritime origin shows small Radon-content in contrast to the south-east wind whose standard value is exceedingly large. The standard values of each wind direction observed at Misasa from September 1952 to May 1953 are shown in Fig. 7. As the observation place of the Misasa Middle School at Misasa is situated to the north-west of the radioactive hot springs, the standard value observed at Misasa is considered to be greatly influenced by the effect of Radon exhaled from the hot springs and their neighbourhood. Concerning the reliability of the difference of the standard value above obtained in case of Tottori, the significance of the difference between those for the north-wind and south-wind was examined by stochastics and the reality of existence was recognized with great certainty in the significant level of 0.1%.

(*c*) *Relation to precipitation*

Maćek (**12**) reported that the precipitation, particularly that of long duration, decreases the Radon-content; this can easily be explained by a decrease of exhalation due to the clogging of the ground capillaries and in addition, the absorption of Radon by rain drops. In the present observation the data on their relation are listed in Table 2,

Table 2. Correlation between precipitation and atmospheric Radon-content.

Precipitation (mm) / Radon cont.	3	8	13	18	23	28	33	38	43	48
0.2										
0.5	1	5	4		1					
0.8	2	3	4		1	1	1			1
1.1	4	3	1							1
1.4	3	2								
1.7	1				1			1		
2.0		1		1						
2.3	1	1		1						
2.6	2									
2.9		2								
—										
—										
5.6			1							

$r \fallingdotseq -0.09$ (correlation coefficient)
Value of "Radon-content" is the ratio to each standard value.

in which the correlation of precipitation during the 24 hours before the time of Radon observation and atmospheric Radon-content is tabulated. In this case, correlation coefficient of -0.09, and significant level of 60% by stochastic calculation, tells us that their correlation may safely be neglected in the present treatment.

(d) Relation to atmospheric temperature

The seasonal variation seems to run generally parallel to the temperature curve as, for example, in the case of Messerschmidt (**13**), but there are some exceptions as in the case of the observation at Innsbruck, where the atmospheric Radon is highest in the cold season. In the present treatment, those data are selected which are between 1015 mb and 1020 mb atmospheric pressure in order to avoid the effect of atmospheric pressure, and the relation between atmospheric Radon-content and atmospheric temperature is investigated. The data are listed in Table 3, and the correlation coefficient calculated is 0.06 in this case. For the test of significance of correlation, the significant level of 70% is derived from stochastic calculation which permits a safe neglect of effect by atmospheric temperature upon the variation of atmospheric Radon in the present treatment.

Table 3. Correlation between at mospheric temperature and atmospheric Radon-content.

atom. temp. (C°) / atom. Rn cont.	1	4	7	10	13	16	19	22	25
0.2							4		
0.5	1			1	2	3	6		
0.8			1	3	4	2	3	3	
1.1		1		1	1	4	1	3	2
1.4					1			2	1
1.7	1	1	1		1			1	
2.0				1		1			
2.3				1					
2.6									2

$r=0.06$
Value of "Radon-content" is the ratio to each standard value.

(e) Relation to atmospheric pressure

According to Maćek (**12**), Kosmath (**14**) and Priebsch (**15**), falling pressure increases the Radon-content and rising pressure decreases it, as is to be expected from the atmospheric influence upon the exhalation, whereas Smyth (**16**) denied these relations. In this section the data of April, May, June and July which seem to show comparatively large variations of atmospheric pressure are selected and listed in Table 4. The correlation coefficient in this case becomes -0.20, and the significant

level, calculated for test of significance, of correlation is 5%, which means a negative low correlation.

Table 4. Correlation between atmospheric pressure and atmospheric Radon-content.

atom. press. (mb) / atom. Rn cont.	998	1001	1004	1007	1010	1013	1016	1019	1022	1025	1028
0.2			2			1					
0.5	1	1		3	6	2	6	2			2
0.8	1		3	2	13	6	3	4	5	2	1
1.1		2	3	3	10	8	3	2		2	
1.4		1		1		5	2				
1.7		1	1	2	1		1				
2.0			2			1	1				
2.3		1									
2.6					1						
2.9					1						
3.2				1							

$r = -0.20$

Value of "Radon-content" is the ratio to each standard value.

(f) Difference of Radon-content due to observation places

According to the large number of data collected by Israël (2), the mean Radon-content of the atmosphere near the surface of the continents amounts to about in the range of $100 \sim 2000 \times 10^{-18}$ C cm^{-3}.

This difference of Radon-content seems to be reduced to the local characteristics of the observatory, for instance to their meteorological type, geographical position, etc. It is well known that the exhalation rate of Radon from the ground surface on the fault line is large. Concerning the local character of atmospheric Radon-content, some observations for comparison at the play ground of the Tottori University, and at the

Table 5. Difference of atmospheric Radon-content observed at Tottori and Misasa.

Place and time	Number of data	$\times$C 10^{-18}cm^{-3}		
		Mean	Max.	Min.
Tottori, Nov. 1952– Feb. 1953	81	119	362	23.9
Misasa, Nov. 1952– Feb. 1953	49	146	478	25.5

ground of the Misasa middle school were made, their results being tabulated in Table 5. The Radon-content at Misasa seems larger than that at Tottori, and the cause may be attributable to the circumstances that Misasa is the place of radioactive hot springs and, moreover, more distant from the sea shore compared with Tottori.

(g) Relation to wind velocity

It is expected that the exhalation of the Radon may have some relation with wind velocity, because it is connected with suction effect of the wind. On some groups of data, which are classified according to the direction of wind, 40 examples of NE wind, 31 examples of NNW wind, 25 examples of S wind, and 22 examples of SE wind, the correlation coefficients were calculated. Tables 6, 7, 8, and 9 show respectively the correlation of wind velocity and atmospheric Radon-content. The correlation coefficients are as follows; NE: −0.05, NNW: 0.017, S: −0.085 and SE: −0.348. The correlation coefficients of these are too small to be discussed, and these results are considered to reveal that the diffusion effect of the wind may be equal to the suction effect of the wind. For reference, the mean value of wind velocity and frequency of wind direction which are observed in Tottori, are shown respectively in Figs. 8 and 9.

Table 6. Correlation between wind velocity and atmospheric Radon-content in case of NE wind direction.

wind velocity (m/sec.) \ Rn cont. (d.p.10 m)	2	5	8	11	14	17	20	22	25	28
1										
2		2		1	1					
3		3	2	3	2	1		1	1	1
4		2	1		2	1				
5		1	2	1		1				
6		2	1	2	1	1				
7				1	1					
8				2						
9										

$r = -0.05$

Table 7. Correlation between wind velocity and atmosperic Radon-content in case of NNW wind direction.

wind velocity (m/sec.) \ Rn cont. (d.p.10 m)	2	5	8	11	14	17	20	22
1								
2		1	1					1
3		3	2	1	1			
4	1	1	5	2				
5		1	3		1		1	
6		1	1			1		
7				1				
8		1						
9					1			

$r = 0.017$

Table 8. Correlation between wind velocity and atmospheric Radon-content in case of S wind direction.

wind velocity (m/sec.) \ Rn cont. (d.p.10 m)	2	5	8	11	14	17	20	22	25
1									
2									
3				1	1	1			
4		1	1	1	1				1
5		1			1	2	1		
6		2	2	1	1	3			
7									
8							1		
9									
10				1					
11									
12									
13									
14									
15									
16				1					

$r = -0.085$

Table 9. Correlation between wind velocity and atmospheric Radon-content in case of SE wind direction.

wind velocity (m sec.) \ Rn cont. (d.p.10 m)	2	5	8	11	14	17	20	22	25	28	31	34	···	48
1						1	1							1
2				2		1	1		1		1			
3				3	1			1		1		1		
4				2			1		1					
5					1									
6					1									

$r = -0.348$

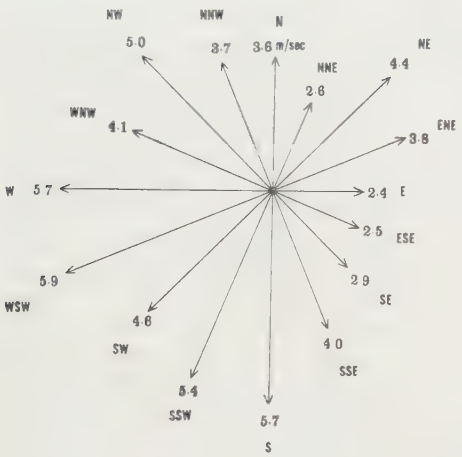

Fig. 8. Mean value of wind velocity for each wind direction at Tottori.

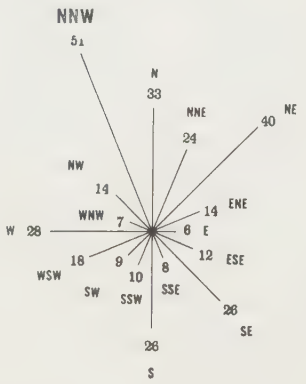

Fig. 9. Frequency of wind for each direction at Tottori.

4. On the relations between atmospheric Radon-content and earthquakes

Considering that the atmospheric Radon is mainly exhaled from the ground surface, it is considered to be worth discussing whether there exists or not any relation between the variation of atmospheric Radon-content and the occurrence of earthquakes, especially of local shocks near Tottori. For the purpose of detecting some influences of an earthquake upon Radon-content, raw materials observed must be corrected for all other conceivable effects other than earthquakes. Fortunately in the present case, the effects of the wind direction is the only thing that needs some consideration, and the relation to atmospheric pressure is not taken up here, for its correlation coefficient is comparatively small. Thus, in the following sections, all data are expressed in their ratio to the standard value for each wind direction, and it is generally considered

that the effect of wind direction may be corrected by this process. For instance, the measured value of 1.5 scale division per minute in case of north-wind is calculated as 2.0 by dividing it with the standard value of 0.75 in N-wind in Table 2 and similarly when south-east wind is blowing, it becomes 0.82. Namely in the former case the measured value of Radon is interpreted as anomalously large, and in the latter case it is an ordinary value in this wind direction.

(*a*) *On the atmospheric Radon-content measured before and after the earthquake*

In this section all data of Radon-content during one year are investigated in regard to the relation with the earthquake. In Table 10, the distribution of the

Table 10. Atmospheric Radon-content observed before and after the occurrence of earthquake.

atom. Rn cont.	Below 0.9		1.0–1.5		More 1.6		More 2.0	
	Number of data (f)	f/e	Number of data (f)	f/e	Number of data (f)	f/e	Number of data (f)	f/e
−3 (3 days before)	34	1.0	19	1.0	10	1.0	5	1.0
−2 (2 days before)	37	1.1	14	0.7	10	1.1	8	1.6
−1 (1 day before)	32	1.0	21	1.1	10	1.0	6	1.2
0 (that day)	37	1.0	17	0.9	7	0.8	7	1.4
1 (1 day after)	30	0.9	17	0.9	12	1.3	9	1.8
2 (2 days after)	32	1.1	17	0.9	13	1.4	10	2.0
3 (3 days after)	30	0.9	18	1.0	13	1.3	7	1.4
4 (4 days after)	27	0.8	23	1.2	11	1.2	8	1.6
5 (5 days after)	30	0.9	20	1.1	10	1.1	8	1.6
6 (6 days after)	34	1.0	17	0.9	8	0.9	5	1.0
Expected number of days (e)	33		19		10		5	

Value of "Radon content" is the ratio to each standard value.

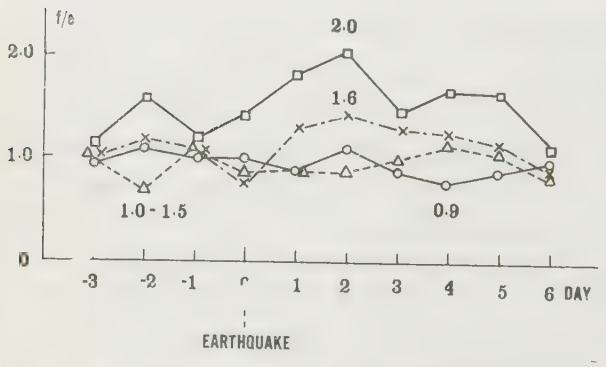

Fig. 10. Relation between the observed intensity of atmospheric Radonc-ontent and the number of days before and after the earthquake occurrence.

observed intensity of atmospheric Radon-content normalised by the standard value is classifiedly tabulated referring to the number of days before and after the earthquake occurrence. The earthquakes listed in the table are a total of 61 earthquakes which were observed during the period of present investigation with the seismometer of the Imamura type at the

Tottori Meteorological Observatory, the free period and magnification of the seismograph being 4.0 sec 40 respectively. The distribution in Table 10 is shown in Fig. 10 in which the ordinate shows the ratio of the observed number to the expected number. Expected numbers are meant the number of days which are theoretically expected to appear and calculated from the frequency distribution of total data. According to Fig. 10 the days of large Radon-content are expected several days after an earthquake has occurred, and considering the process of Radon exhalation from soils and the half-life of Radon, this phenomenon is reasonably explained. To show it more clearly, the distribution of the data during the period of three days after the earthquake is shown in Table 11, according to which, most values larger than 3.0 are observed within three days after the earthquake, and even in the case of values over 2.50, 75% of them are observable in these days, and thus some relationship between Radon-content in the atmosphere and the earthquake occurrence seems to exist, as far as the above argument is concerned. But, by applying the test to ascertain the real existence of different character between two distributions of total data and data during three days after earthquake occurrence which are shown in the percentage columns of Table 11, the significant level of this view that there are some differences between the distribution of these two sets of data, is estimated as 90% by using the distribution of χ^4 of 4 free dimensions in stochastic calculation. Consequently, the prospect for the relation between the atmospheric Radon-content and the earthquake occurrence is calculated to be negative from the test of stochastics so far as all the earthquakes observed at Tottori are concerned.

Table 11. Atmospheric Radon-content observed during three days after the earthquake occurrence.

Rn cont.	Total data		Data in 3 days after the earthquake occurrence	
	Number of data	%	Number of data	%
0.2	15	24.9	7	26.2
0.5	75		33	
0.8	97	26.8	40	26.1
1.1	78	21.5	30	19.6
1.4	37	11.0	13	8.5
1.7	22	16.8	8	19.8
2.0	13		6	
2.3	4		3	
2.6	8		4	
2.9	5		4	
3.2	2		1	
3.5	2		1	
3.8	1		1	
4.1				
4.4	1			
—				
5.6				
5.9	1		1	
6.2	1		1	
Total	362		153	

Value of "Radon-content" is the ratio to each standard value.

(b) Relation between atmospheric Radon-content and local shocks

In the preceding section, the relation between the value of Radon and earthquake

occurrence was not noticed from the standpoint of stochastics, though it seems to exist in appearance as shown in Fig. 10 and Table 11. In this section the same argument as described above will be applied only to the local shocks occurred near Tottori. It

Table 12. Earthquakes which have their epicenters in Tottori Prefecture.

Date of earthquake occurrence	Intensity of earthquake	Epicenter
22h 14th May 1955	I	neighbourhood of Tottori city
15h 19th May	I	neighbourhood of Tottori city
20h 15th Jun.	I	neighbourhood of Chizu
22h 23th Jun.	II~III	upper stream district of Hino river
8h 26th Jun.	II	upper stream district of Hino river
4h 27th Jun.	0	upper stream district of Hino river
2h 30th Jun.	0	upper stream district of Hino river
20h 13th Oct.	III	center of Tottori prefecture
19h 14th Oct.	I	neighbourhood of Tottori city
19h 20th Oct.	I	neighbourhood of Tottori city
23h 18th Nov.	I	neighbourhood of Tottori city
13h 21th Nov.	I	neighbourhood of Tottori city
4h 1th Feb. 1956	I	neighbourhood of Tottori city
22h 24th Feb.	0	west part of Tottori prefecture

is expected that the relation between the atmospheric Radon-content and occurrence of local shocks can, if existing, be fairly well detected, since the intensity of atmospheric Radon-content is supposed to be greatly increased by exhalation from the ground surface near the observation station caused by the violent shaking of local shocks and, moreover, the increased Radon-content will reach the observation station with less absorption and diffusion into the large air mass. Table 12 shows those earthquakes which had their epicenters in Tottori prefecture, and these 14 earthquakes are treated as local shocks in the present case. Referring to the above 14 earthquakes the same procedure was applied as in the preceding

Table 13. Relation between the near earthquake and atmospheric Radon-content.

atom. Rn content	Data of 3 days after earthquake		Total data	
	Number of data	%	Number of date	%
0.2		8.2	15	24.9
0.5	3	27.0	75	
0.8	10	24.4	97	26.8
0.1	9	10.8	78	21.5
1.4	4		38	11.0
1.7	2		22	
2.0	3		13	
2.3			4	
2.6	1		8	
2.9	1	29.8	5	16.8
3.2			2	
3.5	1		2	
3.8	1		1	
4.1				
4.4			1	
5.6	1			
5.9	1		1	
6.2	1		1	
Total	37		362	

Value of "Radon-content" is the ratio to each standard value.

section, the numerals being shown in Table 13. It seems also to show some influence of the earthquake upon Radon-content, and the test of difference of these two distributions was tried by making use of the distribution of χ^4 of 4 free dimensions. The significant level of this test shows 0.1%, i.e. it can certainly be said in this case that when an earthquake occurs near the observatory the Radon in the atmosphere increases. Next, some explanation must be found for the earthquakes which were not accompanied by the increase in Radon-content, namely, the earthquakes on May 14th and May 19th 1955. It may be attributable to the blowing wind from the sea in north direction during these days, because the air mass of maritime origin has low Radon-content, and the Radon exhaled by the shaking of the earthquake from sea side alluvium is of low value and, furthermore, the area which can contribute to Radon exhalation is very narrow in this case.

(*c*) *Relation between atmospheric Radon-content and intensity of earthquake*

The sixty one earthquakes recorded at the Tottori Meteorological Observatory are classified according to their intensity as well as their relation to the atmospheric Radon-content, which was measured during the three days after the earthquake, and they are shown in Table 14. Their correlation coefficient becomes 0.24 and according to the test of significance of correlation, this relation is slightly recognized, but with the significant level of 10%.

Table 14. Correlation between intensity of earthquake and atmospheric Radon-content.

atom. Rn content \ Intensity of earthquake	0	I	II	III
0.2				
0.3	9			
0.8	9	3	2	
1.1	12	2	1	
1.4	11	2		1
1.7	2			
2.0	2	2		
2.3				
2.6	1			1
—				
3.8				
4.4		1		

$r \fallingdotseq 0.24$

Value of "Radon-content" is the ratio to each standard value.

(*d*) *Effect of distant earthquakes traced by air currents*

As mentioned above, the relation between the atmospheric Radon-content and local shocks has been fairly well recognized. In this section we shall briefly discuss the effect of Radon exhaled by a distant earthquake and transported by favourable winds to Tottori from its epicentral region. Concerning the displacement of air mass, the air current in question is blowing near the ground surface, and it may receive much disturbance by the configuration of the ground, but here it is assumed that the air mass is displaced from the epicenter to Tottori retaining most of the Radon caused by the earthquake. For instance it is possible to move 260 km in 24 hours, presuming the wind velocity to be 3 m/sec. From this point of view, the effect in question was

examined for some distant earthquakes, taking wind direction into consideration as deduced from the Far-East weather chart issued by the Central Meteorological Observatory. Fig. 11 shows the relation between the variation of Radon-content observed in Tottori and the direction of wind determined from the weather chart, when the earthquake occurred in Ibaraki Prefecture on June 15, 1955. This is an example of a case of the air mass which is supposed to be transported to Tottori from the epicentral region. Fig. 12 shows the case of an earthquake, occurring in the Tokushima district on August 14, 1955, and it is an example in which the movement of air from the epicentral region to Tottori is not expected.

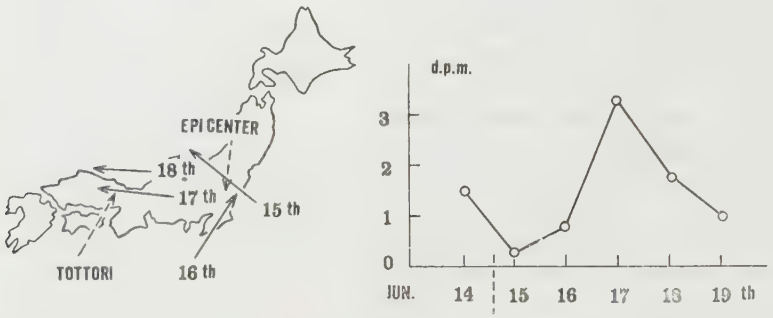

Fig. 11. Relation between the variation of atmospheric Radon-content at Tottori and the direction of wind in case of the distant earthquake in Ibaraki Prefecture.

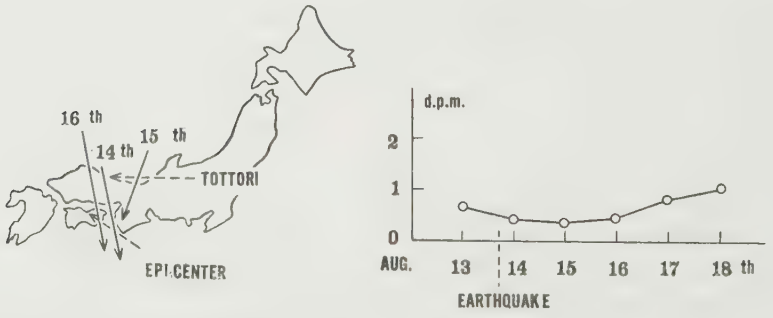

Fig. 12. Relation between the variation of atmospheric Radon-content at Tottori and the direction of wind in case of the distant earthquake in Tokushima Prefecture.

In concluding the present investigation, the fact that the Radon-content in the atmosphere near the ground surface is certainly increased by the occurrence of local shocks near the observation station was fairly ascertained from the standpoint of stochastics. In this case the effects caused by change of barometric pressure, atmospheric temperature, and precipitation, and especially the influence by wind intensity

and direction should carefully be corrected. The effort will be exerted, in a near future, to detect directly the influence of earthquake occurrence upon the change of atmospheric Radon-content for each earthquake by suitable methods of automatic and continuous observation of atmospheric Radon and ground radiation in general.

Acknowledgement

The writer wishes to express his cordial thanks to Prof. E. Nishimura of the Geophysical Institute, Kyoto University, and Prof. K. Kimura of the Physical Institute, Kyoto University for their kind guidance and pertinent advices. The writer's thanks are due to Messrs. T. Tamura, S. Fukunaga, T. Koyano and T. Otagaki for their daily observation during a long period, and also to the Tottori Meteorological Observatory for kind permission for the use of the observation materials. The cost for this study was partly defrayed by a grant-in-aid for scientific research of the Ministry of Education.

REFERENCES

1. J. Elster and H. Geitel, Phys. zs. **2** (1901), 590.
2. H. Israël, Compendium of Meteorology (American Meteorological Society Boston) 155 (1951).
3. R. P. Vancoup, Thesis. Fordham University, New York (1950).
4. A. Sella, Atti. Acad. Lincei. **11** (1902), 57.
5. M. H. Wilkening, Rev. Sci. Instrum. **23** (1952), 13.
6. G. Eckmann, Jb. Radioakt. **9** (1912), 157.
7. H. Gerdien, Phys. zs. **6** (1905), 465.
8. L. A. Bauer, Carng. Instn. Wash. Publ. No. 175 (1916), 3.
9. C. C. Lauritsen and T. Lauritsen, Rev. Sci. Instrum. 8 (1937), 438.
10. A. S. Eve, Phil. Mag. [6] **10** (1905), 98.
11. F. Becker, Beitr. Geophys. **42** (1934), 365.
12. O. Maček and W. Illing, Beitr. Geophys. **43** (1935), 388.
13. W. Messerschmidt, zs. f. Phys. **81** (1933), 84.
14. W. Kosmath, Beitr. Geophys. **43** (1935), 258.
15. J. Priebsch, Beitr. Geophys. **50** (1937), 55.
16. L. B. Smyth, Phil. Mag. **24** (1912), 632.

MEMOIRS OF THE COLLEGE OF SCIENCE, University of Kyoto, Series A,
Vol. XXVIII, No. 2, Article 2, 1956

SEISMOMETRIC INVESTIGATION OF THE EARTH'S INTERIOR

PART III. ON THE STRUCTURE OF THE EARTH'S MANTLE (I)

BY

Yoshimichi KISHIMOTO

(*Received December 20, 1956*)

ABSTRACT

The structure of the earth's mantle, mainly its upper part, having been investigated by the analysis of seismic waves of five Kamchatka-Kurile Islands Earthquakes of shallow focus and some others, the problems on the existence and property of the 20°-discontinuity and the low-velocity layer in the mantle are discussed in some detail. The time-distance graphs is obtained in Japan are in fair agreement with Jeffreys-Bullen's Table (1939), and also the 20°-discontinuity is considered to exist certainly at nearly the same depth as given by Jeffreys. The amplitude relation observed at the epicentral distance near 20° between the direct wave propagating through the medium entirely above the 20°-discontinuity and the refracted wave penetrating down into that discontinuity is just the reverse of that commonly expected, that is, the former being small and the latter large both for the *P*- and *S*- waves. Concerning this phenomenon some arguments are given. Moreover, the existence of a new discontinuity was ascertained at some depth below the 20°-discontinuity, as deduced from the appearance of a prominent later phase. As to the existence of a low-velocity layer in the mantle, it is negatively concluded from the analysis of seismic waves observed at the stations in Japan of the earthquakes of Kamchatka-Kurile Islands, but the possibility of its existence near the crust in the form of pocket or reservoir is supposed to be not unreasonable, its problem being postponed to a succeeding paper.

1. Introduction

On the structures and properties of the earth's mantle, especially its upper part, many investigations have been carried out in various fields of research.

Seismometrically, many authors have published reports in this field, for example, H. Jeffreys (**1**, **2**, **3**, **4**, **5**), B. Gutenberg (**6**, **7**, 8), P. Byerly (**9**), I. Lehmann (**10**, **11**, **12**), and, in our country, H. Kawasumi (**13**, **14**), T. Matuzawa (**15**), and K. Wadati (**16**).

At present, one of the most important and interesting problems with regard to the structure of the earth's upper mantle as well as the crust may be relative to the two essentially different opinions for its construction. So far, most researchers including Jeffreys have held that the seismic wave velocities in the earth's mantle increase with depth and at the so-called 20°-discontinuity (its depth is estimated, for example, as 413 km below the earth's surface by Jeffreys) the rate of increase of velocity

begins to rise abruptly. Jeffreys-Bullen's 1939 Table (**3**) is the most typical work of this opinion. On the other hand, in 1939 B. Gutenberg and C. F. Richter (**6**) initiated an entirely different opinion based on the observations of P-wave amplitude by using the North American earthquakes and observatories, that there exists a layer (so-called the low-velocity layer at present) in which the seismic wave velocities decrease with increasing depth, and which begins at about 80 km below the earth's surface. And they have further developed this opinion. According to Gutenberg's recent investigation (**8**, **17**) it is said that the low-velocity layer exists in ranges between 60 km and 150 km for P and between 60 km and 250 km for S. And, moreover, he says that the 20°-discontinuity never exists at any depth.

I. Lehmann recently entertains a little different opinion (**11**). According to her, a low-velocity layer exists, but it is effective only for shear waves, and not for longitudinal waves and, moreover, far below this layer there exists also a discontinuity corresponding to the 20°-discontinuity at whose surface the change of seismic velocities is strong but gradual. Namely, her opinion is a compromise between the two opinions described above.

Of course, the velocity distributions of seismic waves are the most decisive data for the investigation of structure and properties in the earth's interior, so that the precise determination of velocity distribution is the most important, and the determination of velocity distribution is usually performed by the Herglotz-Wiechert method. But, in the application of this method, the data used have necessarily to belong to the same family of phase. If it is not so, the result of analysis is not correct. And whether a phase belongs to a certain family or not is never determined only by the precise reading of times of the first arrivals. For instance, according to Gutenberg, if there exists a low-velocity layer, only the diffracted waves arrive at as the P-phase in some ranges of epicentral distance and are read as the first P. If that is the case, the application of the Herglotz-Wiechert method will give rise to a faulty result.

To determine what family any phase belongs to is considered to be possible only with a detailed investigation of seismic wave development with distance extending over as wide ranges as possible. Namely, first, the following procedures are needed; 1) to take all later phases into consideration as well as the first arrivals of P and S. 2) to read the travel time, the amplitude, the period and as many other data as possible, and 3) to clarify the properties of each phase by taking all data obtained together into consideration. And by doing so, we shall be able to obtain many properties of each family of seismic waves and also to increase our information concerning the structures and properties of the earth's interior from various points of view.

Recently, this sort of investigation allowing for various observed data including the amplitude as well as the time-distance curve is increasing. Not to speak of

Gutenberg's investigation of the low-velocity layer, Lehmann's investigation above-cited (**11**) is also one in this course. And Bremaecker has recently published an investigation (**18**), in which he inferred the velocity distribution in the earth's mantle only by the observations of the amplitudes of the first P-waves between distance of 3° to 23°.

In the present investigation, several earthquakes which extended over areas of from about 6° to 26° were investigated in the course described above, and some interesting facts were found out, which will be described below in some detail.

2. Seismological data used in the analysis

For various reasons the seismological data used in the analysis are specially selected to fit the following conditions; 1) to use only the seismograms recorded with the seismographs of the same type, 2) to use as many observations as possible extending over the necessary distances, and 3) to use only the observations in nearly the same azimuth as seen from the epicenter. The first condition is convenient for the comparison and discussion on the amplitude and form of the seismic waves at each observatory, and the second condition may minimize the errors caused by the local character of each observatory founded on ground of different geological and crustal structure. The last condition will not approximately necessitate any consideration on the effect caused by the complex mechanism of earthquake occurrence at the hypocenter.

The Japan Meteorological Agency kindly permitted our copying of the seismograms recorded with the Wiechert Seismograph at 23 observatories attached to the Agency. By this courtesy the observations of epicentral distances extending over 6° to 26° were available for the present investigation. The constants of the Wiechert Seismograph used are as follows:

Component	Mass	Magnification	Period	Damping ratio
horizontal	200 kg	70～100	about 5 sec	5～10
vertical	80	50～ 80	,,	,,

The earthquakes examined were five Kamchatka-Kurile Islands earthquakes and some Formosa earthquakes. As the seismograms used in the analysis were obtained at the observatories in nearly the same azimuth seen from the epicenters of Kamchatka or Formosa earthquakes, the problem on the mechanism of earthquake occurrence is, in the present treatment, not taken into consideration. The positions of epicenters and the various data of those earthquakes are shown in Fig. 1 and Table 1 respectively. In this Table, the epicenters, focal depths and magnitudes are those after the United States Coast and Geodetic Survey (U.S.C.G.S.).

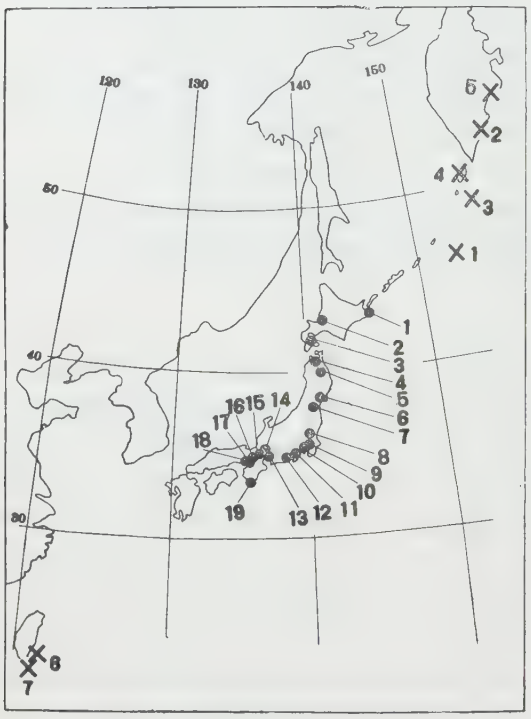

Fig. 1. Epicenters of earthquakes and observatories used in the present analysis. The cross and dot denote the epicenter and observatory respectively. Numbers of epicenter are referred to Table 1, and those of observatory are as follows:

1. Nemuro, 2. Sapporo, 3. Mori, 4. Aomori, 5. Morioka, 6. Sendai, 7. Fukushima, 8. Utsunomiya, 9. Tokyo, 10. Yokohama, 11. Mishima, 12. Shizuoka, 13. Nagoya, 14. Gifu, 15. Hikone, 16. Kyoto, 17. Osaka, 18. Kobe and 19. Shionomisaki.

Table 1. List of the earthquakes used in the present investigation. Latitude and longitude of epicenter, magnitude, focal depth and some of the origin time (*) are after the U.S.C.G.S.. The Greenwich Mean Time is adopted for the origin time.

No.	Date	Origin time (G.M.T.)	Epicentral region	Epicenter N	Epicenter E	Focal depth	Magnitude (Pasadena)	Observational range
		h m s		°	°	km		
1	1952 June 22	21 43 02	SE off Shinshiru Is., Kurile Is.	46,	153½	—	7	6°~17°
2	1952 Nov. 4	16 58 33	Near east coast of Kamchatka	52½,	159	—	8¼	13°~25°
3	1953 Jan. 5	10 06 30	N part of Kurile Is.	49,	156	—	6¾	9°~22°
4	1953 Oct. 11	13 08 34 (*)	"	50,	155½	60	6¾	10°~23°
5	1955 March 18	00 06 46	Near east coast of Kamchatka	54½,	161	—	—	19°~26°
6	1936 Aug. 22	06 51 37	Near SE coast of Formosa	22.1,	121.2	—	—	17°~24°
7	1955 Apr. 4	11 11 21 (*)	"	22,	121	—	6	17°~24°

3. Observational results

i) *Time-distance graph*

A typical example is the earthquake of January 5, 1953 (No. 3 in Table 1), which occurred at the northern part of the Kurile Islands, 49°N and 156°E. The observational data are given in Table 2, and some examples of the seismogram in Fig. 2 are given at the end of this article. Each value in Table 2 was read from the photographic copies of the original seismograms. The time-distance graphs of both P and S are shown in Fig. 3. In this figure, it is to be noted that both P- and S-graphs are divided into two branches intersecting at about 18°, and that the later branches are extended down to 13° in both P- and S-graphs, so that the graphs for the later phase up to 18° read after the first P- or S-phase are interpreted as the extention of the later branch observed beyond the distance of 18°. As will be described in the succeeding sections ii) and iii) and also as clearly seen from the seismograms in Fig. 2, these two phases are so clearly distinguished from one another by difference in their amplitudes and periods that there is no danger of confusing the two phases.

Focal depth of this earthquake is approximately estimated as $0.01R$ according to Jeffreys' notation after pP–S duration at each observatory. Consequently the epicentral distance of about 18° which is the intersecting distance of our two branches stated above, will correspond to the so-called 20°-discontinuity referring to the Jeffreys-Bullen Table. In the J.-B. Table, two branches separated at the epicentral distance corresponding to the 20°-discontinuity are represented by two letters d and r respectively. The earlier branches at distances smaller than 20° are called Pd and Sd, and the later ones beyond 20° Pr and Sr. Namely, Pd and Sd represent the waves having their vertices above the 20°-discontinuity and

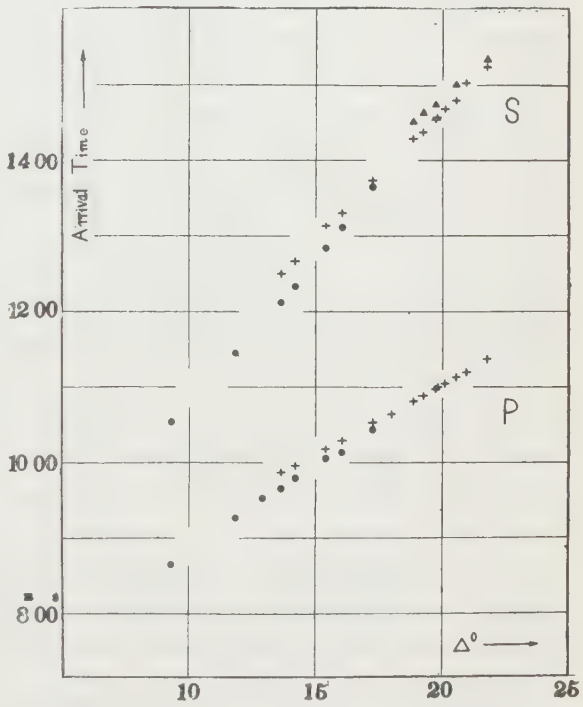

Fig. 3. Time-distance graphs of the earthquake of Jan. 5, 1953. Dots, crosses and triangles represent the d-wave (Pd and Sd), r-wave (Pr and Sr_1) and Sr_2-wave respectively.

Table 2. The earthquake of Jan. 5, 1953, 49°N, 156°E
0 : $10^h06^m30^s$.

Observatory	Δ	Arrival time						O-C						Amplitude						Period				
		Pd	*Pr*	*Sd*	*Sr*$_1$	*Sr*$_2$		*Pd*	*Pr*	*Sd*	*Sr*$_1$	*Sr*$_2$		*Pd*	*Pr*	*Sd*	*Sr*$_1$	*Sr*$_2$		*Pd*	*Pr*	*Sd*	*Sr*$_1$	*Sr*$_2$
	°	m s	m s	m s	m s	m s		s	s	s	s	s		μ	μ	μ	μ	μ		s	s	s	s	s
Nemuro	9.32	8 39.4	—	10 32.2	—	—		− 4	—	+ 5	—	—		6.8	—	147	—	—		0.7	—	—	—	—
Sapporo	11.86	9 16.3	—	11 27.5	—	—		− 1	—	0	—	—		18.0	—	103	—	—		2.6	—	—	—	—
Mori	12.92	31.5	—	—	—	—		+ 1	—	—	—	—		11.5	—	—	—	—		3.7	—	—	—	—
Aomori	13.63	39.2	9 51.7	12 7.1	12 30.0	—		+ 1	+12	− 2	+20	—		8.5	21.0	260	540	—		2.7	—	1.0	4.7	—
Morioka	14.20	47.5	56.9	20.0	39.7	—		0	+10	− 9	+21	—		3.4	—	23	44	—		3.2	5.4	2.5	5.8	—
Sendai	15.41	10 3.1	10 10.5	50.2	13 7.8	—		0	+ 8	− 1	+17	—		5.4	22.4	50	181	—		1.9, 9.3	4.1	1.1	4.0	—
Fukushima	16.03	7.9	17.2	13 6.7	18.1	—		+ 1	+ 6	+ 1	+13	—		3.3	15.1	28	136	—		0.8, 5.2	4.1	1.2	3.6	—
Utsunomiya	17.25	26.1	31.3	38.5	44.0	—		0	+ 5	+ 6	+11	—		1.9	6.8	11	52	—		1.2	3.3	1.9	4.0	—
Tokyo	18.00	—	38.3	—	—	—		—	+ 4	—	—	—		—	4.3	—	—	—						
Mishima	18.85	—	48.3	—	14 17.2	14 29.9		—	+ 4	—	+ 9	+22		—	4.8	—	28	158		—	4.2	—	5.1	4.4
Shizuoka	19.23	—	52.9	—	22.3	37.0		—	+ 4	—	+ 7	+22		—	7.2	—	—	112		—	3.9	—	5.6	4.9
Gifu	19.73	—	58.0	—	32.5	43.4		—	+ 4	—	+ 6	+17		—	23.3	—	57	145		—	4.1	—	5.7	—
Nagoya	19.82	—	59.6	—	33.9	—		—	+ 5	—	+ 6	—		—	21.3	—	54	153		—	3.8	—	—	4.5
Hikone	20.10	—	11 2.5	—	41.3	—		—	+ 5	—	+ 8	—		—	16.3	—	—	—		—	4.4	—	—	—
Kyoto	20.57	—	7.6	—	47.6	59.6		—	+ 5	—	+ 5	+17		—	14.9	—	20	64		—	4.3	—	—	—
Osaka	20.96	—	11.4	—	15 1.5	—		—	+ 5	—	+12	—		—	19.2	—	—	—		—	4.5	—	—	—
Shionomisaki	21.77	—	21.5	—	14.2	15 19.6		—	+ 7	—	+12	+17		—	21.3	—	13	97		—	4.1	—	5.8	5.0

Pr and *Sr* represent the refracted waves at the 20° discontinuity. It is yet unknown whether two branches in our case intersecting at 18° correspond to Jeffreys' or not, but the same notation as Jeffreys' might tentatively be used for two branches in the present graph. Then, the fitness of the present time-distance graph to the J. B. Table will be examined in the next step.

Recently, Jeffreys published (**4**, **5**) the revisions for his 1939 Table and stated the existence of regional differences in three areas, i.e. in Europe, Japan and North America. According to his revision, the 1939 Table is about right up to 17° but a reduction of 2 sec is needed beyond 22° for Japanese area. But, in the present treatment, the 1939

Table will tentatively be used. O–C in Table 2 shows the residual from the J.–B. 0.01 curve, taking $10^h\,06^m\,30^s$ as the origin time. These residuals were obtained in the following manner: Considering mainly the phase of *Pd* and moreover taking the other phases (*Pr*, *Sd* and *Sr*) for reference purposes, it was ascertained that the J.–B. 0.01 curve rightly fits for the present graph and the origin time was deduced as above mentioned. It is to be remarked that the J.–B. 0.005 curve calculated from the given 0.00 and 0.01 curves is practically most suitable for the present observed graph, but, in the present treatment, the difference of fitness for 0.005 and 0.01 curves is beyond our discrimination in respect to observational and analytical errors. If the focal depth is approximately assumed to be in the order of magnitude of $0.01R$ (R is the radius of the earth) the turning point of time-distance graph for the so-called 20°-discontinuity will be shifted to the epicentral distance of 18°, and it is well in accord with the present case. The *Pd*-branch fits best into the J.–B. 0.01 curve up to about 18°, and the fitness of the *Pr*-branch is comparatively good referring to its gradient although there are systematically positive residuals of a few seconds. The *Sd*-branch show some fluctuations, whose residuals, however, show minus signs at smaller distances and change their signs at larger distances, thus giving a little larger gradient than the J.–B. curve. But the *Sd*-branch is continuously traced up to 18° and no gap is observed on the time-distance graph. The *Sr*-branch roughly fits into the J.–B. curve referring to the gradient, but has systematically positive deviations in this case also.

The earthquake of November, 4, 1952 was one of the severest shocks and has been investigated in various research fields. The observational data are given in Table 3. This earthquake shows also the same tendency as that above-mentioned with regard to the development of seismic wave with distance. Namely, the time-distance graph of P-wave (as to S-wave, they were not accurately read due to scale-out in the seismograms or to extraordinarily large amplitudes) has two branches intersecting at about 18°. The residuals of both *Pd* and *Pr* from the J.–B. 0.01 curve, adopting the origin time, $16^h\,58^m\,33^s$, are given in Table 3. The fitness is fairly good not only for *Pd* but also for *Pr*, and the systematically plus residuals of *Pr* are not observed. On this point, the present earthquake differs from the previous one, which will be discussed in some detail in section **4**.

Besides these two earthquakes, the following three were treated, their observing data being tabulated in Tables 4, 5 and 6 respectively. On the earthquake of June 23, 1952, only *Pd* and *Sd* were available owing to the smallness of the observing distance, and the fitness of P into the J.–B. 0.01 curve is fairly good. The earthquake of October 11, 1953 gave results similar to those of the two cases treated earlier. Lastly, the earthquake of March 18, 1955 also gave similar results, in which, however, only *Pr* and *Sr* were available owing to the largeness of observing distance. *Pr* and

Table 3. The earthquake of Nov. 4, 1952, $52\frac{1}{2}°$N, 159°E
$0:16^h58^m33^s$

Observatory	Δ	Arrival time		O-C		Amplitude		Period	
		Pd	*Pr*	*Pd*	*Pr*	*Pd*	*Pr*	*Pd*	*Pr*
	°	m s	m s	s	s	μ	μ	s	s
Nemuro	12.97	1 34.4	1 51.0	− 1	+16	11	14	0.9, 17.1	—
Urakawa	15.18	2 4.9	—	+ 1	—	12	—	1.1, 14.7	—
Sapporo	15.23	4.3	2 11.9	0	+ 8	13	22	—	—
Mori	16.33	18.5	24.5	0	+ 7	11	—	18.6	—
Aomori	17.18	27.5	33.0	− 1	+ 5	10	—	1.2, 15.7	—
Morioka	17.85	35.9	40.4	− 1	+ 4	—	19	—	4.0
Akita	18.35	43.1	47.1	+ 1	+ 5	—	14	—	6.3
Sendai	19.13	—	47.7	—	+ 2	—	—	—	5.1
Fukushima	19.75	—	59.5	—	+ 2	—	16	—	5.0
Utsunomiya	21.01	—	3 11.9	—	—	—	8	—	—
Nagoya	23.48	—	35.6	—	+ 1	—	16	—	5.8
Toyooka	24.22	—	45.0	—	+ 3	—	9	—	3.9
Shionomisaki	25.46	—	57.5	—	+ 6	—	—	—	—

Sr gave systematically plus residuals referring to the J.-B. 0.01 curve, in which the origin time was estimated as $00^h\ 06^m\ 46^s$ by comparing *Pr*-branch in this case with that of the earthquake of January 5, 1953. Since the positions of observatories are all nearly on a straight line seen from the epicenter of each earthquake in analysis, a small shift of epicenter will change their epicentral distances and azimuths slightly and to the same degree. Consequently, the gradient of the time-distance graph may be considered almost unchangeable and, moreover, a certain J.-B. curve to which each phase shows the best fit is kept also unchangeable by a small shift of epicenter.

Thus, from the results above-obtained, it may be concluded, at least from the standpoint of time-distance curve, that *Pd* and *Sd* correspond to the direct waves propagating through the material above the 20°-discontinuity and *Pr* and *Sr* are the refracted waves penetrating down into the 20°-discontinuity and again coming up to the earth's surface, both waves as being defined by Jeffreys in the J.-B. 1939 Table. In addition, the extending of *Pr*- and *Sr*-branches backward down to about 13° well coincides with what was discussed by Jeffreys in his 1939 paper (**3**). Therefore, it may safely be said that the existence of the 20°-discontinuity was ascertained by an analysis of the time-distance graph with regard to the data of earthquakes near Japan.

But, a question is left as to whether the 20°-discontinuity is of the first order or the second order. This question will be solved by finding a loop of the time-distance graph or the reflected wave at the discontinuity concerned. A P-phase was observed shortly after *Pr* on the seismograms of January 5, 1953, which forms a time-distance graph approximately similar to the upper branch of the loop or the reflection branch.

Table 4. The earthquake of June 22, 1952, 46°N, 153½°E
0 : $21^h43^m02^s$

Observatory	Δ	Arrival time		O–C	
		Pd	*Sd*	*Pd*	*Sd*
	°	m s	m s	s	s
Nemuro	6.36	43 34.0	44 48.7	− 1	+ 2
Sapporo	9.22	44 13.3	46 0.7	0	+ 5
Mori	10.17	27.4	22.1	+ 1	+ 3
Aomori	10.73	32.1	36.1	− 2	+ 3
Morioka	11.13	38.6	43.8	− 1	+ 2
Fukushima	12.84	45 3.3	47 29.6	+ 1	+ 7
Utsunomiya	14.04	18.3	—	+ 1	—
Tokyo	14.75	28.4	48 18.0	+ 2	+10
Yokohama	15.00	31.2	20.9	+ 1	+ 7
Mishima	15.62	39.4	35.2	+ 2	+ 7
Shizuoka	16.00	46.4	44.3	+ 4	+ 8
Nagoya	16.66	53.6	—	+ 3	—
Hikone	16.99	57.1	—	+ 2	—

Table 5. The earthquake of Oct. 11, 1953, 50°N, 155½°E
0 : $13^h08^m34^s$

Observatory	Δ	Arrival time		O–C		Amplitude		Period	
		Pd	*Pr*	*Pd*	*Pr*	*Pd*	*Pr*	*Pd*	*Pr*
	°	m s	m s	s	s	μ	μ	s	s
Nemuro	10.02	10 51.0	—	− 6					
Sapporo	12.32	11 28.4	11 38.5	+ 1	+11	7.6	15.5	1.4	2.6
Mori	13.41	41.4	56.5	0	+15	5.2	18.7	3.3	3.5
Aomori	14.23	53.2	—	+ 1	—	3.2	—	—	—
Morioka	14.90	59.1	—	− 2					
Sendai	16.18	12 18.7	12 22.5	+ 2	+ 6	2.8	8.2	—	6.0
Fukushima	16.79	23.4	30.2	− 1	+ 6	2.8	8.5	1.1	—
Utsunomiya	18.05	39.4	43.3	0	+ 5	0.2	6.9	—	3.6
Tokyo	18.83	—	—	—	—	—	2.7	—	—
Yokohama	19.09	—	54.1	—	+ 3	—	0.5	—	3.7
Mishima	19.65	—	58.5	—	+ 1	—	5.4	—	5.4
Shizuoka	20.03	—	13 4.3	—	+ 3	—	4.5	—	6.5
Nagoya	20.53	—	8.8	—	+ 3	—	6.5	—	4.6
Hikone	20.78	—	11.4	—	+ 3	—	3.8	—	4.2
Kyoto	21.23	—	17.3	—	+ 4	—	4.5	—	4.2

Table 6. The earthquake of March 18, 1955, 54½°N, 161°E
0 : $00^h06^m46^s$

Observatouy	Δ	Arrival time			O—C			Amplitude			Period		
		Pr	Sr_1	Sr_2	*Pr*	Sr_1	Sr_2	*Pr*	Sr_1	Sr_2	*Pr*	Sr_1	Sr_2
	°	m s	m s	m s	s	s	s	μ	μ	μ	s	s	s
Aomori	19.35	11 10.4	14 42.5	14 56.0	+ 4	+ 8	+21	—	82	312	—	5.2	—
Morioka	20.05	16.3	51.8	15 8.1	+ 3	+ 3	+19	3.5	10	89	4.7	—	5.4
Sendai	21.35	30.4	15 20.7	28.2	+ 3	+ 7	+15	19.0	36	158	5.6	—	5.7
Fukushima	21.97	36.4	32.5	38.1	+ 3	+ 8	+14	11.3	41	92	5.0	5.3	6.4
Utsunomiya	23.24	49.5	—	56.8	+ 4	—	+10	10.6	—	50	4.4	—	4.1
Tokyo	24.03	58.4	—	—	+ 5	—	—	—	—	—	4.9	—	—
Yokohama	24.28	12 1.0	—	16 15.0	+ 5	—	+11	—	—	—	—	—	—
Mishima	24.86	7.1	—	23.7	+ 6	—	+10	12.8	—	42	4.9	—	4.8
Shizuoka	25.21	10.2	—	29.9	+ 6	—	+10	7.9	—	51	5.2	—	5.4
Gifu	25.57	12.0	—	35.0	+ 4	—	+ 9	5.1	—	12	5.2	—	5.2
Nagoya	25.68	12.8	—	—	+ 4	—	—	—	—	—	—	—	—
Hikone	25.91	15.8	—	37.1	+ 5	—	+ 6	5.7	—	10	5.0	—	—

But, its duration from *Pd* or *Pr* is much longer than that given in the J.-B. Table. Thus, in the present article, this problem must be left as unsolved, and will be investigated and reported in a succeeding paper.

ii) *Amplitude relation*

Concerning the phases *Pd* and *Sd* (both referred to as *d*-wave) and *Pr* and *Sr* (both referred to as *r*-wave), a clear and interesting fact is that the amplitude of *d*-wave becomes smaller and smaller with increasing distance, and the amplitude of *d*-wave is much smaller than that of *r*-wave near the distance of 18°. At the observatories of epicentral distance smaller than 13°, the seismograms are begun on the clear arrival of a *d*-wave and no *r*-wave is observed. At about 13° the arrival of a *r*-wave is first observed after the *d*-wave phase, and on the seismograms from 13° up to 18°, the *d*-wave of small amplitude is observed as the first motion, being followed by the *r*-wave of large swing as a later but clear phase. At the epicentral distance beyond 18° a *r*-wave of large amplitude first arrives and the following small *d*-wave cannot usually be identified, because it is disturbed by the wave train of the large *r*-wave of first arrival.

In Figs. 4, (a) and (b), some examples of amplitude-distance relation are given and the observed data are tabulated in the respective tables. The amplitude relation between *d*- and *r*-waves mentioned above is clearly observed on these graphs, in which the plotted points represent the amplitudes of horizontal movement owing to the lacking of vertical seismograms at many observatories, and moreover double amplitude is taken for the *S*-wave. In Fig. 5, the relation between the arrival time

and observed amplitude for both P- and S-waves with respect to d- and r-waves are schematically shown which will afford a good guide for discussing the nature of this sort of phenomena.

This fact with regard to the amplitude relation of d- and r-waves is very interesting. Since, at the crustal discontinuity including the Mohorovičić discontinuity, this sort of phenomenon is never observed, the behaviour of seismic waves with relation to the 20°-discontinuity, if existing, has to be considerably different from that at the crustal discontinuity. Therefore, the amplitude relation above-mentioned is

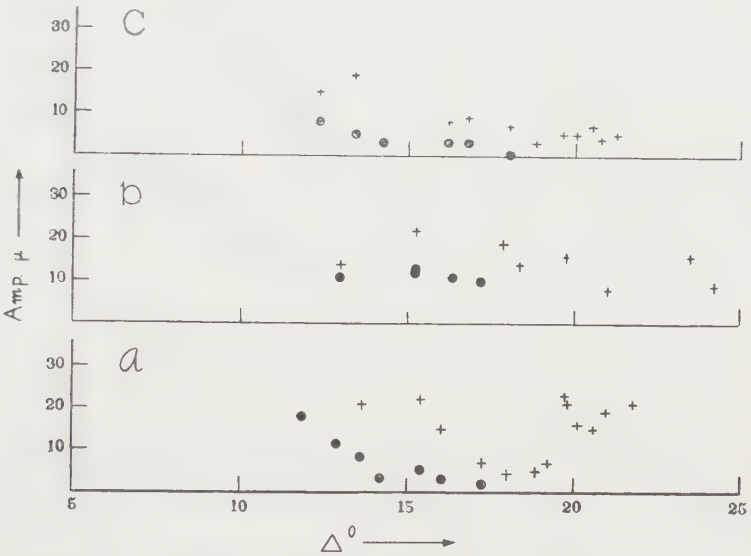

Fig. 4. a) Amplitude-distance graphs for P-wave. Notations have the same meanings as in Fig. 3.
a) The earthquake of Jan. 5, 1953
b) The earthquake of Nov. 4, 1952
c) The earthquake of Oct. 11, 1953

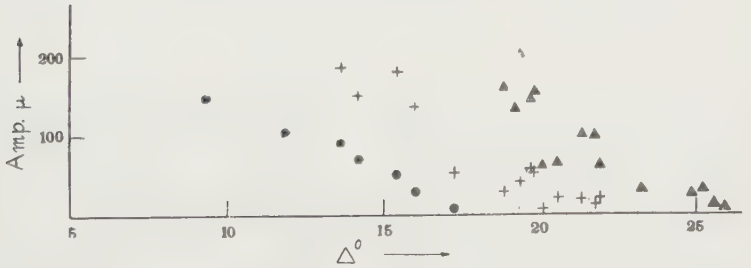

Fig. 4. b) Amplitude-distance graph for S-wave superposed of two earthquakes of Jan. 5, 1953 and March 18, 1955. in which the corrections are made for some observatories allowing for the local structural character. Notations have the same meanings as in Fig. 3.

considered to be an important key for the solution of the mantle structure, and will be discussed again in some detail in the later section **4**, i).

iii) *Wave period of each phase*

The periods of four phases, *Pd*, *Pr*, *Sd* and *Sr* of five earthquakes in Table 1 are plotted together in Fig. 6 with the period and epicentral distance as ordinate and abscissa respectively.

The *r*-wave periods are concentrated in a range of about 4 sec to 6 sec, independently of epicentral distance, observatory and earthquake. On the other hand, *d*-wave periods differ considerably. In some cases the very short period, and in other cases the fairly long period is prevailing, and, in addition, the superposition of the short period and the long one are sometimes observed. Roughly speaking, the periods of *d*-wave consist of periods shorter than about 2 sec and one longer than about 8 sec. Anyhow, it can safely be said without exception, at least in the earthquakes used in the present investigation, that *d*- and *r*-waves are clearly distinguished from each other alsofrom their differences in period. These data also possibly contribute to the investigation of the mode of propagation of both *d*- and *r*-waves and the properties of the mantle.

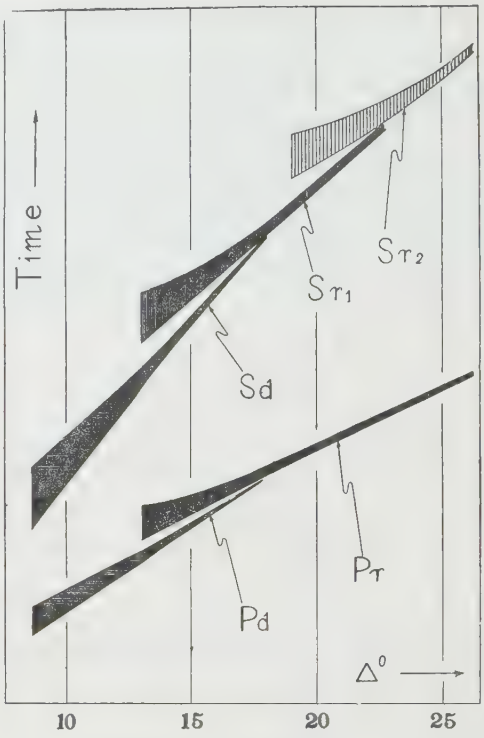

Fig. 5. Schematical illustration of the amplitude-distance relation. The breadth of each branch corresponds to the amplitude at the respective distances.

iv) *Sr_2-wave*

Concerning the earthquake of January 5, 1953, another fact is recognized. The *Sr*-wave amplitude described earlier decreases rapidly and a phase of large amplitude is observed after *Sr* beyond about 19°, and the duration between *Sr* and this phase becomes shorter and shorter with increasing distance. These aspects are clearly seen in Figs. 3 and 5. Thus, this phase seems to belong to a new branch different from that of the *Sr*-wave, and hereafter this phase and the previous *Sr* will be called Sr_2 and Sr_1 respectively. The time-distance graph of Sr_2 is nearly a straight line, whose apparent velocity is 6.4 km/sec. From the diminishing of duration between Sr_1 and

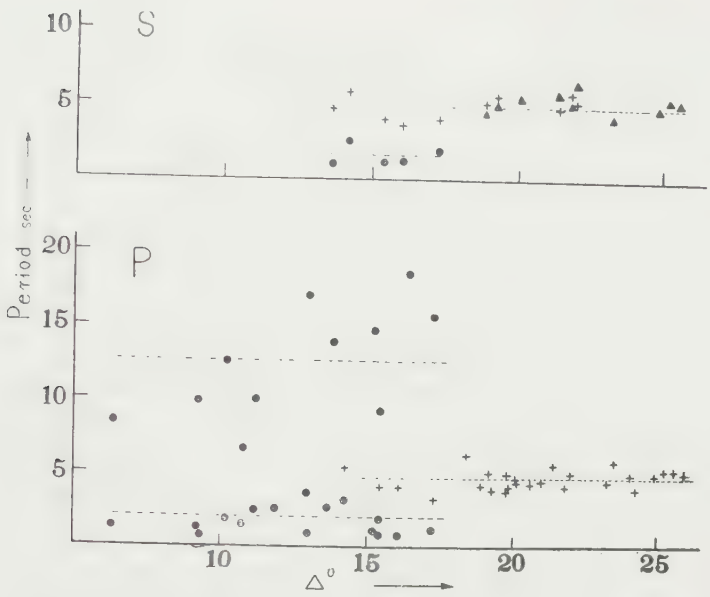

Fig. 6. Period-distance relation of each phase. Notations have the same meanings as in Fig. 3.

Sr_2 with increasing distance, these two branches are finally to intersect at a certain distance, but unfortunately, we have no observation beyond 22° as to this earthquake, so that we are obliged to examine this problem by an earthquake presenting more data.

The earthquake of March 18, 1955, mentioned above in § 3, i), is suitable for the present purpose, because this earthquake has the observational data from about 19° up to 26°. Some seismograms are shown in Fig. 7. In this case also, the time-distance graph of S-curve is divided into two branches which intersect at about 24°, and the apparent velocities of these two branches are 5.4 km/sec and 6.6 km/sec respectively. These numerals, 5.4 km/sec and 6.6 km/sec, coincide very well with those of the earthquake of January 5, 1953. The residuals of Sr_1 and Sr_2 from the J.-B. 0.01 curve are tabulated in Table 6 in the previous section i). In Fig. 8, the travel-time graphs of these two earthquakes are shown, calculated from the respective origin times. In this figure, it is clearly recognized that the behaviours of S waves of both earthquakes are in a fairly good agreement. Moreover, in most seismograms, as seen in Fig. 7, the commencement of Sr_2 is so clear that we can easily identify the appearance of Sr_2-wave. And the amplitude-distance relations of Sr_1 and Sr_2 are nearly the same in both earthquakes as seen in Fig. 4, b).

Thus, from the data above-mentioned, it is roughly concluded that there may be

a discontinuous plane at some depth below the 20°-discontinuity, namely that Sr_2 at distance smaller than about 24° is the backward extension of the branch beyond 24°. Concerning this problem, it can be stated that at about 24° the J.-B. 0.01 curve shows a clear change, though gradual, of its gradient.

It is to be noted that this result was deduced only from the analysis of the *S*-wave, and as to the *P*-wave no later phase was observed at the distances concerned. Although the amplitudes of the first *P* shows a maximum near the critical distance, say about 24° and it seems that there exists a change of waveform suggesting the superposition of two waves near the critical distance, these are less reliable than those of the *S*-wave. Consequently, this new discontinuity, if existing, is considered to be more effective for *S* than *P*. Needless to say, this problem on new discontinuity should be discussed by much more abundant and more accurate data, but the above-observed fact is considered to be useful for a new development of the investigation of the earth's mantle.

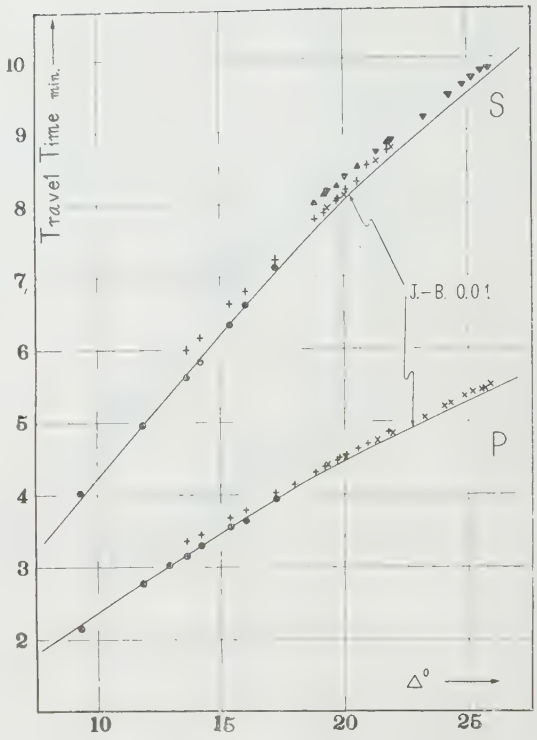

Fig. 8. Travel time-distance graphs superposed of two earthquakes of Jan. 5, 1953 and March 18, 1955. ●, + and ▲ belong to the former, and × and ▼ represent the *r*-wave and Sr_2-wave for the latter respectively.

In connection with the newly proposed discontinuity, Nishitake (**19**) recently discussed the property of the earth's mantle and obtained the distribution of k/μ (k and μ are the bulk modulus and rigidity respectively) with depth as deduced from the J.-B.'s seismic velocity distribution. In his paper it was reported that an abrupt decrease takes place at about 100 km below the 20°discontinuity and this decrease keeps on for about 100 km. The decrease of k/μ corresponds to the larger increase of μ compared with that of k with increasing depth, and this behaviour of k/μ seems to relate possibly to the present new discontinuity.

4. Some considerations

i) *On the amplitudes of d- and r-waves*

Gutenberg previously stated (**7**) that the amplitude of the first *P*-wave shows an abrupt decrease at about 5° and is very small at distances up to about 15°, and beyond 15° becomes gradually large with increasing distance. And he attributed the cause of these phenomena to the existence of a low-velocity layer in the mantle, namely, the waves of small amplitude at 5° to 15° are the diffracted waves due to that low-velocity layer and the large waves observed beyond 15° are the wave penetrating down into this low-velocity layer and again rising up to the earth's surface. According to his recent paper (**8**), this diffracted wave of the normal earthquake composes a nearly straight time-distance curve whose apparent velocity is 7.74 km/sec and deviates considerably from the the J.-B. curve. On the other hand, as to the *S*-wave, it is said that there is no observation in the range of about 10°~17°.

In any case, since the amplitude variation with distance stated by Gutenberg seems to be similar in some points to the facts described in §**3**, ii), a consideration on Gutenberg's structure is to be made. The conception of 'low-velocity layer' by Gutenberg is assumed on the basis of the following two phenomena; namely, 1) the sudden diminution of amplitude at about 5° and its continuation up to about 15°, and 2) the gradual and monotonous increase of amplitude from about 15° up to beyond 20°. Accordingly, these two points should be examined regarding the earthquakes concerned here. In order to examine the first relation, the amplitude-distance relations of the first *P*-motion of three earthquakes at short distances near 5° were investigated, whose results are illustrated in Figs. 9, a), b) and c). Of these earthquakes, the first was the Akita-Oga Earthquake on May 1, 1939 whose focal depth was considered to be shallower than 10 km. The second was the earthquake of July 28, 1951 whose epicenter and focal depth were estimated as 37.5°N, 143.5°E and about 10 km respectively, and the third was the Yoshino Earthquake of July 17, 1952 whose focal

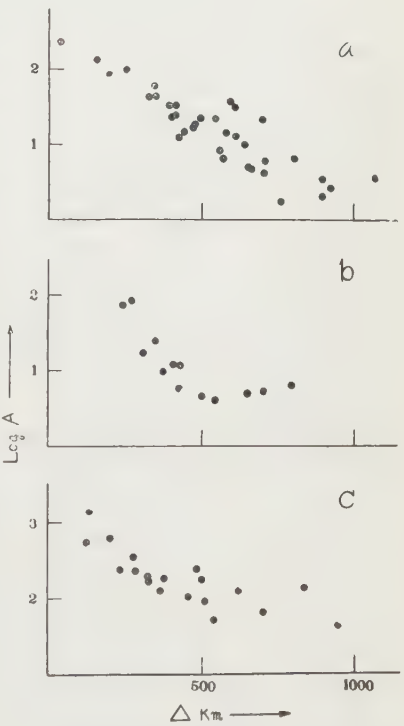

Fig. 9. Amplitude-distance graphs for the first *P*-motion at short distances. a) The Akita-Oga Earthquake of May 1, 1939, b) The earthquake of July 28, 1951, and c) The Yoshino Earthquake of July 17, 1952.

depth was estimated as 70 km below the earth's surface and this depth corresponds to the top of low-velolocity layer, if it exists. In Fig. 10, the natural logarithm of amplitude is plotted against the epicentral distance. In any case, the sudden diminution of amplitude at about 5° as assumed by Gutenberg was not observed. Next, for the second relation, as was already described, the *d*–waves are observed equally on both *P*– and *S*–waves, and continue with no gap up to about 18° at which the *d*–waves are overtaken by the *r*–waves, and, moreover, the amplitudes of *d*–wave decrease monotonously up to 18° and never increase again. In addition, the time-distance graphs of *d*–waves fit fairly well into the J.–B. Table from about 6° to 18° as was mentioned in the previous § **3**, i). Considering these results, it is reasonably concluded that the present case differs certainly from that of Gutenberg, and so the existence of a low-velocity layer in the mantle is considered questionable at least in the case of Japanese earthquakes.

According to the recent investigations of Jeffreys cited in the previous § **3**, i) (**4**, **5**), there exist considerable regional differences between the time-distance curves in European, Japanese and North American regions, and these differences imply the regional difference of the mantle structure down to considerable depth. On the other hand, Lehmann (**11**, **12**) also found that the time-distance graphs of the *S*–wave give the different aspects in Europe and North America. Reflecting upon these facts, the allowance for the regional difference may be possibly assumed in the present investigation.

In any way, however, the phenomena mentioned above in § **3**, ii) concerning the amplitudes of *d*– and *r*–waves will be interpreted as caused by an abnormally strong attenuation of *d*–waves observed near the epicentral distance of 18° or by an abnormal enlargement of *r*–waves owing to some causes. In order to examine this point, a deep earthquake was treated for reference. This earthquake occurred on February 28, 1950 and its epicenter and focal depth were 46.0°N, and 143.8°E, and 350 km respectively, and so this earthquake is considered to have been seated above the 20°–discontinuity but below the low-velocity layer, if existent. In Fig. 10, the amplitude of the first *P* arrival is plotted against the epicentral distance. Since this earthquake was a very large one and the onsets of the first *P* arrival was very clear, there is no doubt with regard to the readings of amplitude.

In this figure, the amplitudes are small in some ranges before about 12°, and increase abruptly at about 12° which may nearly correspond, allowing for the focal depth, to the amplitude relation which should be observed near the epicentral distance of 20° in the case of shallow earthquakes. Thus the deep earthquake, if its focus is above the 20°–discontinuity, shows the same behaviour with regard to the anomalous diminution of amplitude at an epicentral distance at which *Pr*–wave is expected to appear first.

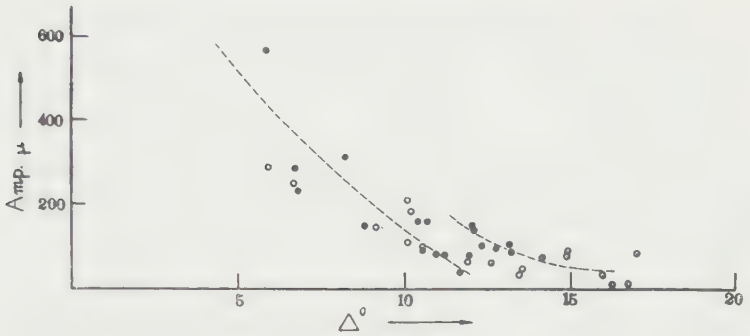

Fig. 10. Amplitude-distance graph for the first *P*-motion of the deep earthquake (350 km) of Feb. 28, 1950.

Then, the reasonable interpretation of the behaviours of amplitude of both *d*- and *r*-waves is fairly difficult. One probable interpretation is the diminution of the *d*-wave due to the existence of a transient layer just above the 20°-discontinuity which makes the amplitudes of both *P* and *S* diminish equally. On the other hand, the enlargement of the *r*-wave may possibly be considered as reflecting the constancy of *r*-wave period and the possible existence of another discontinuity below the 20°-discontinuity as mentionedin § **3**, iv). The emphasis on a specified period of the critically refracted wave in the case of a layer overlying a semi-infinite medium was worked out by Sato (**20**) and Officer (**21**). These investigations seem to be worthy of examination in the present case, although it is problematical whether or not these are valid for a layer in the earth's interior.

Finally, some remarks are conveniently added in this occasion. As was mentioned in § **3**, i), *Pr*- and *Sr*-waves showed positive residuals of a few seconds compared with the J.-B. curve for some earthquakes, but this is not the case for others. This phenomenon may be related with the magnitude of earthquake and with the sensitivity of seismograph. On the earthquake of November 4, 1952, the *P*-wave of clear onset beyond about 18° was forerun by a weak vibration which fitted into the J.-B. curve. On the earthquake of October 11, 1953, the Galitzin-type seismograph of high magnification (about 2000) at the Kamigamo Geophysical Observatory, Kyoto University, showed a similar weak vibration forerunning *Pr* of clear onset. On these two earthquakes, the weak vibration fits into the J.-B. curve and the following wave of clear onset (*Pr*) is delayed by a few seconds. Other earthquakes show only a *Pr*-wave of clear onset, missing the weak vibration. These facts may be justified by the explanation that the weak vibration is missed by refraction at the 20°-discontinuity in some cases.

ii) *On the Formosa earthquakes*

As the comparison of northern earthquakes seen from Japan (Kamchatka-Kurile

Table 7. The earthquake of Aug. 22, 1936, 22.1°N, 121.°2E
0 : 06h51m37s

Observatory	Δ	Arrival time			O—C			Period of *Pr*
		Pd	*Pr*	*S*	*Pd*	*Pr*	*S*	
	°	m s	m s	m s	s	s	s	s
Kobe	17.44	55 37.0	55 45.4	59 11.4	− 2	+ 6	+21	3.7
Kyoto	18.00	46.8	51.0	19.9	+ 1	+ 5	+17	3.7
Nagoya	18.87	57.4	56 00.2	34.5	+ 1	+ 3	+12	3.3
Gifu	18.89	55.8	00.1	32.0	− 1	+ 3	+ 9	3.4
Mishima	20.13	—	11.4	58.5	—	+ 1	+ 8	5.0
Nagano	20.59	—	15.4	00 6.7	—	0	+ 8	3.6
Tokyo	21.01	—	21.6	—	—	+ 2	—	6.5
Kumagaya	21.02	—	20.5	19.3	—	0	+12	6.0
Fukushima	22.69	—	36.7	42.1	—	0	+ 4	3.5
Sendai	23.27	—	41.0	50.8	—	− 1	+ 2	3.4
Morioka	24.34	—	51.0	01 12.5	—	− 2	+ 5	5.5

Islands) with southern earthquakes, two Formosa earthquakes, mainly that of August 22, 1936, were likewise analysed with regard to the travel-time, amplitude and period of each phase. The earthquake of August 22, 1936 is considered to be very shallow-seated in the crust, because this earthquake did some damages to the buildings near its epicenter. The observational data are given in Table 7 and some examples of seismogram in Fig. 12. The time-distance graphs of both *P* and *S* are shown in Fig. 11, in which, unfortunately, the seismograms at distance smaller than about 17° were not available. As shown in Fig. 11, the abrupt change of gradient is clearly observed at about 20° as to the time-distance graph of *P*-wave. This value

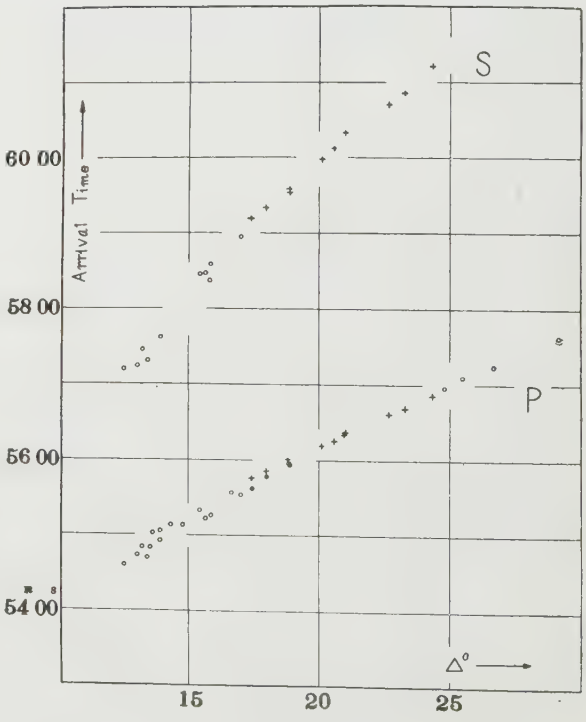

Fig. 11. Time-distance graphs of the Formosa earthquake of Aug. 22, 1936. Circles are the readings after the Japan Meteorological Agency added for reference, and other notations are referred to Fig. 3.

of 20° is well accordant with the so-called 20°-discontinuity as observed in shallow earthquake, and clearly shows the existence of a 20°-discontinuity in the Japanese area.

The first *P* waves at distances up to about 20° are weak and their periods are short, and moreover, they are followed by waves of clear onset and long period. On the other hand, beyond 20°, the seismograms are commenced by a wave of clear onset which corresponds to the latter *P*-wave at distances up to about 20°. This change of the appearance of the first *P* arrival with increasing distance is the same as that of the Kamchatka earthquake; accordingly, we may call them *Pd* and *Pr* respectively. *Pd*-waves up to about 20° fit fairly well into the J.-B. 0.00 curve, as seen in Table 7, allowing for the first *P* arrivals from 2° to 7° in Formosa observatories which are considered the *Pd*-waves. And, moreover, *Pr*-waves beyond 20° approximately fit to the same curve. But, there exists a slight difference between the Formosa and the Kamchatka earthquakes. In the latter case, *Pr*-branch beyond 18° (corresponding to 20° in the Formosa earthquake) was extended back almost linearly down to about 13°, but in the former, two *Pr*-branches, say, one up to 20° and the other beyond 20°, have the different slopes and intersect at about 20°, as seen in Fig. 11. Therefore, judging only from this fact alone, it is naturally to consider that there exist two branches belonging to different families, and this consideration is suggested by another phenomenon, namely, the period of *Pr* which is about 3.5 sec up to about 20°, becoming 6.0 sec at 21°, and thereafter returning to about 3.5 sec. Recently, Z. Suzuki (**22**) stated that a similar phenomenon was observed at the superposition of direct and refracted waves at the so-called critical distance on the small scale explosion experiment. If a similar explanation is valid in the present case of natural earthquakes, it results that three branches, say, *Pd* and two *Pr*'s, meet at about 20°. In the present state, however, it is impossible to accurately determine as to whether there exists a difference between the observed materials of both the Kamchatka- and Formosa-earthquakes, because the observed materials of Formosa earthquakes are far inferior to those of Kamchatka-Kurile Islands in the points of example-number and distribution of observatories.

Next, concerning the *S*-wave, the arrival time observed of the *S*-phases observed after the distance of 20° is approximately accordant with the J.-B. 0.00 Table, but the *S*-phase clearly observed before the 20° is considered to be the *Sr*-wave and not the *Sd*-wave, as shown in Fig. 12 and Table 7. Contrary to the case of Kamchatka-Kurile Islands, it is difficult to find the *Sd*-wave preceding the *Sr*-wave in a distance shorter than 20°. And moreover, in case of Formosa earthquake, the available observatories are lacking between 2°- and 17°-epicentral distance. Under such disadvantageous circumstances the discussion of the comparison between the earthquakes of

northern and southern origin seen from Japan is inappropriate in the present state, but the minute regional difference of the mantle structure, if existing, will be discussed in greater detail in a succeeding paper.

iii) *On the* 13°*-discontinuity*

In 1951, the writer (**23**) reported that an abrupt change was observed at about 13° of the gradient of superposed time-distance graph of about ten shallow earthquakes having occurred in the same epicentral region of Japan and having nearly equal focal depths, and he provisionally called it a 13°–discontinuity. It was left unexplained, however, as to whether it corresponded to a real discontinuity or was only an apparent phenomenon

Now, reflecting upon the facts described in this article and allowing for the apparent velocity, 9.5 km/sec, of the branch at range between 13° and 20° in our article above-cited, it may naturally be inferred that the abrupt change of gradient of superposed time-distance graph at 13° is caused by missing of *Pd* owing to its weakness and misreading of *Pr* as the first motion at many observatories. And, moreover, a considerably large fluctuation of the observed *P*–time at distances near 13° may possibly support the interpretation above-mentioned. And moreover, the epicentral distance of 13° is estimated to be the shortest distance at which the *Pr*–wave is expected to be clearly observed. Consequently the anomalous appearance in the time-distance graph whihc was previously reported as the 13°–discontinuity is, after all, reasonably explained by the refracted waves connected with the existence of 20°–discontinuity in the earth's mantle.

5. Summary

Seismograms observed at observatories in Japan of five prominent earthquakes of Kamchatka-Kurile Islands were analysed to investigate the existence and nature of the 20°-discontinuity and the low-velocity layer in the earth's mantle. Some results obtained in the present treatment are as follows:

i) The existence of the 20°–discontinuity was ascertained in Japan, but its order of discontinuity remains undetermined.

ii) The existence of low-velocity layer was negatively concluded, at least in Japan.

iii) The abnormal diminution of amplitude of direct seismic wave and, reversely, the large and clear appearance of a refracted seismic wave through the 20°–discontinuity were definitely observed for both *P*– and *S*–phases near the epicentral distance of 20°. For these remarkable facts two explanations of the large attenuation of direct wave at the transition layer close above the 20°–discontinuity or any enlargement-effect for the refracted wave by the

layer-channel between the 20°-discontinuity and the 25°-discontinuity newly found, were tentatively postulated.

iv) From the present treatment, it is reasonably concluded that the nature and structure of the earth's mantle may have somewhat regional character when they are compared for the regions in Europe, America, Asia, etc.

Acknowledgement

The writer wishes to express his hearty gratitude to Prof. E. Nishimura for his kind guidance throughout the present investigation, and also to the directors and members of the Japan Meteorological Agency for their generous permission for copying many seismograms. The cost for the present study was partly defrayed by a grant-in-aid for Scientific researches of the Ministry of Education.

REFERENCES

1. H. JEFFREYS, The structure of the Farth down to the 20°-discontinuity, Mon. Not. Roy. Astr. Soc., Geophys. Suppl., **3** (1936), 401–422.
2. ———, ——————————————— (second paper), Mon. Not. Roy. Astr. Soc., Geophys. Suppl., **4** (1936), 13–43.
3. ———, The times of *P*, *S* and *SKS*, and the velocities of *P* and *S*, Mon. Not. Roy. Astr. Soc., Geophys. Suppl., **4** (1939), 498–533.
4. ———, The times of *P* up to 30°, Mon. Not. Roy. Astr. Soc., Geophys. Suppl., **6** (1952), 348–364.
5. ———, The times of *P* in Japanese and European earthquakes, Mon. Not. Roy. Astr. Soc., Geophys. Suppl., **6** (1954), 557–565.
6. B. GUTENBERG and C. F. RICHTER, New evidence for a change in physical conditions at depths near 100 km, Bull. Seism. Soc. America, **29** (1939), 531–537.
7. B. GUTENBERG, On the layer of relatively low wave velocity at a depth of about 80 kilometers, Bull. Seism. Soc. America, **38** (1948), 121–148.
8. ———, Low-velocity layers in the earth's mantle, Bull. Geol. Soc. America, **65** (1954), 337–348.
9. P. BYERLY, The Montana earthquake of June 28, 1925, Bull Seism. Soc. America., **16** (1926), 209–265.
10. I. LEHMANN, Transmission times for seismic waves for epicentral distances around 20°, Geod. Inst. Kobenhavn, Med., **5** (1934), 1–46.
11. ———, *P* and *S* at distances smaller than 25°, Trans. Amer. Geophys. Union, **34** (1953), 477–483.
12. ———, The times of *P* and *S* in Northern America, Estratto da Annali di Gecfisica, **8** (1955), 351–370.
13. H. KAWASUMI and S. HONMA, On a problem concerning the internal structure of the earth as discussed from the time-distance curve of the Formosa Earthquake of April 20, 1935, Bull. Earthq. Res. Inst., **14** (1936), 201–221.
14. H. KAWASUMI, Study on the propagation of seismic waves (the first paper), Bull. Earthq. Res. Inst., **10** (1932), 94–119.
15. T. MATUZAWA, Seismometrische Untersuchungen des Erdbebens von 2, März 1933, I. Bestimmung des Herdes, Bull. Earthq. Res. Inst., **13** (1935), 171–193.

16. K. WADATI and K. MASUDA, On the travel time of earthquake waves (Part V), Geophys. Mag. **7** (1933), 269–290.
17. B. GUTENBERG, Wave velocities at depths between 50 and 600 kilometers, Bull. Seism. Soc. America, **43** (1953), 223–232.
18. J. CL. DE BREMAECKER, Use of amplitudes, Part I: Pn from 3° to 23°, Bull. Seism. Soc. America, **45** (1955), 219–244.
19. T. NISHITAKE, Elastic properties of rocks with relation to the earth's interior, Mem. Coll. Science, Kyoto Univ., A, **28** (1956). 73–98.
20. Y. SATO, Study on surface waves, VI Generation of Love and other types of SH waves, Bull. Earthq. Res. Inst., **30** (1952), 101–120.
21. C. B. OFFICER, Jr., The refraction arrival in water covered areas, Geophysics, **18** (1953), 805–819.
22. Z. SUZUKI, On the forms of seismic wave generated by the explosion (3rd paper), Bull. Research Group of Seismic Exploration, **7** (1956), 43–59 (in Japanese).
23. Y. KISHIMOTO, On a 13°-discontinuity of the earth's mantle, Zisin, 2nd Ser., **5** (1951), 7–12 (in Japanese).

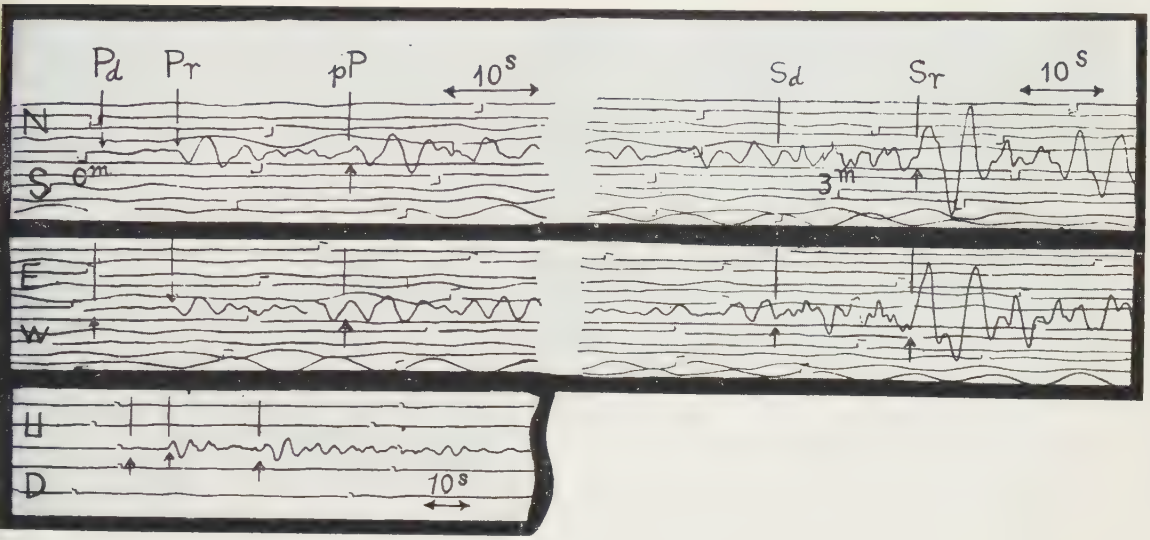

Fig. 2. Wiechert-seismograms, Jan. 5th 10h 06m 30s, N Part of Kurile Islands (referred to Table 2)
(a) Sendai (Δ=15.41°) The weak *Pd* and *Sd* appear as the first motion, being followed by *Pr* and *Sr* of large swing.
(By the courtesy of the Sendai Observatory)

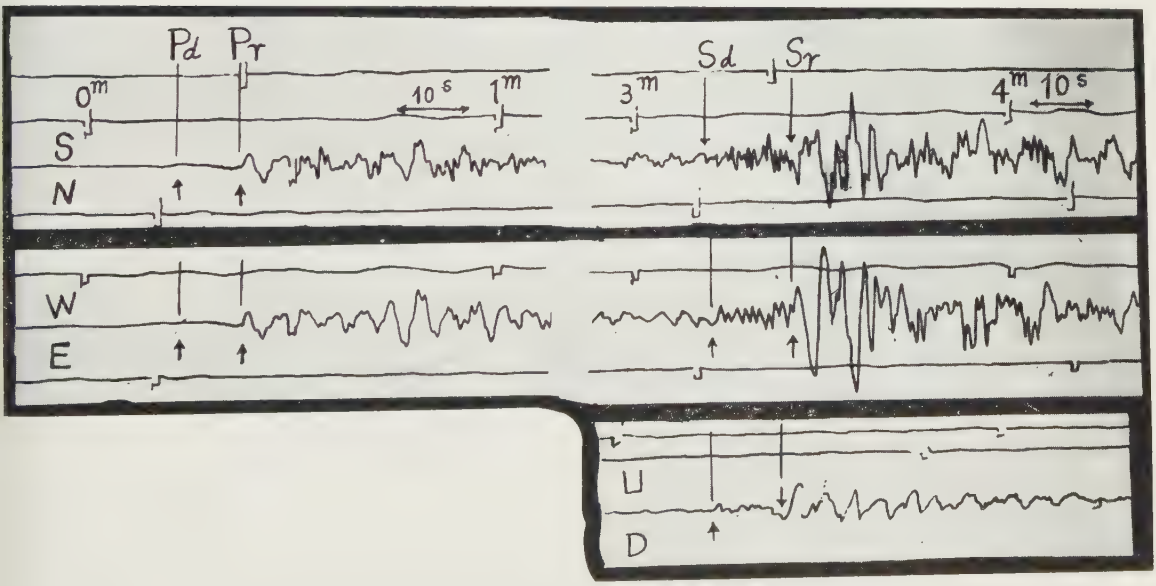

Fig. 2. (b) Fukushima (Δ=16.03°) The behaviours of *P*- and *S*-waves are the same as at Sendai.
(By the courtesy of the Fukushima Observatory)

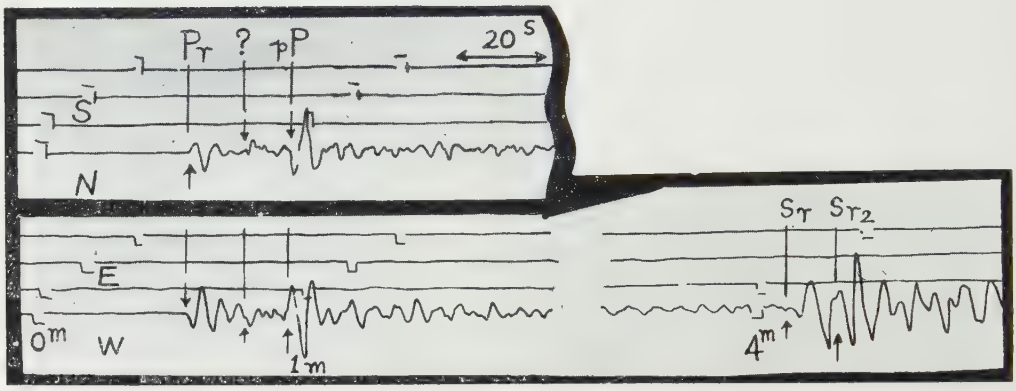

Fig. 2. (c) Gifu (Δ=19.73°) *Pr* and *Sr* appear as the first motion with the clear onset.
(By the courtesy of the Gifu Observatory)

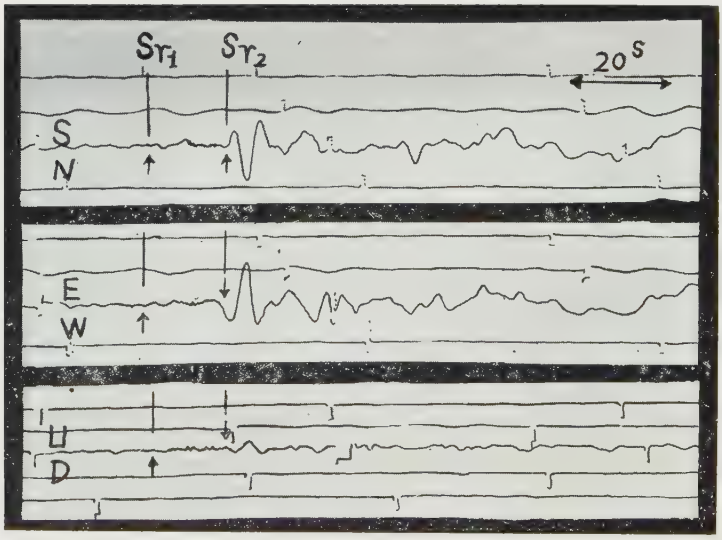

Fig. 7. Wiechert-seismograms, March 18th 00h 06m 46s, Near east coast of Kamchatka (referred to Table 6)
(a) Morioka (Δ=20.05°) A large Sr_2 arrives, forerun by a weak Sr_1.
(By the courtesy of the Morioka Observatory)

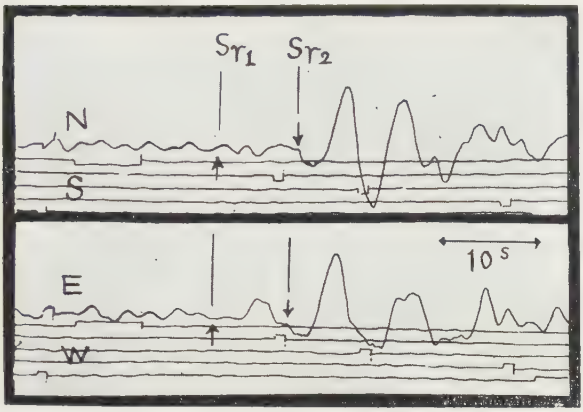

Fig. 7. (b) Sendai (Δ=21.35°) The behaviour of S wave is the same as at Morioka.
By the courtesy of the Sendai Observatory)

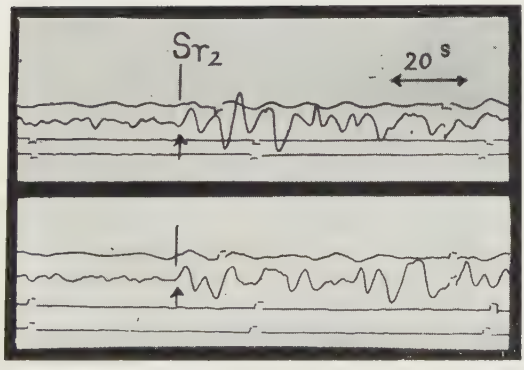

Fig. 7. (c) Shizuoka (Δ=25.21°) A clear Sr_2 appears as the first S-arrival.
(By the conrtesy of the Shizuoka Observatory)

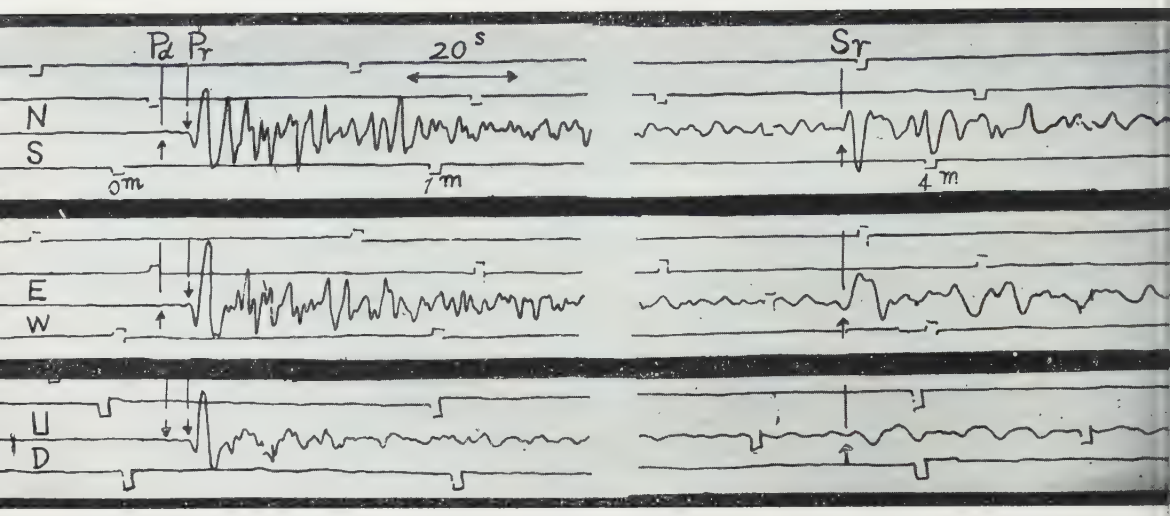

Fig. 12. Wiechert-seismograms, Aug. 22nd 06h 51m 37s, Near SE coast of Formosa (referred to Table 7)
(a) Kyoto (Δ=18. 00°) A weak *Pd* appears as the first *P*-motion, followed by a large *Pr*. As to *S*, the *Sd* being not observed, the *Sr* is only observed.
(By the courtesy of the Kyoto Observatory)

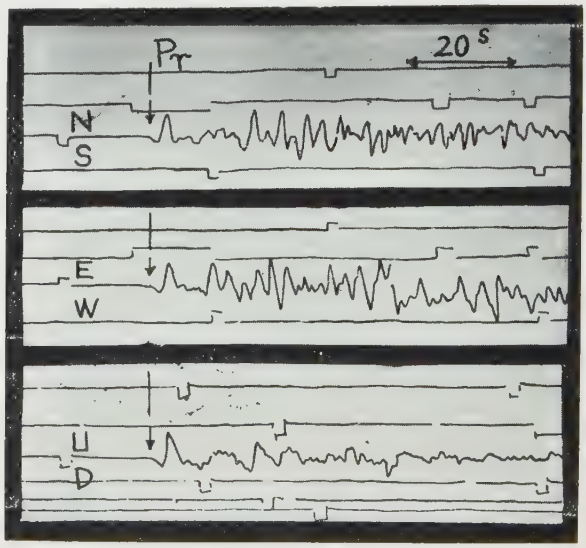

Fig. 12. (b) Sendai (Δ=23.27°) A clear *Pr* appears as the first motion.
(By the courtesy of the Sendai Observatory)

MEMOIRS OF THE COLLEGE OF SCIENCE, University of Kyoto, Series A,
Vol. XXVIII, No. 2, Article 3, 1956

ON THE SEISMIC WAVES REFLECTED AT THE MOHOROVIČIĆ DISCONTINUITY (I)

BY

Akira KAMITSUKI

(*Received December 21, 1956*)

ABSTRACT

The seismic waves reflected at the Mohorovičić discontinuity of the earth's crust are discussed on the basis of seismograms recorded at the stations near the epicenter of natural earthquakes. It was profitably proved from both observational and theoretical sides that the seismic waves reflected at the Mohorovičić discontinuity in earthquakes of shallow origin are clearly identified in the seismograms recorded at observation stations of several kilometers distance from the epicenter, and this affords a powerful means for the investigation of the crustal structure. In this paper the seismograms of some earthquakes of short distances of within 70 km, and shallow focus of less than 20 km depth, were examined, and those of middle distance will be treated in a forthcoming paper.

1. Introduction

In 1909, A. Mohorovičić found by the analysis of the travel time-distance curve of near earthquakes that the velocity of seismic waves increases abruptly at the depth of about 55 km below the earth's surface and its discontinuity surface is called the Mohorovičić discontinuity, being considered as the bottom of the earth's crust. Since then the nature of the earth's crust has been an important and attractive problem in seismology. In recent years, many investigations of the earth's crust have been carried out in various regions of the world, analysing the seismic waves not only of natural earthquakes but also of artificial explosions. They have yielded many important results, while many problems have remained unsolved.

It is well known that most of the earthquakes have their foci in the earth's crust and their seismograms recorded at the stations on the earth's surface are considerably complicated. This complexity may be attributed to the fact that the seismograms contain the superposed effects caused by the emission mechanism at the focus, the various phenomena in the seismic paths through which the waves are transmitted, the local condition of the observation stations and the characteristics of the seismographs, etc. The assumption of layers separated by discontinuity surfaces in the earth's crust affords a reasonable explanation of the various sets of phases which appear on the records of such earthquakes. Namely, when the seismic waves are

incident at the discontinuity surface, the reflected and refracted waves are generated and the waves are transformed from P- to S-type or inversely.

Reflecting upon the many investigations made up to the present, they have almost all been carried out by using the direct and refracted waves, while the reflected and transformed waves have scarcely been treated, particularly in the case of natural earthquakes (**1**, **2**, **3**, **4**, **5**, **6**, **7**, **8**, **9**, **10**). This is mainly attributed to the difficulty of phase identification in the case of the reflected and transformed waves. In normal cases the direct and refracted waves in seismograms are easily discriminated from other waves, while the reflected and transformed waves are complicatedly mixed in seismograms, and their separation and identification are usually a troublesome but fruitless task. But, considering the fact that the analysis of reflected and transformed waves in co-operation with the direct and refracted waves will certainly afford a powerful method of investigating the structure of the earth's crust and earth's deep interior, any useful method of easy and unmistakable identification of phase of reflected and transformed waves should be pursued for the advancement of our knowledge on the nature of the earth's interior. In the following series of investigations some useful methods for the analysis of reflected and transformed waves will be discussed in detail and applied to practical cases.

In the present paper, the shallow earthquakes of which foci are situated in the crust, are selected and the S-waves reflected at the Mohorovičić discontinuity (S_MS) are especially investigated among the various phases appearing in the seismograms. And by the application of the reflection analysis, the local structural character in our country is discussed in some detail.

2. The earthquake of December 21, 1954

The local earthquake occurred near Kyoto City on December 21, 1954. It seemed to be shallow because the P~S time at the Kamigamo Geophysical Observatory was only about 2 sec, and in the vertical seismogram of the large Wiechert seismograph, a prominent phase was found out about 10 sec later after the direct S-wave, as seen in Fig. 1. It is to be mentioned that the horizontal component in this case was out of scale owing to the large amplitude of horizontal movements. With regard to this prominent wave phase, some detailed arguments will be developed in the following.

a) *Travel time-distance graph*

Recently, Y. Kishimoto insisted on the regional character of the crustal structure in our country by the analysis of the refracted waves recorded on many seismograms obtained at the Kamigamo and Abuyama Observatories (**11**, **12**). By his method, it was found that the several regions around Kyoto have a crust whose thickness varies within the range between 25 km and 50 km from region to region and their diversity

is mainly due to the various thicknesses of the basaltic layer. In his paper, he gave the figure shown in the annexed table as the crustal structure of the Kyoto region. This structure is tentatively adopted in the present investigation.

Layer	V_p (km/sec.)	V_s (km/sec.)	Thickness (km)	
				earth's surface
granitic	5.4	3.1	6	
				g-g discontinuity
granodioritic	5.8	3.3	14	
				g-b discontinuity
basaltic	7.0	4.0	10	
				M-discontinuity

Generally speaking, in seismometric investigations of the earth's crust, the accurate determination of the location of epicenter and the focal depth is the most essential. From this point of view, it is also desirable in the present study on the reflected wave that there be many observatories around the epicenter and, moreover, that the focus be seated as shallow as possible. Needless to say, the more observatories available in seismogram-analysis, the more accurately the various elements in seismometry are determined and also the shallow-seated earthquakes result generally in a sharp and clear separation of reflected waves from other wave phases in their seismograms, owing mainly to the longer interval of arrival time between various phases compared with that in the case of earthquake of deep crustal origin. In these points, the earthquake in question is regarded as the most suitable for reflection analysis.

The data observed at each station are tabulated in Table 1. And the seismograms are shown in Figs. 1 and 2, the former being at Kamigamo ($\Delta = 4$ km) of the very short distance and the latter at Hikone ($\Delta = 51.5$ km) near the critical distance.

When the theoretical travel time-distance curves are drawn referring to the direct P- and S-wave in case of earthquakes whose foci are situated at depths of less than

Table 1. The earthquake of Dec. 21, 1954.
Epicenter $\varphi = 35.1°$N $\lambda = 135.7°$E Focal depth = 11 km

No.	Station	Epicentral distance	P~S time
1	Kamigamo	4.0 km	1.9 sec.
2	Kyoto	5.0	2.0
3	Abuyama	26.5	3.7
4	Nara	38.5	5.2
5	Ôsaka	47.5	6.6
6	Hikone	51.5	7.0
7	Kôbe	65.5	8.8
8	Kameyama	67.0	9.3
9	Tsu	78.0	10.3

20 km, they can safely be treated as a straight line within the range of observation accuracy at the epicentral distance between about 30 km and 80 km. The reason is that at distances below the above-mentioned range, the effect of the focal depth must be considered and at the larger distances the refracted waves forerun the direct wave. For this reason, the data of stations which are at shorter distances (Kamigamo, Kyoto and Abuyama) and at larger distances (Owase and Shionomisaki) are temporarily excluded in the first step of drawing the P～S time-distance graph. Using the P～S times of the remaining six stations (Nara, Osaka, Kobe, Hikone, Kameyama and Tsu), the location of the epicenter and the P～S time-distance curve was determined by the following procedure.

Now one point near the approximately assumed epicenter was arbitrarily taken as the origin and the co-ordinates of each station were determined in relation to the rectangular co-ordinate axes. Then taking account of the linear relation of the P～S times to the epicentral distance, the following equation was postulated.

$$t_i = p\Delta_i + h$$
$$= pv\sqrt{(x-x_i)^2+(y-y_i)^2} + h$$

where t_i is the P～S time observed at each station,
x_i and y_i are the co-ordinates of each station,
x and y are the co-ordinates of epicenter,
p is the gradient of P～S time-distance curve and
h is the intercept time of the curve on the time axis.

The four unknowns x, y, p and h were determined by the method of least squares. The locations of observation station and epicenter thus determined are shown in Fig. 3. Taking account of the gradient and intercept time of the P～S time-distance curve, the focal depth was calculated as 11 km. Moreover, this value was also ascertained by the identification of the S-wave reflected at the g-b discontinuity surface ($S_{g-b}S$). The theoretically calculated travel time-distance curve is shown in Fig. 4, the duration between the direct P-wave and the respective phases being plotted against the epicentral distance. On the basis of the above-mentioned procedure, the values of arrival time of the clearly observed phase at each station are in a fairly good coincidence with the curve calculated as the S-wave reflected at the M-discontinuity (S_MS), and in this case, the calculated curves for the S_MS under other conditions of focal depth and crustal thickness are far out of conformity with the observed values. Consequently it is safely said that, at least, from the point of arrival time, the prominent phases observed in the present case are correctly interpreted as the S-wave reflected at the M-discontinuity, and it is also ascertained that Kishimoto's model of the crustal structure around Kyoto is reasonably applicable to

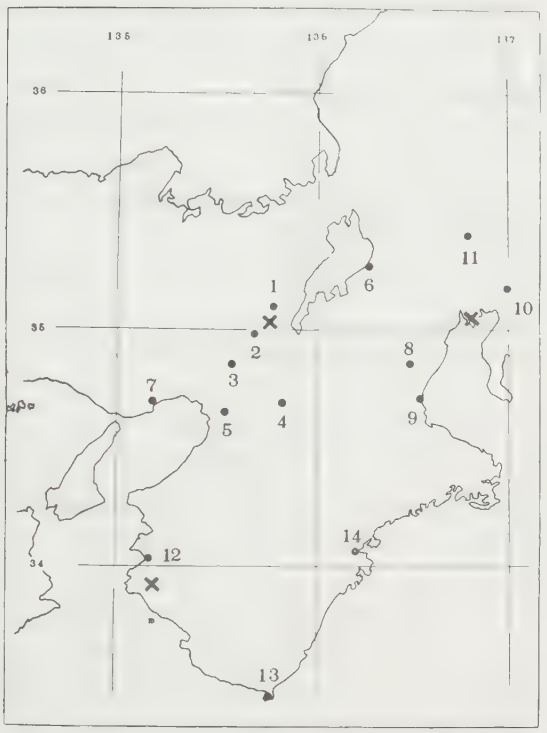

Fig. 3. The location of epicenters and observation stations tabulated in Table 1, 3 and 4.

Earthquake	Date	Epicenter
1)	1954 Dec. 21	$\varphi=35.1°$N, $\lambda=135.7°$E in section 2
2)	1955 Feb. 12	$\varphi=35.1°$N, $\lambda=136.8°$E in section 3
3)	1955 Dec. 3	$\varphi=33.8°$N, $\lambda=135.1°$E in section 3

Station number
1) Kamigamo, 2) Kyoto, 3) Abuyama, 4) Nara, 5) Ôsaka, 6) Hikone, 7) Kôbe, 8) Kameyama, 9) Tsu, 10) Nagoya, 11) Gifu, 12) Yuasa, 13) Shionomisaki, 14) Owase

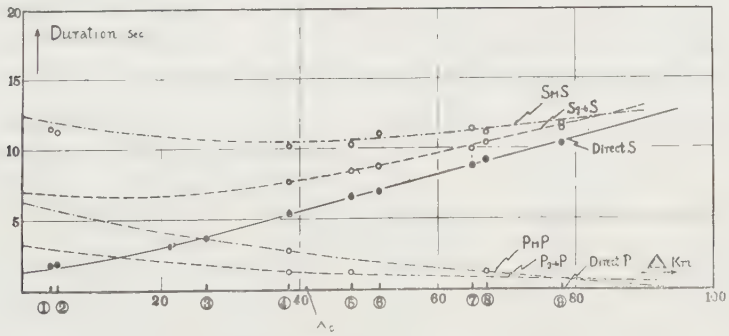

Fig. 4. Travel time-distance graph of the earthquake of Dec. 21, 1954 tabulated in Table 1.

the present investigation.

b) *Amplitude-relation*

In the next place, a further step toward the investigation of amplitude variation with the epicentral distance will be taken, which is another important clue to seismometric investigation of the earth's interior. At first, under the following assumption, the theoretical calculation of amplitude was carried out (**13**, **14**, **15**, **16**, **17**).

1) On the emission mechanism at the focus, the waves are emitted with the

same magnitude in all directions. In other words, the initial amplitude is independent of θ and φ, where θ is the angle between vertical and the direction of the ray of respective waves and φ is the azimuth referring to the epicenter.

2) The reflection and refraction coefficients of waves incident at each discontinuity surface are calculated as for plane waves.

3) Divergence factor due to spreading as the spherical wave is considered to be inversely proportional to r^2 where r is the path length (**18**).

4) Absorption effect due to the departure from perfect elasticity of the crustal material is omitted (**19**).

5) The effect due to the existence of sedimentary layer was considered to be negligible (**11**, **20**, **21**).

In general, on the transversal wave, it is theoretically advantageous to treat the amplitude as separated into two components; SV and SH. And the discussion of vertical motion of the seismogram is simpler than that of the horizontal, because the former is contributed by the SV-component only, while the latter from both SV- and SH-components.

The stations equipped with vertical seismographs are five in number (Kamigamo, Abuyama scale out, Osaka, Hikone and Kameyama). It is favourable for the present analysis that they all are equipped with the vertical component of large or small Wiechert seismograph which has the same natural period of about 5 seconds. The observed values obtained at the respective stations are tabulated in Table 2. In Figs. 5 (a) and (b), in which the theoretical values are compared with the observed ones, the following tendencies were clearly recognized.

Table 2. The observed amplitudes of the earthquake of Dec. 21, 1954.

No.	Station	Epicentral distance	Amplitude			Seismograph
			Direct S	$S_{g-b}S$	S_MS	
1	Kamigamo	4.0 km	21,400μ	time markμ	6,800μ	large Wiechert
5	Ôsaka	47.5	690	990	960	small "
6	Hikone	51.5	670	1,420	2,090	" "
8	Kameyama	67.0	670	1,350	1,160	" "

1) The amplitude of direct S-wave is almost constant against the epicentral distance between about 40 km and 70 km.

2) The curves of the waves of $S_{g-b}S$ and S_MS, have their peaks respectively in the above-mentioned range of distance.

3) There is the range of distance at which the amplitude of S_MS is larger than that of $S_{g-b}S$ and both are larger than that of direct S-wave.

With regard to the emission mechanism at the focus, the angle θ of the waves

arriving at three stations concerned in this analysis are nearly equal and the effect due to the different azimuths does not seem to be large. And so the above-mentioned characteristics of the amplitude variation support our identification of reflected waves which are expected in this analysis.

Really, the phase of S_MS observed at Kamigamo is very remarkable as seen in Fig. 1, and this is interpreted to be due to two causes. First, as shown in Fig. 5, the direct SV-wave amplitude is reduced at a certain short epicentral distance (8 km in the present case) by the interference effect between incident and reflected waves at the earth's surface and consequently the phase of the reflected SV-wave is sharply

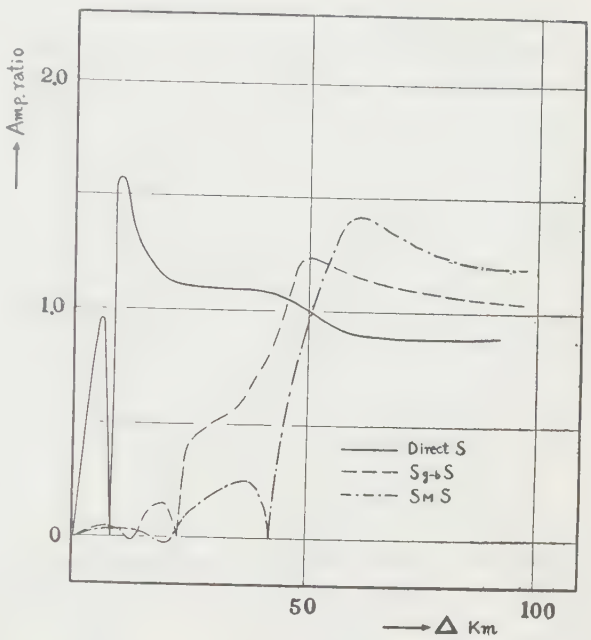

(a)

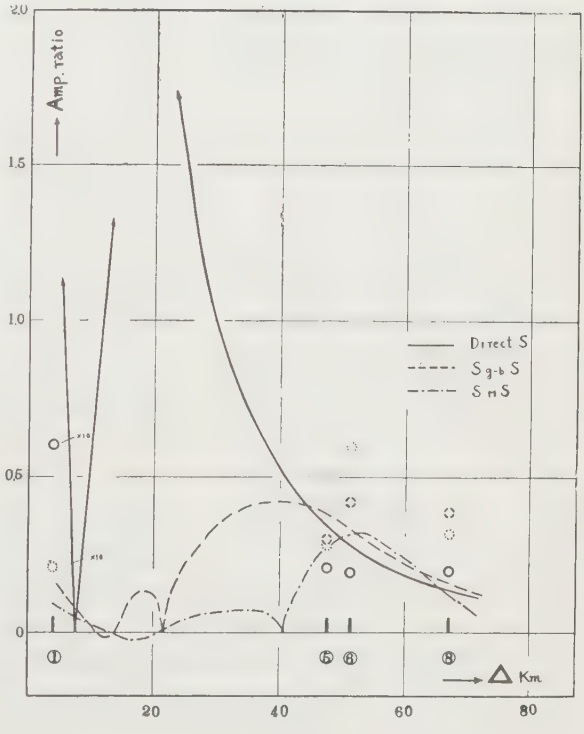

(b)

Fig. 5. The amplitude variation with the epicentral distance in the case of vertical component referring to SV.
(a) The curves are not corrected by the divergence factor $1/r^2$.
(b) The curves are corrected by the divergence factor $1/r^2$. Station numbers are tabulated in Table 2. O, ◌ and ◌ denote the observed amplitudes of direct S, $S_{g-b}S$ and S_MS waves respectively tabulated in Table 2.

and distinctly observed in contrast to that of direct SV-wave. Secondly, as shown in Fig. 4, the difference of arrival times between the direct and reflected waves becomes larger and larger as the observation station approaches the epicenter, and it naturally results in a good separation of respective phases at such short distance. These are considered to be a main reason for a remarkable appearance of S_MS wave in the vertical seismogram obtained at Kamigamo. The amplitudes of the direct and reflected waves at M- or g-b discontinuity surface observed at Kamigamo, however, are very large compared with those observed at the larger distances from the epicenter. This is explained to be owing to the effect of the divergence factor $1/r^2$ due to the spherical spreading of the waves, the hypocentral region being assumed to be a sphere of 1 km radius in the present case. The absorption effect is out of the question for this fact.

Next, in the case of the horizontal component, the problem of polarization must be considered in addition. Tentatively assuming that the transversal wave is emitted at the focus with the ratio 1 : 1 for SV : SH, the theoretical calculation has been carried out as shown in Fig. 6. The observed values are in fairly accord with the theoretical ones at the respective stations.

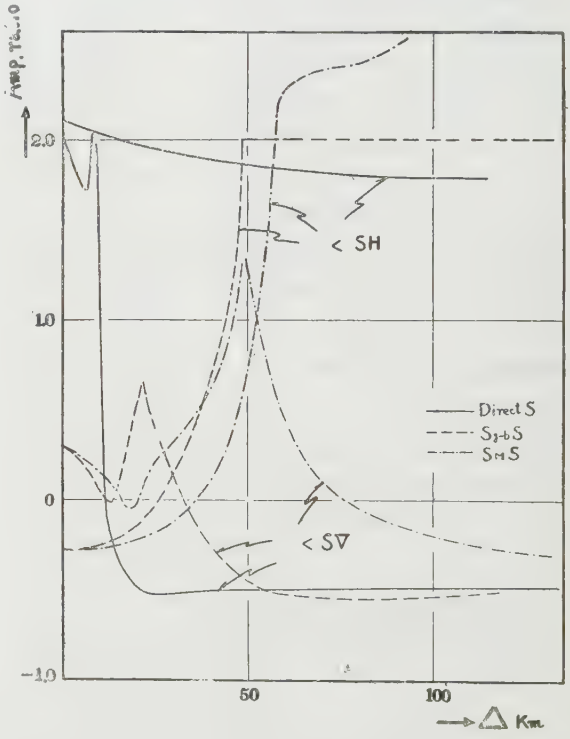

Fig. 6. The amplitude variation with epicentral distance in the case of horizontal component referring to SV and SH.
<SV and <SH are the amplitudes contributed by SV and SH respectively.

Discussing the merit and defect on the whole of the analysis method of S-wave reflected at the M-discontinuity for the investigation of crustal structure, the following will generally be concluded. As seen in Figs. 5(a) and (b), the amplitude of S_MS is certainly large at the critical distance of total reflection of 50～60 km in the present case, but as clearly understood in Fig. 4, the difference of arrival times of each phase is fairly small, being practically within the error of time measurement. The example in this case is seen in Fig. 2, being the seismograms recorded at Hikone. On the

contrary the separation of each phase is fairly good at the short epicentral distance and favourably the amplitude of S_MS at the epicentral distance of 20～30 km is fairly large especially in the horizontal seismogram. As shown in Fig. 6, the phase of reflected S-wave in the horizontal seismogram may become very prominent at a short epicentral distance in a certain case where the amplitude ratio of SH to SV is favourable, or in other words, the S-wave is polarized in the SV-type, and really such cases are frequently observed and they are of great service in the analysis of reflected waves. With regard to the case of very short distance (about 8 km in the present case), the amplitude of the direct S-wave in the vertical seismogram is exceedingly reduced as seen in Fig. 5 and consequently the reflected S-wave appears as a prominent phase which affords a sharp and accurate clue for the seismometric investigation of the crustal structure. This example is seen in the vertical seismogram obtained at Kamigamo.

Referring to the P-wave, the P-waves reflected at the crustal discontinuity are generally inconvenient for seismometric analysis, especially in the case of natural earthquakes. The reason for this is first that the amplitude of P-wave is usually quite small compared with that of the S-wave, and, secondly, that the P-wave reflected at any discontinuity surface is frequently confused with other phases such as the transformed and refracted waves which are usually observed during the arrival time of the direct P- and S-waves. But it should be mentioned that the reflection method for P-waves in the case of artificial explosion for the exploration of underground resources and the determination of geological structure is the superior one, as the confusion of phases above stated can for the most part be avoided by regulating the surface explosion.

Summarizing it may be considered that the analysis method of seismic S-waves reflected at the crustal discontinuity surface is quite serviceable for the seismometric investigation of the crustal structure when the seismograms obtained at the suitably short distance from the epicenter are available for earthquakes of shallow origin. In the following section some additional examples will be presented in support of the above arguments.

3. Other examples

In order to investigate the regional difference of the crustal structure, an analysis similar to that mentioned in § 2 was applied to the two following earthquakes.

Date	Epicenter
1955 Feb. 12, 10^h 47^m	Near the mouth of the river Kiso
„ Dec. 3, 23^h 28^m	Near the Kii Yuasa

The locations of stations and epicenters are shown in Fig. 3 and the data used

in the following analysis are tabulated in Tables 3 and 4 respectively. As in §2, on the basis of P~S time-distance curve, their epicenters and focal depths were determined. In these cases, the forerunner durations at some stations were available. The travel time-distance graphs are shown in Figs. 7 and 8. The focal depths are fixed for about 20 km in both cases. In the case of the Tôkai region, the P- and S-waves reflected at the M-discontinuity were found at several stations and in the

Table 3. The earthquake of Feb. 12, 1955.
Epicenter φ=35.1°N λ=136.8°E Focal depth=20 km

No.	Station	Epicentral distance	P~S time	Forerunner duration
10	Nagoya	22.5 km	3.8 sec.	— sec.
8	Kameyama	34.5	5.2	
11	Gifu	38.5	5.7	—
6	Hikone	53.0	7.4	—
1	Kamigamo	91.0	11.9	0.7
4	Nara	94.5	12.4	1.3
3	Abuyama	111.5	14.6	1.2
5	Ôsaka	120.5	15.4	1.6

Table 4. The earthquake of Dec. 3, 1955.
Epicenter φ=33.8°N λ=135.1°E Focal depth=15 km

No	Station	Epicentral distance	P~S time	Forerunner duration
12	Yuasa	11.5 km	3.2 sec.	— sec.
13	Shionomisaki	77.0	9.5	0.7
5	Ôsaka	87.0	11.5	1.2
14	Owase	95.5	11.8	1.3
3	Abuyama	108.5	13.9	1.1
1	Kamigamo	136.5	17.1	1.4

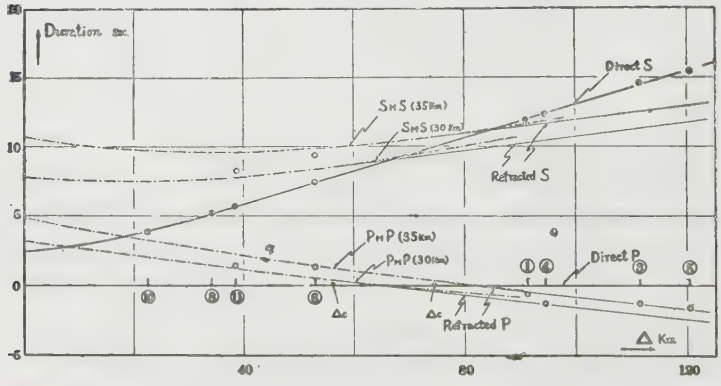

Fig. 7. Travel time-distance graph of the earthquake of Feb. 12, 1955 tabulated in Table 3.

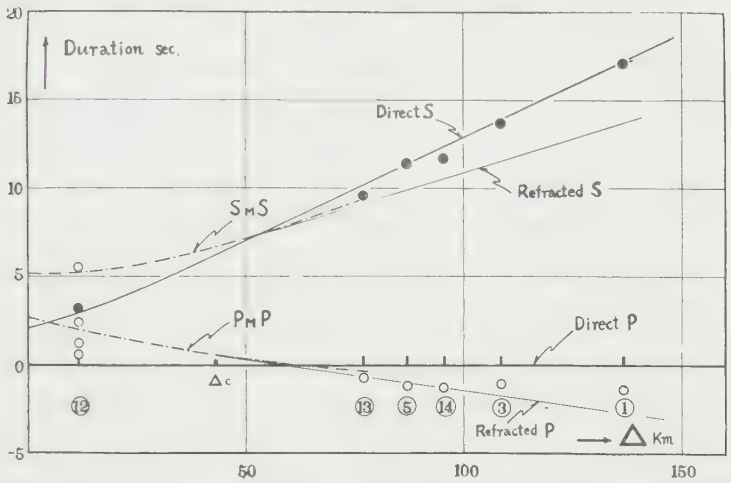

Fig. 8. Travel time-distance graph of the earthquake of Dec. 3, 1955 tabulated in Table 4.

case of the Kii region the point at which the reflected waves could be observed, was Yuasa only. The seismograms obtained are inserted in Figs. 9 and 10, one being those obtained at Gifu (Δ=38.5 km) and the other at Yuasa (Δ=11.5 km). From these, the depth of the M-discontinuity was roughly estimated to be in the range from 30 km to 35 km in the Tôkai region and less than 30 km in the Kii region. These results are in good agreement with those derived from the Bouguer anomalies of the gravimetric measurement (**22**) and the seismic refraction method (**12**).

It will be expected that a more detailed study of the crustal structure can be accomplished when the frequently occurring shallow earthquakes are selected and the thus analysed regions centering around their epicenters are successively overlapped by each other.

4. Further application

In the preceding section, the merit and applicability of the seismometric analysis method using the S-wave reflected at the discontinuity surface for the investigation of the earth's crust were discussed in some detail. In this section, the seismograms obtained at two places in our country are investigated where the crustal structure is considered to be largely different from that at other places as deduced from the results of gravity survey, etc. For this purpose, the local and shallow earthquakes observed at the Nagano Meteorological Observatory (φ -36° 40′N, λ-138° 12′E) and the Aso Volcanological Laboratory (φ=32° 53′N, λ=131° 00′E), were selected. Their seismograms are shown in Figs. 11 and 12. In the following the analytical method of S_MS-wave will be applied to those earthquakes, and the results of analysis are

Table 5. Some local earthquakes observed at the Nagano and Aso Observatories and the durations of $S_{g-b}S$ and S_MS.

Observation station	Date	Duration		
		P～S time	P～$S_{g-b}S$	P～S_MS
Nagano	1952 Sept. 5th 0h52m	3.4 sec.	7.5 sec.	13.0 sec.
〃	〃 Dec. 27 14 59	3.3	12.1	24.3
〃	1954 Feb. 15 14 44	4.5	7.2	12.1
Aso	1954 Aug. 11 12 43	2.6	5.8	7.3
〃	1956 Apr. 20 4 42	2.9	5.7	7.8

tabulated in Table 5. In these cases, the precise determination of the crustal structure are difficult, because the available seismogram is from one station only. But it can reasonably be estimated from the difference of interval of arrival times between the direct S-wave and the presumed S_MS-wave as seen in Table 5, that the depth of M-discontinuity under the area of Nagano is much larger than that of Aso. They are roughly calculated to be 45 km and 30 km for Nagano and Aso respectively. This sort of comparison of the depth of M-discontinuity between two distant areas can easily be put in practice using the suitable seismograms of local earthquakes of shallow origin at each area, and really many examples are now being analysed and the results will be reported in a near future.

5. Summary

Considering the present state of distribution of the seismological observation stations and their accuracy of observation, the investigation of the crustal structure by the analysis of seismic reflected wave may be generally considered to be less utilisable compared with that of refracted wave, especially in the case of natural earthquakes. But the seismic waves reflected at the discontinuity surface will profitably be applicable to the investigation of the crustal structure under such favourable conditions as earthquakes of shallow origin, observation at short epicentral distances, the analysis of S-type waves, etc. These conditions are remarkably advantageous for the analysis of the reflected wave, because the shallow focus does not make the undesirable transformed waves which greatly disturb the identification of phase of reflected wave, and moreover the shallowness of focus serves for the separation between the direct and reflected waves. And in particular the seismograms obtained at a suitably short distance from the epicenter, are usefully analysed because of the comparatively large amplitudes of reflected waves and the good separation between both waves as discussed in some detail in the main section. As practical examples three local earthquakes of shallow origin were selected. Studying their travel time-distance graphs and amplitude variation with distance, the waves reflected at the M-discontinuity were identified.

Applying these analyses to the Kyoto, Tôkai and Kii regions respectively, the regional character of the crustal structure were investigated. The results are in good agreement with ones derived by other methods. Moreover, it is especially remarkable that there exists such a very short distance as Kamigamo as seen in the case of § 2 at which the reflected waves are noticeably recognized. Some suitable examples of local earthquakes which were observed at the Nagano and Aso observatories respectively, were selected and it was verified that this method is useful for the investigation of the crustal structure.

In the middle distances, larger than those concerned in this paper, the refracted waves begin to appear and the reflected waves are concealed in much complexity. But, in such cases, the new phases derived from other sources are prevailingly observed. Some studies on these problems will be made in a forthcoming paper.

Acknowledgements

The writer wishes to express his hearty thanks to Prof. E. Nishimura for his kind guidance and encouragement throughout the present study. The writer is also deeply indebted to the directors and members of various meteorological observatories in Japan for their generous permission for copying seismograms recorded at their observatories. The cost of the present study was partly defrayed by a grant-in-aid for scientific research of the Ministry of Education.

REFERENCES

1. L. Don Leet, Travel times for New England, Bull. Seism. Soc. America, **28** (1938), 45–48.
2. B. Gutenberg, Travel times of principal P and S phases over small distances in Southern California, Bull. Seism. Soc. America, **34** (1944), 13–32.
3. ———————, Energy ratio of reflected and refracted seismic waves, Bull. Seism. Soc. America, **34** (1944), 85–102.
4. ———————, Reflected and minor phases in records of near-by earthquakes in Southern Galifornia, Bull. Seism. Soc. America, **34** (1944), 137–160.
5. ———————, Revised travel times in Southern California. Bull. Seism. Soc. America, **41** (1951), 143–163.
6. A. Kamitsuki and T. Mikumo, Investigation of the earth's crust in relation to local earthquakes, Bull. Disaster Prevention Res. Inst., **6** (1953), 39–47.
7. H. Reich, Über seismische Beobachtungen des PRAKLA von Reflexionen aus grossen Steinbruchsprengungen in Blaubeuren am 4 März und am 10 Mai, 1952, Geol. Jahrbuch, **68** (1953), 225–240.
8. H. E. Tatel, L. H. Adams, and M. A. Tuve, Studies of the earth's crust using waves from explosions, Proc. American philos. Soc., **97** (1953), 658–669.
9. M. A. Tuve, H. E. Tatel and P. J. Hart, Crustal structure from seismic explosion, Journ. Geophys. Res. **59** (1954), 415–422.
10. The Research Group for Explosion Seismology, The fifth explosion seismic observations carried out in the North-eastern Japan, Bull. Earthq. Res. Inst., **38** (1955), Part 4.
11. Y. Kishimoto, Seismometric investigation of the earth's interior, Part I, On the structure of the earth's upper layer, Mem. Coll. Science, Kyoto Univ., A **27** (1954), 125–143.

12. ————————, Ditto, Part II, On the structure of the earth's crust, Mem. Coll. Science, Kyoto Univ., A **27** (1955), 243–288.
13. J. B. MACELWANE, *Introduction to Theoretical Seismology* (New York, John Wiley and Sons, Inc. (1936)).
14. H. JEFFREYS, Reflexion and refraction of elastic waves, Mon. Not. Roy. Astr. Soc., Geophys. Suppl., **1** (1926), 321–334.
15. L. B. SLICHTER and V. G. GABRIEL, Studies in reflected seismic waves, Beitr. z. Geophys., **38** (1933), 228–256.
16. H. KAWASUMI and T. SUZUKI, Reflection and refraction of seismic waves at plane interface of the earth's surface crust, Zisin, **4** (1932), 277–307 (in Japanese).
17. T. MATUZAWA, An example of surface refletion of elastic plane waves, Zisin, **4** (1932), 7–12 (in Japanese).
18. C. S. CLAY and MCNEIL HALCYON, An amplitude study on a seismic model, Geophysics, **20** (1955), 766–773.
19. B. GUTENBERG, *Handbuch der Geophysik*, Bd. IV. Lief. 1 (1932), 255.
20. T. SUZUKI, On the angle of incidence of the initial motion observed at Hongô and Mitaka, Bull. Earthq. Res. Inst., **10** (1932), 517–530.
21. K. SEZAWA and K. KANAI, Reflection and refraction of seismic waves in a stratified body, Bull. Earthq. Res. Inst., **10** (1932), 806–816.
22. C. TSUBOI, Gravity survey along the lines of precise levels throughout Japan by means of a Worden gravimeter, Part IV, Bull. Earthq. Res. Inst., Suppl. Vol. IV, Part III (1954).

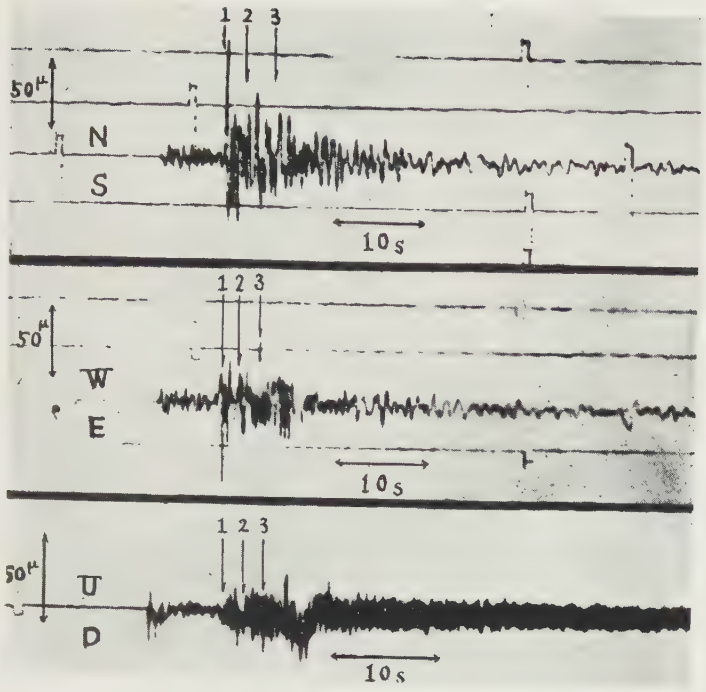

Fig. 2. The small Wiechert seismogram, Dec. 21, 1954, recorded at Hikone near the critical distance (Δ= 51.5 km).
(By the courtesy of the Hikone Meteorological Observatory)
1) direct S, 2) $S_{g-b}S$, 3) S_MS

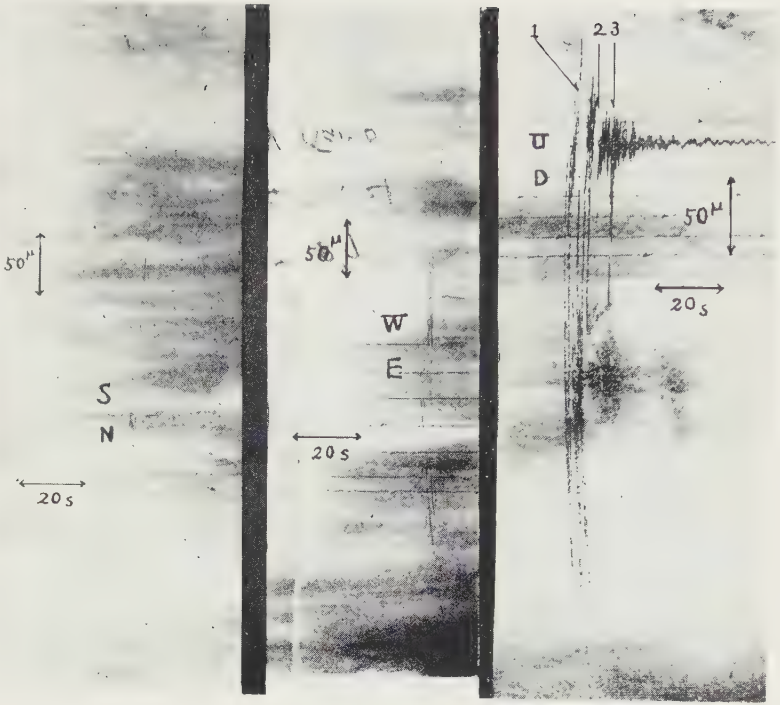

Fig. 1. The large Wiechert seismogram, Dec. 21, 1954, recorded at Kamigamo in the epicentral region (Δ=4 km).
1) direct S, 2) $S_{g-b}S$, 3) S_MS

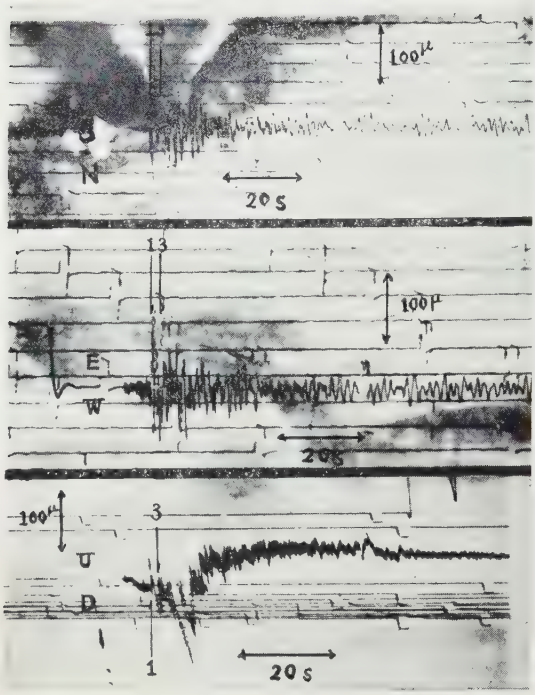

Fig. 9. The small Wiechert seismogram, Feb. 12, 1955, recorded at Gifu of the short epicentral distance (Δ=38.5 km). (By the courtesy of the Gifu Meteorological Observatory)
1) direct S, 3) S_MS

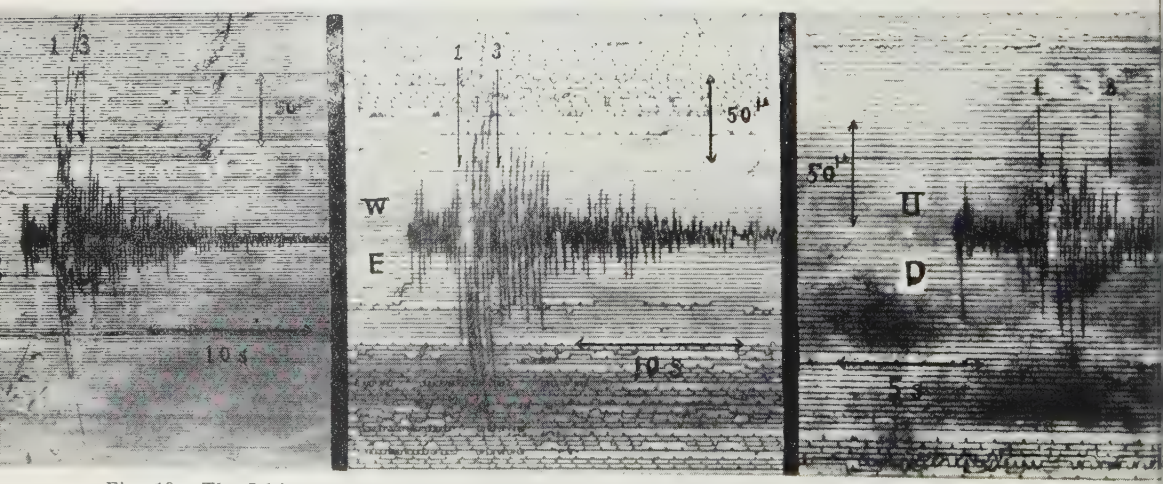

Fig. 10. The Ishimoto type-acceleration seismogram, Dec. 3, 1955, recorded at Yuasa of the short epicentral distance (Δ=11.5 km).
(By the courtesy of the Taikyu High School)
1) direct S, 3) S_MS

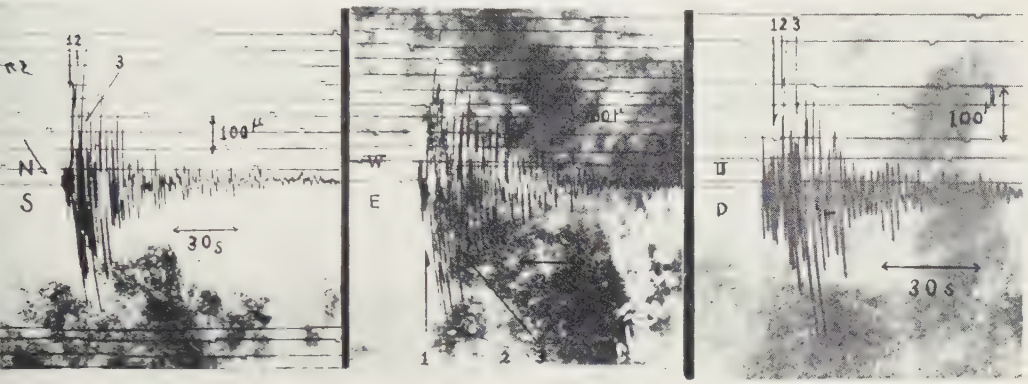

Fig. 11. The small Wiechert seismogram, Feb. 15, 1954, recorded at Nagano in the epicentral region ($\Delta < 10$ km).
(By the courtesy of the Nagano Meteorological Observatory)
1) direct S, 2) $S_{g-b}S$, 3) S_MS

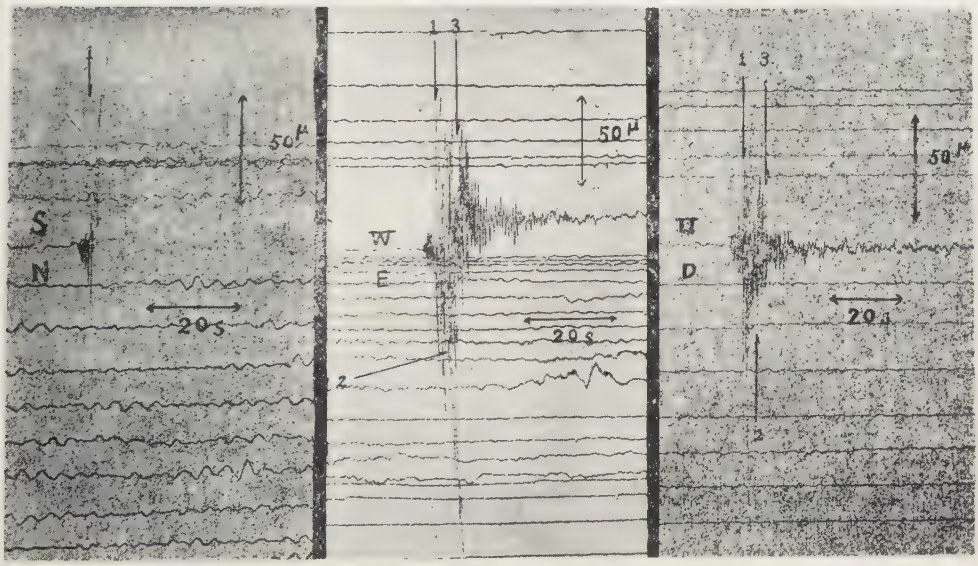

Fig. 12. The large Wiechert seismogram, Apr. 20, 1956, recorded at Aso in the epicentral region ($\Delta < 10$ km).
1) direct S, 2) $S_{g-b}S$, 3) S_MS

MEMOIRS OF THE COLLEGE OF SCIENCE, University of Kyoto, Series A,
Vol. XXVIII, No. 2, Article 4, 1956

PRECISE SEIMOMETRIC OBSERVATIONS IN THE EPICENTRAL REGION OF LOCAL SHOCKS

BY

Takeshi MIKUMO

(Received January 30, 1957)

ABSTRACT

The precise observations of local earthquakes were carried out in Wakayama District with many sets of high magnification seismometer, for the purpose of studying the crustal structure and the nature of local shocks.

The travel-time anomalies were detected on the time-distance curves when the focus was determined in either case, both from the arrival times and from the P–S times at each station. The anomalous travel-time curves were separable into two groups which seemed to be related with the recorded directions of initial motion of the local shocks at their respective stations. These anomalies may safely be regarded as being attributed to the nature of hypocentre and mechanism of earthquake occurrence.

With regard to the structure of the crust in the district concerned under the assumption of horizontal parallel layers, the velocities in the surface layer, second, and third layers were estimated to be 4.3, 5.4～5.6 and 6.0 km/sec for the P waves and 2.5, 3.2 and 3.4 km/sec for the S-waves, and the thickness of surface layer about 4 km, respectively.

1. Introduction

The seismometric study on minor earthquakes, as the local shocks and the aftershocks, has successively been made by many researchers in our country since the observation (**1**) of aftershocks accompanied by the Tango Earthquake in 1929. And a great many results of investigations were already published as regards the aftershocks following great earthquakes, for example, the Tango, Formosa, Niijima, Ogashima, Tottori, Tonankai, Mikawa, Nankai, Fukui and Imaichi Earthquake, and the earthquake-swarms in North-Idu and Wakayama Districts.

But, in spite of the gradual amelioration of observation methods with the considerable advance of instrumental functions: for example, for the seismograph, the recording apparatus and the time marking, most studies thus far made were prone to remain within the field of estimating the positions of hypocentre of these microearthquakes by the P–S duration times and discussing the time variation of seismic activities, the spatial distribution of foci, the frequency distribution of P–S times and of maximum amplitudes and so forth, as pointed out by S. Miyamura (**2**).

While in recent years, noticeable results have been obtained in new fields of research with improved accuracies of observation. For instance, S. Omote (**3**) tried to determine the focus from the measurement of arrival times at five different stations, in his observation of an aftershock of the Fukui Earthquake. He also compared the position of hypocentres respectively determined by these methods using the commencement times of the P- and S-waves and P-S times, and discussed the travel time curves. But the time accuracy of the above observation did not seem to be sufficiently high. In the case of aftershocks of the Fukui and Imaichi Earthquake, T. Asada and Z. Suzuki (**4**, **5**) estimated the apparent velocities of longitudinal waves by the tripartite station method and presumed that there was a simple crustal structure from the relations between their velocities and the P-S times. This method is excellent, but the actual velocity in the crust cannot be obtained favourably on account of the unknown focal depths. Omote (**6**) furthermore made a trial, in the Imaichi aftershocks, for determination of the underground structure by means of incident angles of the initial waves.

Of the same case, R. Ikegami (**7**) discovered two prominent phases between the P- and S-waves on the seismograms obtained with a displacement seismograph of low magnification, and estimated the depth of the discontinuity surface, considering these phases to be the seismic waves reflected from the bottom of a granitic layer. It is said, however, according to another report of Asada and Suzuki (**8**), that many phases could be picked out between the P-S interval in the observation of aftershocks at Fukui and Imaichi with sensitive seismometers, and no regularity in these distributions was recognized.

Omote (**3**, **6**) constructed a map of hypothetical distribution of 'push' and 'pull' fro mmany data taken from a few observation stations, under the assumption that all aftershocks at Fukui or Imaichi occurred at the same depth with the same mechanism. But the results of this study suggest the invalidity of the foregoing assumption.

The observations of minor earthquakes, of the same kind as stated above, have also been made at Witwatersrand District in South-Africa (**9**). H. J. Logie (**10**) determined the velocities of the P- and S-waves from many minor shocks under the assumption of uniform medium. Accurately observing a host of tremors which generated in Witwatersrand mine, P. G. Gane and others (**11**) compared the actual position of tremors with the hypocentre determined from the times of occurrence of shock at six stations, and discussed the relationship between the geological structure and tremor-occurrence in reference to the distribution of initial directions of surface movement. P. L. Willmore and others (**12**) successfully determined the structure of the crust in the district concerned, not only from the data of those stations but by many seismograms obtained in distant stations.

Presumption of local crustal structure merely from very near shocks of small magnitude seems to be much more difficult than from distant earthquakes, in spite of the various fore-mentioned attempts.

In recent years, however, artificial explosions were utilized for the investigation of the structure of crust, and explosion seismic experiments on a large scale were successfully executed several times in Japan (**13**). It cannot be denied that the artificial explosion method is more accurate in determining the underground structure than natural earthquakes on account of the previously known position and time of origin. However, in explosion the mechanism of fracture at the origin and the nature of seismic waves are regarded as being considerably different from the natural earthquake. In the sense stated above, the precise observation of minor earthquakes seems to be of great interest not only from the standpoint of the study of their nature, but, moreover, far the study of the nature of great earthquakes by extension of results obtained from these observation of minor ones. And in this case, the fact that a great many shocks will be observed in the very vicinity of epicenter in some suitably selected area is expected to offer an effective clue to the mechanism of earthquake occurrence, the nature of various seismic waves, and other problems, as well as indicating crustal structures.

It is well known that in Wakayama District local earthquake have frequently occurred since 1920 with a diversity to some extent in the location and frequency of their generation, although these shocks were of very slight magnitude, and their range which can be observed even with a sensitive seismograph was only a score of kilometres at most. Moreover, several destructive earthquakes, for example, the Nankaido Earthquake in 1946, occurred during this period, and these great earthquakes and the crustal deformation in the Kii-Peninsula may be considered to have some effects on the vicissitudes of local shocks in this region.

A. Imamura and others (**14**, **15**) had previously studied the earthquake-swarms in Wakayama District, but recently the Earthquake Research Institute of Tokyo University in co-operation with the Geophysical Institute of Kyoto University began more detailed studies on these shocks. A. Kamitsuki and myself, both of the Geophysical Institute, made preliminary observations with a seismometer of high magnification at Yura in Wakayama Prefecture twice in 1952 (**16**). From these observations the later phases which may be regarded as the seismic waves reflected from several discontinuity surfaces in the crust could be learned, but conclusive presumptions were avoided because the observations were made at only one station. The Earthquake Research Institute also made successive seismic observations in this region during every year since 1952 (**17**).

The present observations were executed with many seismographs of high magnification for the purpose of studying in detail the unsolved problems of minor local

earthquakes and the underground structure in Wakayama District from the precise observation of these shocks in their epicentral region.

In this paper the results obtained from the observations in 1954 and 1956 will be reported and discussed.

2. Seismometric Observation

(1) *Observation stations*

The present seismometric observations were carried out from Nov. 24th to Dec. 2nd in 1954 (**18**) and from April 10th to April 22nd in 1956.

Temporary observation stations were installed so as to be situated in the epicentral area at a limited region of 10 km in radius with Kainan City as its centre, where minor shocks frequently occur. For the geological structure of the area concerned, the ground rocks of the superficial layer consist of metamorphic rocks, being the crystalline shist and phyllite, belonging to the Sanbagawa system and the Mikabu series. This area covers the region which Imamura (**14**) had already observed. All of our station sites were selected within this region of metamorphic rocks, so that the superficial condition of ground rock on which the observation instruments were installed should be identical. The number of our stations were 4 in 1954 and 6 in 1956, and the three of these stations were fully equipped with three components of seismometers and the others with only vertical component. The united observations were carried out in close connection with the Earthquake Research Institute. The locations of all stations are shown in Tables 1 and 2 and Fig. 1. These co-ordinates were determined from triangulations and aerial photographs furnished by the Earthquake Research Institute (abbr. E. R. I.) and theirs errors are considered to be approximately 10 m. These

Table 1. Observation stations in Wakayama District

Station	Location		Elev.	Seismometer	Observers	Obs. Period
	λ	φ	h			
Wakanoura (W)	135°10′04″.4 E	34°11′23″.1 N	35 m	V1	Y. Okamoto	1956
Kimiidera (Km)	11′29″.6	10′44″.5	25	V1, H2	T. Mikumo, Y. Itô	1954
Idakiso (I)	15′14″.3	11′53″.4	35	V1	Y. Tanaka	1954 1956
Fuyuno (F)	12′59″.6	10′49″.8	40	V1	K. Hosoyama, Y. Itô	1956
Kainan (K)	13′31″.4	08′42″.0	50	V1, H2	T. Mikumo, Y. Yamamoto	1956
Nokami (N)	17′50″.0	09′46″.8	80	V1, H2 H1	M. Ōtsuka, K. Zako M. Ōtsuka	1954 1956
Yoro (Y)	09′40″.4	06′54″.0	15	V1	Y. Kishimoto A. Kamitsuki I. Nakagawa	1954 1956

Table 2. Co-ordinates of Observation Stations

Stations		X_i	Y_i
		km	km
Wakanoura	(W)	0	0
Fuyuno	(F)	1.04	4.45
Idakiso	(I)	−0.91	7.90
Nokami	(N)	2.99	11.76
Kainan	(K)	4.94	5.15
Yoro	(Y)	8.10	−0.69
Kimiidera	(Km)	1.27	2.20
Todoroki	(R_2)	3.19	12.88
Shimotsu	(R_3)	8.53	−4.04
Kanaya	(L_1)	15.58	8.79
Idakiso	(L_2)	−0.91	7.90
Kainan T.	(Kh)	4.55	3.72
Kotonoura	(Ko)	3.82	2.08
Taisei H. S.	(T)	3.44	12.87
Dejima	(D)	0.49	−0.33
Sanda	(S)	−0.80	3.62
Niitakamachi	(Ni)	−1.00	0.32
Kotonoura	(Ko′)	3.84	2.08
Kanan H. S.	(Ka)	4.34	5.72
Taisei H. S.	(T′)	3.41	12.87
Minoshima	(M)	11.67	−4.47
Yuasa	(Yu)	17.49	1.49

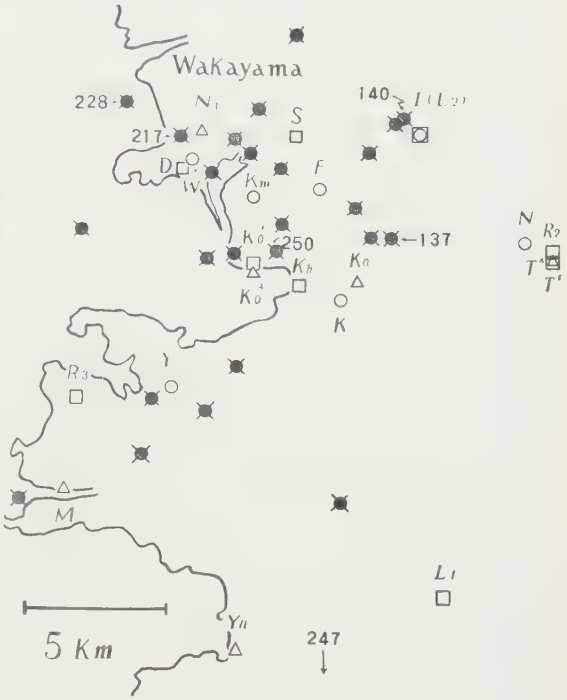

Fig. 1. Positions of the observation stations and the epicentres of the earthquakes mentioned.
□; observation stations of the E.R.I. with electromagnetic seismometers.
△; observation stations of the E.R.I. with acceleration seismographs.
○; observation stations of the Kyoto Univ. with electromagnetic seismometers.
✱; epicentres.

determined co-ordinates were used in our analysis by the courtesy of the E.R.I.. The origin point of the co-ordinate was selected at Wakanoura, taking the X-axis southwards and the Y-axis eastwards.

(2) *Instruments*

The instruments used in the present observations were the electromagnetic seismometers of the variable reluctance type with short period and high magnification, which were designed and constructed especially for the purpose of observing small earthquakes and artificial explosions. The detailed properties of these seismometers named R_2-type will be described in the last paragraph of this paper as an appendix.

Both the vertical and horizontal seismometers were used in the conditions of 0.45 sec in natural period and 1.79 volt/kine in voltage-sensitivity. Maximum magnification of these seismometers in direct connection with the galvanometer of 0.35 sec

in free period and 3.20×10^{-8} amp/mm in direct current sensitivity is approximately 80,000 at the optical distance of 1 metre.

The time marks, at all stations, were recorded on the oscillogram by interruption of a light beam with a relay-apparatus for receiving the time signals of JJY standard short wave (4 or 8 Mc) of every second kept by the Tokyo Astronomical Observatory. Reception conditions of the short wave were excellent during about 3/4 of the daytime. The rotation speed of the oscillogram winding around a recording cylinder was nearly 5.0 mm/sec. The time error accompanied with precise readings on seismograms is less than 1/20 sec.

Most stations of the E.R.I. carried out an observation with electromagnetic seismometers using a line carrier telerecording (**19**) or a radio telerecording (**20**), and a part of them with acceleration seismographs. The time signals were marked by chronometer (**21**) at all stations of the E.R.I., and paper speed was about 4 mm/sec. The time marks resulting from this chronometer system were compared with those resulting from JJY standard time at our stations, chiefly by the commencement times of initial shock recorded with two kinds of seismometer which were installed at Idakiso, and partly by a close examination several times each day.

(3) *Observed results*

Our observations were made during a day-light hours (08h00m–20h00m) only. It is by reason that there is no need for this study to observe the total number of shocks during a day. The number of earthquakes recorded at each station was from only two or three to ten or more. Those shocks observed at more than three of the four stations first established amounted to 56 in the primary observation, and those at more than five of six stations were 44 in the second observation. The maximum amplitude in the greater part of these shocks is estimated to be approximately $1/10\mu$.

The P–S duration times recorded, for the most part, are within the range from 0.5 to 4.0 sec. Constructing the frequency spectrum of the P–S times observed at each station, the highest frequency lies in the period of 0.5~1.0 sec at Kimiidera and Fuyuno, 0.5~1.5 at Wakanoura, 1.0~1.5 at Idakiso and Yoro, 1.0~2.0 at Kainan and 1.5~2.0 at Nokami, respectively. Therefore, the majority of shocks mentioned here are considered, as a result of this examination, to have occurred within a very short range from these stations.

With respect to the correlation between the maximum amplitudes and the number of shocks accompanying them, the Ishimoto-Iida's formula does not seem to hold always, evidencing a deviation especially in larger amplitudes, for a large percentage of these minor quakes recorded at each station, as pointed out also by Miyamura (**23**).

The especially well-recorded earthquakes which seem to have occurred inside or

near our observation network were selected from the shocks observed at more than five stations and used in the analysis. In the ensuing discussions the data obtained by the E.R.I. will synthetically be used with those of our own.

3. Anomalous Time-Distance Curves

In determining the hypocentres of the previously mentioned earthquakes, the crust in this region was assumed to be of a homogeneous medium as a first approximation. And since the difference in the elevation of these stations is less than 50 meters we may safely say that they are of the same elevation, as such a slight discrepancy, in comparison with the mutual distances between the respective stations, could hardly effect the final outcome.

First a trial was made to estimate the position of foci from the arrival times of the initial wave observed at each station, but the hypocentres, for the most part, could not analytically be determined by this means.

(1) *Determination of hypocentres by the P–S times and the time-distance curves*

The next trial of determining the hypocentre was made by a graphical method or the method of least squares from the P–S times clearly recorded at more than four stations, as was the general case in the observation of aftershocks. In the case of ours the P–S times recorded with seismographs of the same type were utillized for the most part, and the horizontal directions of initial motion at the stations with three components of seismometers were taken into account. When this method was adopted (**18**), the epicentre could be determined without much conflicting evidence and the errors in this determination are estimated to be less than several hundred metres. Omori's constants calculated are from 5 to 8.

When the arrival times of the P– and S–waves at each station are plotted against the hypocentral distance on a time-distance graph with regard to each 17 of the shocks whose focus was determined by the above method, the plotted points excessively diverged in a wide range. It is to be remarked that the hypocentral distance, instead of the epicental, was taken as abscissa for convenience sake in this case, because the focal depths calculated are comparable with the epicentral distances.

If the time-distance curve is provisionally represented as a mean straight line the gradient of this line, in other words the reciprocal of the propagation velocity of waves, has a great diversity in every shock, and as is the case even in several shocks which occurred at approximately the same depth in the same area. In these cases, the values of velocity of the P–waves are from 2 to 8 km/sec, and the maximum deviation of travel times at each station from the mean straight line reaches to 0.3 sec, being beyond the limit of observational errors. However, the time-distance

curves could successfully be represented as straight lines only in the two of 17 shocks and their velocities of the P-waves are 5.6, 5.0 km/sec, respectively.

For this reason it is undesirable to represent the time-distance curve for most of the shocks as a straight line. Considering, then, the travel-time curve to be a straight band line with a certain time range, or to consist of several minor groups of straight lines, from another point of view, it can naturally and favourably be divided into two systems of straight line, with respect to 15 of the shocks discussed here. The respective groups of the time-distance curve can plausibly be represented as straight lines approximately paralleling each other with the travel-time difference of about 1/4 sec, having small deviation of observed values at each station from either line. This fact can be found for the S-waves as well as for the P-waves. The velocity differences estimated from these two straight lines are within 0.1 km/sec, and the propagation velocities themselves obtained from the above 15 shocks are 4.3～5.3 km/sec for the P-waves and 2.3～2.8 km/sec for the S-waves, respectively. These values are not so diverse in every earthquake as in our previously findings and are considered to be reasonable ones for the velocities in the crustal upper layers.

Furthermore, even when the uncertainty of the positions of hypocentre due to measuring errors of the time at each station was taken into consideration, the general tendency that the time-distance curves are separable into two straight lines is not altered, even though the values of velocities and of time difference would be changed in small percentage.

Comparing the relation between the commencement times and the P-S times at two stations, the P-S time recorded at the first station, in some cases, was of longer duration in spite of the earlier commencement time than at the other. These conflicting cases are not always unreasonable, if consideration is permitted that the travel-time curves consist of two groups.

Then, the correlations between the travel times at the stations in each group of time-distance curves and the following items were next examined throughout all the 15 shocks, provided that the time-distance curve is tentatively divided into two groups:

i) the geographical locations in which the observation points are situated.
ii) the positions of epicentres; the focal distance.
iii) the directions from the epicentre.
iv) the directions of the initial movement recorded at each station.

Regarding points i) and ii), these correlations were not so distinctly recognized. That is, neither station nor group of stations in a fixed region have a tendency of always belonging to a fixed group of the travel-time curve, even in the case of similar positions of hypocentres. Moreover, the stations at shorter distance do not always belong to the group with shorter travel time.

Furthermore, the relation between the direction of initial movement recorded at each station and the travel-time curves was then investigated. In the earthquakes here studied, the distribution of 'push' and 'pull', or of an initial anaseismic and kataseismic movement on a map indicated that it is of the four quadrant type, if the nodal curves were assumed to be a pair of lines intersecting at the epicentre, and the recorded first amplitudes at various stations were taken into account. But these lines did not always intersect at right angle. The 'push' and 'pull' in the initial motion at any station, mereover, was not always the same throughout all shocks.

Returning to the subject, it seems in every shock that the arrival times at the respective stations in two groups of the time-distance curves are closely related to the recorded direction of the first movement at each observatory. Namely, the travel times at the stations in the initial anaseismic area have a tendency to belong to either group or the straight lines of either side on the time-distance graph, and the other group consists of travel times at the stations in the kataseismic region. In other words, these groups of travel time have a relation to the direction from the epicentre. The examples of time-distance graphs are shown in Figs. 2 and 3. At the stations near the nodal lines, however, some exceptional cases were found that undoubtly belong to the other group.

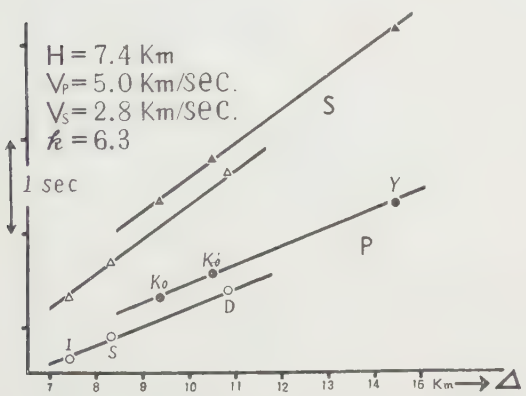

Fig. 2. Time-distance curves. (No. 140)
○ ; stations with the initial anaseismic motion.
● ; stations with the initial kataseismic motion.
△ ; hypocentral distance.

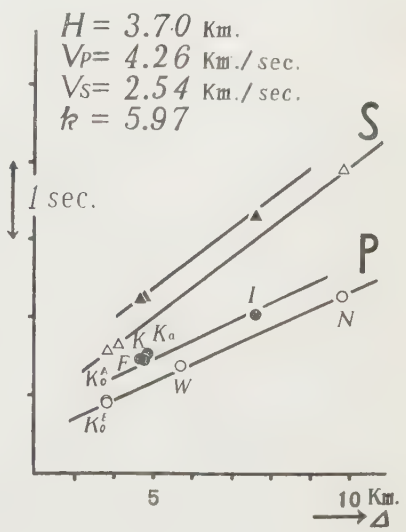

Fig. 3. Time-distance curves. (No. 250)

In two of 17 shocks, the time-distance curve could be represented as a straight line, as shown in Fig. 4, but the recorded directions of the initial movement are anaseismic at all stations.

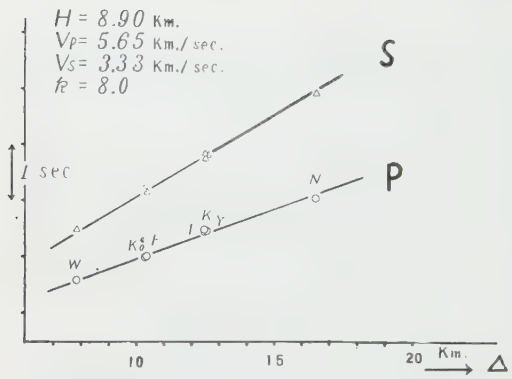

Fig. 4. Time-distance curves. (No. 228)

Taking these points into consideration the group of travel time curves may probably be defined by the initial direction at each station. Of the 15 shocks discussed above, the stations with the initial anaseismic motion belong to the group of shorter travel time and the initial kataseismic stations belong to that of the longer in some cases, and in other cases these relations were found to be reversed.

(2) *Determination of hypocentre from the arrival times and the time-distance curves*

In determination of a hypocentre from the arrival times at each station, the solution of the simultaneous linear equations of four dimensions, or the graphical method was used in the case of five observation stations, and a least square method in the case of more than five stations. When the arrival times were made use of, the focus, for most of the shocks, could not be determined with some exceptions, as already mentioned. That is, their focal depths resulted in imaginary values or the velocities were calculated as unreasonable values. Miyamura also indicates the same findings (**22**, **23**).

Hence, the problem in which case it is possible or not to determine focus from the arrival times, were investigated in every earthquake, with reference to analysis by means of the P–S times. The following results were obtained.

a) When the directions of first mevement recorded at all stations are the same, in other words, only in the anaseismic or kataseismic sense, the focus could be determined with good accuracy, and the time-distance curves could be represented as straight lines with small probable errors. And the reasonable velocities were obtained for the P– and S–waves in this case. Fig. 5 shows an example of the time-distance curves in these 6 cases. Seismograms of the presently mentioned shock recorded at six stations are shown in Fig. 11.

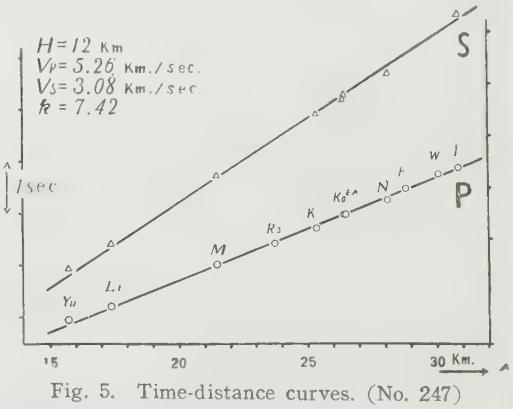

Fig. 5. Time-distance curves. (No. 247)

b) When both the anaseismic and kataseismic first movements were recorded at various stations, the hypocentre was correctly determined if only the arrival times of the P-waves at the stations with the same initial direction were used in calculation. On a time-distance graph, the travel times at these stations successfully lie on a straight line. But the travel times at other stations with the another initial direction, which were out of this calculation, deviate from the above line, and the straight line suitably connecting these plotted points, if possible, approximately parallels the former with a time difference of 0.2~0.4 sec. The reasonable velocities were also obtained. These two examples are shown in Figs. 6 and 7.

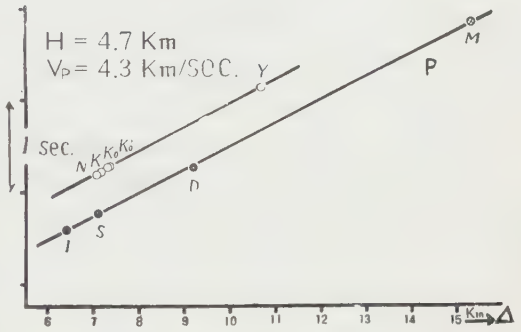

Fig. 6. Time-distance curves. (No. 137)

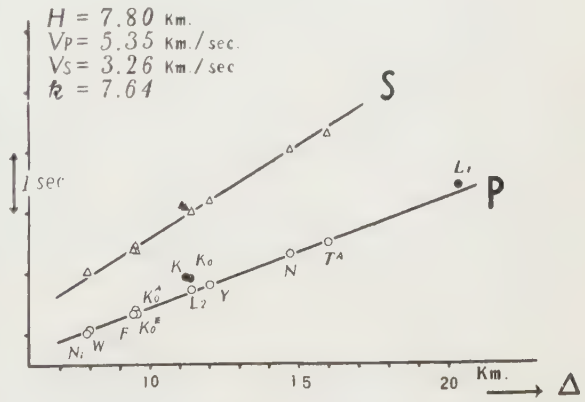

Fig. 7. Time-distance cuaves. (No. 217)

In the present observations, however, there was no earthquake which could be observed at respective more than five stations; both with the initial ana seismic and with kataseismic directions, and so the foci respectively determined from two combinations of the stations with the same direction could not be compared with each other.

c) Again the commencement times at all stations were used in calculation by a least square method without reference to the respective initial directions. If the stations with either initial direction is considerably more than those with another direction, the focus was determinable in a few cases, but the values of velocities became unreasonable or the probable errors in the travel-time curves were found to be very large. When the numbers, both for the former and the latter stations are nearly equal, the hypocentre could not generally be determined.

It was in 6 earthquakes by means of method a) and in 7 shocks by method b) that the focus could be determined from the arrival times of the initial wave. Also, in these methods, as well as the results of the P-S times, the travel time curves are

separable into two groups, or parallel straight lines, relating to the direction of initial movement. But such a fact for the S-waves seems not so clear as in the case of using the P-S times. There were two instances, also, where the earthquakes' focus was determined by these methods. That is, the stations with the initial anaseismic movement belonging to the group of the shorter travel time in one case and the initial kataseismic stations belong to that group in the other.

With regard to the presently discussed methods, Miyamura pointed out the following exceptional cases. Namely, he says in his private communication that the hypocentre of a few earthquakes was not determined by the analysis of arrival times at a certain set of five stations with the same initial direction, but this problem should be solved by a further observations.

(3) *Synthesized results*

As described in detail in this paragraph, the time-distance curve has an indication both for the P- and for the S-waves that the travel times are separated into two groups in connection with the direction of initial motion of shocks at each station, when the arrival times as well as the P-S times were made use of in determination of the focus. In other words, the travel times and the 'push' and 'pull' of first motion at the respective stations may be considered to be related each other.

Table 3. List of number of shocks in reference with the direction of initial motion and group of travel time at each station.

	U	D	T
1	8	4	12
2	5	1	6
N.G.	5	0	5
T	18	5	23

W

	U	D	T
1	3	2	5
2	3	2	5
N.G.	4	0	4
T	10	4	14

F

	U	D	T
1	1	2	3
2	3	4	7
N.G.	4	0	4
T	8	6	14

K

	U	D	T
1	7	3	10
2	6	5	11
N.G.	6	0	6
T	19	8	27

I

	U	D	T
1	4	6	10
2	4	5	9
N.G.	6	0	6
T	14	11	25

N

	U	D	T
1	8	3	11
2	3	1	4
N.G.	5	0	5
T	16	4	20

Y

	U	D	T
1	4	3	7
2	5	8	13
N.G.	6	0	6
T	15	11	26

Ko

U; Up, D; Down, T; total number of shocks, 1; first group of travel time, 2; second group of travel time, N.G.; no group in travel time.

Table 4. Analyzed results.

Shock No.	X (km)	Y (km)	Z (km)	Anal. Method.	Vp (km/sec.)	Vs (km/sec.)	Vp/Vs	k	Time-Distance Curves	δT
121	12.17	5.20	11.20	P S	4.83	2.58	1.87	5.54	(1) Y, N(D) ; (2) Km, D, I(U)	0.20 sec.
122	0.47	3.15	3.70	P S	4.36	2.40	1.82	5.34	(1) Ko, Ko′, Y*, N(D) ; (2) Km, I(U)	0.20
123	2.77	6.20	3.30	P S	4.25	2.43	1.75	5.68	(1) I, Km*, Y(U) ; (2) Ko, N(D)	0.35
124	−0.28	6.20	4.40	P S	5.04	2.52	2.00	4.78	(1) Y(U) ; (2) I, Ko, N(D)	0.25
135	3.57	0.60	4.60	P-S	4.64	2.47	1.87	5.30	(1) D, Y, S(U) ; (2) Ko, I, N(D)	0.20
136	7.37	1.50	4.70	P-S	4.62	2.54	1.82	5.65	(1) Y, D*, I(U) ; (2) Ko, Km, N(D)	0.25
137	2.77	6.95	4.75	P	4.40				(1) I, S, D, M*(D) ; (2) Km, N, Ko, Ko′, Y(U)	0.45
140	−1.23	7.35	7.40	P S	5.07	2.81	1.81	6.31	(1) I, S, D*(U) ; (2) Ko, Ko′, Y(D)	0.25
151	1.72	5.40	5.80	P S	4.73	2.70	1.85	5.88	(1) Km, I, S, D(U) ; (2) Ko, N, Y*(D)	0.20
201	25.65	5.67	10.30	P	5.11	2.92	1.75	6.84	(1) L_1, Y, R_3, K, Kh, Ko, N, I(U)	—
202	2.45	−3.85	6.20	P	5.10	(3.38)			(1) F, K*, I, N*(U) ; (2) Ni, Ko, Ko′, R*$_2$, Kh, L_1, (D)	0.20
206	11.97	−5.98	9.25	P	5.43	3.13	1.74	7.35	(1) M, R_3, Y, Ko, Ko′, Kh, K, W, Ka, L_1, L_2, T′(D) ; (2) Yu(U)	0.15
207	2.30	3.05	3.60	P-S	4.31	2.67	1.62	(7.01)	(1) Y, N (D) ; (2) Ko, Ko′, K, W, I(U)	0.40
217	−0.98	−0.36	7.90	P	5.35	(3.56)	(1.58)	7.64	(1) Ni, W, F, Ko, Ko′, L_2, Y, N, T′(U) ; (2) K, Ka, L_1(D)	0.20
220	−1.20	7.25	5.10	P	4.66	2.85	1.64	7.35	(1) W(D) ; (2) I, F, N, K, Ko′, L_1(U)	0.35
222	8.35	−1.25	4.40	P	4.72	2.96	1.60	5.94	(1) Y, Ko, K, W, F*, I, N(U)	—
223	3.35	1.59	5.15	P S	4.72	2.72	1.73	6.41	(1) Ko, W, Y, I, N(U) ; (2) F(D)	0.20
224	−0.70	0.65	8.90	P-S	5.38	2.91	1.85	6.35	(1) F, Ko (D) ; (2) W, I, N(U)	0.25
228	−2.05	−2.30	7.25	P	5.65	3.54	1.60	—	(1) W, Ko, F, I, Y, K, N(U)	—
230	0.45	0.65	8.40	P	5.65	(2.60)	—	—	(1) F, I(D) ; (2) W, Ko, K, N, Y, (U)	0.20
236	10.50	−1.75	6.30	P	4.83	2.93	1.65	7.45	(1) L_1, N, R_2 (D) ; (2) Y, Ko, Ko′, K*, Ka, W, F, I(U)	0.25
247	27.30	4.15	12.00	P	5.26	3.08	1.71	7.42	(1) Yu, L_1, M, R_3, K, Ko, Ko′, N, F, W, I(U)	-
248	−0.17	2.00	4.55	P S	4.93	2.66	1.87	5.63	(1) W, Y(U) ; (2) F, Ko, K, I(D)	0.40
249	−1.87	2.30	8.80	P-S	5.33	3.20	1.68	(8.00)	(1) W, F, Ko, N(U) ; (2) I(D)	0.20
250	3.20	2.80	3.70	P S	4.26	2.54	1.73	5.97	(1) Ko, Ko′, W, N, R_2*, (U) ; (2) F*, K, Ka, I(D)	0.30
251	8.96	0.46	5.30	P	4.86	(3.23)	—	—	(1) Ko, Ko′, F, W, I, N(U)	—
253	−4.10	3.60	6.60	P-S	5.00	2.88	1.80	6.78	(1) I, W, Ko, Ko′, K, N, R_2, Y(U)	—

X, Y ; location of epicentre, Z ; focal depth, Analytical method : P-S ; using the P-S times, P ; using the arrival times of the P waves, Vp ; velocity of the longitudinal waves, Vs ; velocity of the transversal waves, k ; Omori-constant, (1), (2) ;groups of travel time, U ; initial 'Upward'-motion, D ; initial 'Downward'-motion. δT ; difference of the travel times between two groups. The shoulder mark * indicates that the direction of inital motion at the station recorded the opposite one or it was not clearly recorded.

The observed data (the arrival times of the P and S waves and the recorded directions of initial motion) at the stations of the E.R.I. : R_2, R_3, L_1, L_2, Kh, Ko, Ko′, T, T′, Ni, Ka, M and Yu, were used in the present analysis by the courtesy of the Institute.

In several shocks the positions of hypocentre determined from the above two methods were compared, but the discrepancy between the two positions seems to be within the range of the observational errors.

Putting together all of 27 shocks analysed here, the time-distance curve could be represented as a straight line in 6 shocks and could be separated into two groups in 21 shocks. In the former cases the initial direction at the respective stations are all identical, and in the latter the stations with the initial anaseismic direction belong to the group of the shorter travel time, and the initial kataseismic stations form that of the longer one in 12 shocks, and contradictory cases to these are found in 9 shocks. The travel time difference is in the range from 0.2 to 0.4 sec.

The directions of initial movement and the group in travel times in the main observation stations are shown for every shock in Table 3. The initial motion recorded at any station were not always of the same kind and the travel times did not always belong to the same group.

The location of epicentre, focal depth, velocities of the P- and S-waves, Omori's constant, the travel-time difference in the two groups and the abbreviations of observation stations constructing the time-distance curves, in every shock, are listed on Table 4.

4. Crustal Structure in Wakayama District

The analysis was thus made assuming that the crust as a first approximation was of a uniform medium. The problem whether this assumption may be used as a first

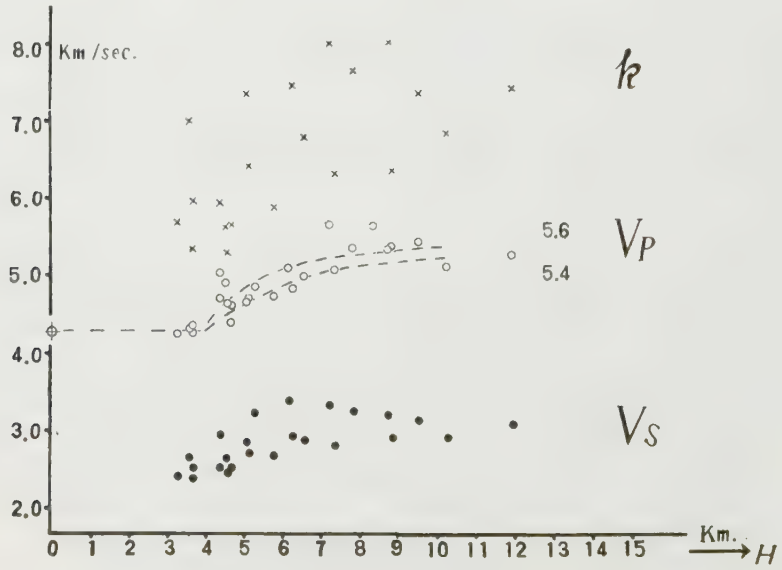

Fig. 8. Velocity-focal depth graph.

approximation or not is certainly an essential one. And next, in this section, a simple model of horizontally layered structure will be treated as a second approximation.

The trials for determining the fine regional structure from the aftershocks or local shocks have been made by various methods, as stated in the first paragraph. In the present study the following method was tentatively adopted, making use of a great number of minor shocks which occurred within a considerably limited region.

The velocity–focal depth graph in many shocks obtained from calculations under the uniform medium assumption is shown in Fig. 8, where the velocities in this case are the calculated ones from either method of the P–S times or the arrival times. In the ensuing discussions the validity of the values of velocity obtained by the above method will be premised.

(1) *Surface layer*

As easily seen in Fig. 8, a clear relationship between the velocities and focal depths seems to be shown by the P–waves, but the relationship of this kind is not so clear for the S–waves and the values of k. It is perhaps disturbed by the observational errors in the case of the S–waves.

The velocity of the P–waves tend to increase with increasing focal depth. According to the results obtained, on the other hand, in the seismic prospecting carried out by A. Kubotera and T. Yoshizawa (**24**) at Shimotsu in the area concerned, the velocity of the longitudinal waves in the upper surface layer of a metamorphic rock, named serpentine, was estimated to be 4.27 km/sec, as plotted at zero-depth in Fig. 8. Of the shocks, moreover, whose focal depth were less than 4 km, the calculated velocity for the P–wave is approximately 4.3 km/sec, and therefore, the surface layer consisting of the metamorphic rock with the longitudinal velocity of 4.3 km/sec is estimated to have a layer thickness of 4 km. The mean velocity of the S–waves in this layer is estimated to be about 2.5 km/sec. In addition, the velocity of the elastic waves from the quarry blasts at Kotonoura was measured by the E.R.I., but the observed value seems to be too large for the velocity in the superficial layer.

(2) *Second layer*

The structure of the horizontal parallel layers will then be assumed to be a second approximation, considering that the velocity of the P–waves in the case of uniform medium tend to gradually increase with increasing focal depth of more than 4 km. However, the focal depths in that case are not, of course, regarded as the actual depths because of the existence of a surface layer with a lower velocity. Secondly, the trial for determination of the longitudinal velocity in the second layer was made so as to be adapted to the distribution of the uniformly assumed velocities against the depths, on the grounds of previous knowledge about the thickness and velocity in the

surface layer. In the present method, the travel times to the respective observation stations from the hypothetical foci which were assumed to be at various depths in the second layer were calculated, taking the velocity in that layer as a parameter. Regarding, then, these travel times as the arrival times at the respective stations, the theoretical relation between the velocities and focal depths was learned from their respectively calculated values under the postulation of a homogeneous medium. Needless to say, this relation is variable with the geographical distribution of the observation stations used in these analyses, but ought not to change in its general appearance. The relations indicated by two broken curves in Fig. 8 were derived from the calculation with the uniform medium-assumption by means of the hypothetical arrival times at five stations, namely, W, F, K, Y and N (abbreviated), when the velocity of the P-waves in the second layer was assumed to be 5.4 and 5.6 km/sec, respectively. These curves show fairly good agreement with the actual distribution of the observed values, and therefore the velocity of the P-waves in the second layer was estimated to be in the range from 5.4 to 5.6 km/sec. The suitable velocity of the S-waves was estimated to be 3.2 km/sec, provided that the Poisson's ratio is 0.25.

In order to estimate the thickness of the second layer we tried to make use of the seismic waves which were emitted from a shock in this layer and reflected at the bottom of the layer mentioned. That is, several prominent phases were chosen from the seismograms recorded at the respective stations, and the duration times between the initial P-wave and the later phases concerned were plotted against the epicentral distance. While the theoretical curves indicating this relation were calculated and drawn on this graph with the variously assumed thickness of the second layer. The later phases seeming to be reflected waves were detected in a few examples. Some phases may probably be regarded as the transformed waves PS or SP, and from the duration times of these waves the already ascertained thickness of surface layer is reliable.

(3) *Third layer*

During the present observation of local shocks, a distant earthquake of small magnitude which occurred in the vicinity of Kyoto was recorded by chance at five temporary stations of ours in Wakayama District. The location and focal depth of hypocentre in this earthquake was roughly estimated to be about 135°32′.5 E, 35°01′.5 N and 11 km from the P-S times and the horizontal directions of initial motion recorded at the Kamigamo and Abuyama Seismological Observatory of the Kyoto University and the Kyoto Meteorological Observatory. On constructing the time-distance curves merely from the above five stations, the mutual differences of their epicentral distances and the directions from the epicentre become the subject of discussion, and the absolute values of epicentral distances are only supplementarily

treated. Even if the epicentre was not so accurately determined in this case, the effects on the travel-time curves are considered to be very slight, because the distance from Kyoto is much larger than the mutual differences. Actually in this case, the recorded directions of first motion were 'push' at all stations. The time-distance curves could be represented as a straight line with a good accuracy for the P- and S-waves as shown in Fig. 9. The apparent velocities of the longitudinal and transversal waves are 6.00 and 3.40 km/sec, respectively. A example of seismograms of the earthquake is shown in Fig. 12.

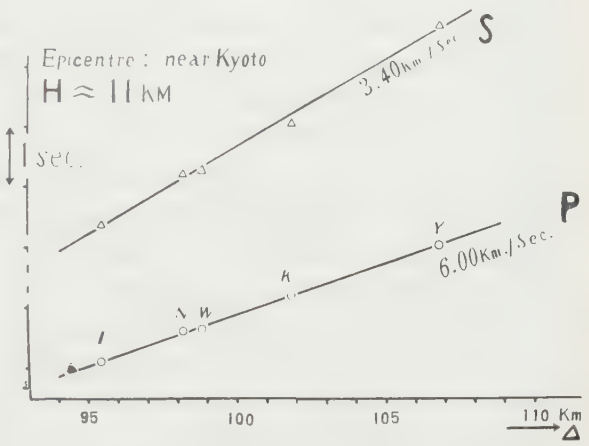

Fig. 9. Time-distance curves. (No. 240)
△ ; epicentral distance.

The tripartite station method for estimating the apparent velocity and the propagating direction of waves by the arrival times at three stations in a small area was thus far adopted in some observations of aftershocks, but the method here used may be regarded as an extension of the prior one.

If the thickness of the second layer was now assumed to be about 6 km, being equivalent to that of the granitic layer in a model of the horizontal structure in Kinki District as derived by Y. Kishimoto (**25**), the depth of the bottom of the second layer is found to be 10 km, which is nearly equal to the focal depth in this case. As the epicentral distances are about 100 km, the initial waves observed at the above five stations are presumed to be the longitudinal waves which horizontally propagated in the main along and just under the interface between the second and third layers. Hence, it may safely be considered that the apparent velocities observed should represent the actual ones in the third layer.

	P	S
4 km	4.3	2.5
(6 km)	5.4 ~5.6	(3.2)
	(6.0)	(3.4)

Fig. 10. Horizontal structure in Wakayama District.

The estimated velocities and thickness in the respective layers are as shown in Fig. 10, when the horizontal parallel structure of the crust was assumed in Wakayama District.

5. Discussions

In the present observations the unanticipated results stated above were obtained.

The various problems in the analysis will be mentioned and discussed under this heading, and in addition, some presumable interpretations for these results tentatively will be given.

1) *Accuracy of time*

The cause of diversity of travel times in the seismometric observations hitherto made was attributed, for the most part, to the unsatisfactory time-keepings, and really the time accuracy in the past observations is considered to be inadequately low for observation of minor earthquakes.

From this point of view, the common times from the JJY standard waves were marked every second on seismograms at our six stations by means of the same type of time-marker in the present observations. The rotation of a recording drum was actuated by a synchronus motor and the irregularity of rotation owing to a voltage fluctuation is less than 0.2 mm/sec. At the stations of the E.R.I. the common times transmitted from one chronometer were placed on seismograms, and two systems of the time mark were checked by a close examination, as stated in the second paragraph. The time errors accompanied by a precise reading of seismograms by a comparator are considered to be less than 1/50 sec in especially good records and within 1/20 sec in poorer ones, judging from the clearness of the initial P– and S–waves in most of the shocks analysed here. Therefore, the large deviations in the travel times as stated in the third paragraph are not regarded as resulting from time errors because of the high accurary in the present observations.

2) *Discrimination of initial wave*

In the present observations, the stations with a low ground noise-level were selected, but it seems undesirable to consider that there are no mis-discrimination of the initial wave, when it is of smaller amplitude than that of the second movements. Namely, the question may arise whether the separation of the time-distance curves into two groups is due to a mis-discrimination of the initial wave in 1/2 cycle or one cycle, on account of their small amplitudes recorded at the respective stations belonging to the group with apparently longer travel time. As the wave frequency in the initial part of seismic motions is more than 5 cycles, the time error resulted from a mis-discrimination of 1/2 cycle is less than 0.1 sec being insufficient to the travel time difference from 0.2 to 0.4 sec between two groups. And seeing also that the distribution of the 'push' and 'pull' in the initial movements shows that of four quadrant type, a possibility of mis-discrimination of 1/2 cycle is difficult to be anticipated. The following facts, moreover, may be regarded as the counter-evidences to the above questions. That is, in the group of the longer travel time many stations with the clearly recorded initial wave of large amplitude are included. And the time-

distance curve could reasonably be represented as a straight line in the case of only the stations with a same initial direction, and otherwise it was in many shocks separable into two groups.

3) *Accuracy in determination of the hypocentres*

On an estimation for the errors of the focal position due to the observational time errors, some studies have been made. N. Nasu (**1**) investigated them using the P S times at four stations in the observation of aftershocks of the Tango Earthquake. Y. Miyayama (**26**) examined these results in detail and stated that the inevitable errors in determination of a hypocentre is about 1 km. But it is possible to become larger when the P–S times at more than four stations are used in combination by a graphical method. The accuracy of hypocentre's determination in artificial explosions was investigated by S. Asano (**27**), when a least square method from the arrival times of initial wave at many stations were used in the analysis. When the calculated focus was compared with the actual position of a shot point, the epicentre could be determined with small discrepancy from the latter of about one fiftieth of a span of observation network, and with the probable errors of the same order. And it is stated that the accuracy of the velocity was considerably good, but the origin time and focal depth were not determinable with such a good accuracy as was possible in locating the epicentre.

The theoretical estimate of the probable errors in determination of focus is very troublesome, because it is concomitant to the geographical distribution of stations, the arrival times and their probable reading errors at the respective stations, and differs in every shock.

At any rate, the uncertainties from the time errors in the present observations are presumed to be less than several hundred metres in the positions of epicentre and 1 km or so in the focal depths by either method of the P–S times or of the arrival times under the uniform medium assumption. However, the general appearance on time-distance curves is not changed within those ranges.

4) *Effect of crustal structure*

In this section the amount of error in the focal position and the degree of effect on the travel-time curves will be investigated, when the analysis is made referring to a horizontally layered structure instead of a homogeneous medium. Namely, for such a purpose, it is needed to compare the respective positions of focus determined from the arrival times at each station assuming the structure of horizontal parallel layers, and of the uniform medium, and examining the incidence of travel-time curves in both cases. But calculation in the former case is difficult, and so the following method was used. The already-presumed horizontal structure was here made use of

as an example. Now the hypothetical focus was assumed to be in the second layer, and the travel times of the P-waves from it to each station were calculated. The discrepancy between the position of hypocentre which was calculated from these travel times and the previously assumed one was 1 km at most. The appearance of time-distance curves are not greatly influenced by the errors of the above order as to the position of focus.

Applying the analysis of this kind to the actual earthquake No. 217 or 250, when only the stations with the same direction of initial motion were used in calculation, and or when all stations were used, the focus was well determined, indicating a slight discrepancy of a few hundred metres from the hypothetical one. In both cases, the derived time distance curves can be represented as a straight line with only small probable errors being less than 5/100 sec.

Such large diviations in the travel time that the time-distance curves were separable into two groups cannot be explained from the effects of such a simple model of the horizontal structure. If we interpret this fact merely from the effects of crustal structure, the more complicated structures, as the dipped discontinuity surfaces, many discontinuities in the lateral directions or fault planes need consideration. Even in these cases, a similar systematic deviation on the travel times is expected to be shown for the shocks in similar positions, when the time-distance graphs are constructed under the uniform medium supposition. But no regularity as above described was recognized, and the travel times at any station did not always belong to a fixed group.

From the various reasons already stated, it may safely be said that the cause of large anomalies in travel times is attributable to the effects of focal conditions, such as the mechanism of earthquake occurrence, or the form of the hypocentral region.

5) *On the origin of local shocks*

Logically, it is not until the underground structure can be determined in detail that the problems of the mechanism of earthquake occurrence should be investigated. In the natural earthquakes, in comparison with the artificial explosion, the condition of the hypocentre will, to some extent, influennce the travel times, as well as the properties of the medium of wave propagation. In this sense, the determination of the more detailed structure of crust by means of the artificial explosion is desirable in the district concerned in future. In the present case, however, it is unreasonable, as already discussed, to attribute the travel-time anomalies observed in local shocks in this area to the effect of crustal structure. Consequently, some simple interpretations for the mechanism or condition of earthquake occurrence will tentatively be given.

In the analysis already made, the seismic focus was provisionally regarded as a point source, but, in reality, the hypocentre is considered to have a certain extent named focal region.

On this dimension, Y. Inouye (**28**) considered in relation to his theoretical study on the origin of the earthquake that its diameter is of comparable order to the emitted wave length, if the focal region is assumed to be a sphere. Furthermore, K. E. Bullen (**29**) investigated theoretically the relation between the linear dimension and the times of the first P and S half-oscillation, under the same assumption. According to these studies, the dimension of focus of the shocks here discussed seems to be less than several hundred metres, and not distinguished from the uncertainty of the position of hypocentre in the analysis.

On the other hand, R. Yoshiyama (**30**, **31**) is the first who made a practical trial for estimating the size of a hypocentral region from the travel-time analysis. He presumed it from the difference between the apparent origin time at the centre of focus calculated from the time-distance curves of the P-waves and the origin time at the surface of focal region by means of the relation of arrival time-P-S duration. Moreover, S. Takagi (**32**) estimated a dimension of focal region comparing the observed $\triangle$-P-S curve with that calculated from the assumed structure of the crust. Their studies, however, are such that the dimension was estimated by the data at distant stations in considerably large earthquakes, supposing the focal region to be a sphere, and no investigation on such a case of the minor earthquakes as the present one was made.

Provided that the cause of the travel time anomalies in this study is attributed to the dimension of hypocentre, there seems to be no help for it but to consider that the hypocentral region is not a sphere, but an ellipsoid or a line source. Namely, if the elastic waves were simultanaeously emitted from the surface of them, the travel-time difference between two groups as referred to the third paragraph is approximately explainable. Here, the difference between the longer and shorter dimension of focal region seems to be from 1 to 2 km as deduced from the point of the travel-time gap.

B. Gutenberg and C. F. Richter (**33**) tried to estimate a dimension of focus by an entirely different hypothesis from the above ones. That is, supposing that the earthquake occurs with generation of faulting, they pointed out, the existence of the region in which the S-waves emitted with the travel of fracture arrive faster than the first S-waves from the centre of fracture, when the travel speed of fracture is slower than the velocity of the P-waves and faster than that of S-waves in the medium. From such an idea, the linear dimension of fault and the travel speed of fracture were tentatively estimated by the mean travel-time difference of the two types of S-waves at the whole observed area. But S. Takagi denied this postulation from the results of studies on Japanese earthquakes.

If we try to interpret the observed results here studied with the similar supposition in relation to the mechanism of earthquake occurrence, we cannot but consider that

the travel speed of fracture or shock wave is faster than that of the P-waves, though it is a question whether this hypothesis is mechanically possible or not. When the fracture travels emitting the elastic waves from a position (a centre of fracture) for some distance along a straight line with the velocity faster than that of the P-waves, the region in which the P-waves propagate with the ordinary velocity and that in which the P-waves propagate with an apparently enlarged velocity effected by the travelling of fracture, are divided into four quadrants by a pair of 'nodal curves' differentiated only by their travel times. The travel-time difference of the first P-waves in two kinds of regions is maximum at any two points on the intersecting straight lines at right angle, dividing these areas into two equal parts. Hence, from the observation of the above travel-time difference and the intersecting angle of 'nodal curves', the linear dimension and travel speed of the fracture is expected to be known.

Inversely speaking, the observed maximum difference of travel times in two groups in the present case seems not to be totally unexplainable, provided the travel speed of fracture can be considered to be twice the order of the longitudinal wave velocity, and the linear dimension to be about 2 km. If the above assumption on the fracture is possible and we are permitted to consider that the 'push-pull' regions in the directions of initial motion agree with two kinds of regions defined by the travel times, it seems possible in some part to interpret our observed results in light of the present observations.

In summary, it is too premature to deduce a definite conclusion from the present observed results, but some possible interpretations were tentatively given.

The anomalous fact of separation of travel times into two groups in the present observation of local shocks in their epicentral region was considered to be intimately related with the nature of hypocentre and mechanism of earthquake occurrence. With a view to clarify the effects on the origin of earthquakes, the more precise seismometric observations of natural earthquakes in their epicentral region with dense nets of high magnification seismometers and high accuracy of time determination are recommended at various places of seismically active areas.

Acknowledgement

The writer wishes to express his cordial thanks to Prof. E. Nishimura for his kind guidance and encouragement throughout the present study. The author also expresses his heart-felt gratitude to Assist. Prof. S. Miyamura, Mr. M. Hori and others, members of the Earthquake Research Institute of Tokyo University, for their generous permission in analysing the data obtained at their observation stations. The writer is greatly indebted to the kind co-operation during these observations by the following members of our institute: Messrs. K. Hosoyama, Y. Kishimoto, A. Kamitsuki, Y. Itô, I. Nakagawa,

Y. Tanaka, M. Ōtsuka, K. Zako and Miss. Y. Okamoto. The writer is also thankful for the kind help during the observation to Messrs. Y. Inouye and Y. Yamamoto of the Wakayama University, and Mr. K. Shinya, Mr. H. Imamura and many other persons in Wakayama District. Finally, the author again expresses his sincere thanks to Mr. M. Ōtsuka for his valuable advice and earnest discussion on this study.

The expense for the present observations was partly defrayed by a grant-in-aid for Scientific Research of the Ministry of Education.

REFERENCES

1. N. Nasu, On the aftershocks of the Tango Earthquake, (in Japanese), Bull. Earthq. Res. Inst., **6** 1929), 245; **7** (1929), 133; **8** (1935), 335.
2. S. Miyamura and T. Akima, Über die Beobachtung der Nachbeben des Imaichi-bebens am Dorfe Hunyu Provinz Totigi, (im Japanischen), Bull. Earthq. Res. Inst., **28** (1950), 421.
3. S. Omote, On the aftershocks of the Fukui Earthquake, Bull. Earthq. Res. Inst., **28** (1950), 311.
4. T. Asada and Z. Suzuki, On microearthquakes having accompanied aftershocks of the Fukui Earthquake of June 28, 1949, Geophysical Notes, Tokyo Univ., Vol. 2, No. 16 (1949), 1.
5. T. Asada and Z, Suzuki, On micro-earthquakes observed after the Imaichi Earthquake, Dec. 26, 1949., Bull. Earthq. Res. Inst, **28** (1950), 415.
6. S. Omote, Aftershocks of Imaichi Earthquake observed at Nishi-Oashi station, Bull. Earthq. Res. Inst., **28** (1950), 401.
7. R. Ikegami, On aftershocks of Imaichi Earthquake observed at Kanuma station, Bull. Tokyo Gakugei Univ., Vol. 4 (1953), 3.
8. T. Asada and Z. Suzuki, Unknown phases in earthquake motion of very near shocks, (in Japanese), Journ. Seism. Soc., Japan, Ser. 2, Vol. 5, No. 2 (1952), 30.
9. P. G. Gane, A. L. Hales, and O. Oliver, A seismic investigation of the Witwatersrand District earth tremors, Bull. Seism. Soc. Amer., **36** (1946), 49.
10. H. J. Logie, The wave velocity of seismic waves on the Witwatersrand, Bull. Seism. Soc. Amer., **41** (1951), 109.
11. P. G. Gane, P. Seligman, and J. H. Stephen, Focal depths of Witwatersrand tremors, Bull. Seism. Soc. Amer., **42** (1952), 239.
12. P. L. Willmore, A. L. Hales, and P. G. Gane, A seismic investigation of crustal structure in western Transvaal, Bull. Seism. Soc. Amer., **42** (1952), 53.
13. The Research Group for Explosion Seismology; The explosion seismic observations in north-eastern Japan, Bull. Earthq. Res. Inst., **29** (1951), 27; **30** (1952), 279; **31** (1953), 281; **32** (1954), 79; **33** (1955), 699.
14. A. Imamura, T. Kodaira, and H. Imamura, The earthquake swarms of Nagusa and vicinity, Bull. Earthq. Res. Inst., **10.** (1932), 3.
15. C. Iwanishi, On the Nagusa seismic zone in Kii District, (in Japanese), Journ. Seism. Soc., Japan, Vol. 3, No. 5 (1931), 257.
16. A. Kamitsuki and T. Mikumo, Investigation of the structure of the earth's crust in relation to local earthquakes (Preliminary), Bull. Disaster Prevention Res. Inst., Kyoto Univ., No. 6 (1953), 38.
17. Earthq. Res. Inst.; General report of research on earthquake swarms in Wakayama District. (in Japanese), 1955.
18. T. Mikumo, On anomalous time-distance curves observed in local earthquakes, (in Japanese), Journ. Seism. Soc., Japan, Ser. 2, Vol. 8, No. 3 (1955), 158.

19. S. Miyamura and H. Matsumoto, Line carrier telerecording seismograph (abbr. LTS), (in Japanese), Bull. Earthq. Res. Inst., **33** (1955), 715.
20. S. Miyamura and M. Tsujiura, A VFH radio telerecording seismograph (abbr. RTS), (in Japanese), Bull. Earthq. Res. Inst., **33** (1955), 725.
21. S. Miyamura and M. Tsujiura, Line carrier telerecording chronograph (abbr. LTC) for local seismological network, (in Japanese), Bull. Earthq. Res. Inst., **33** (1955), 709.
22. S. Miyamura, *et al.*; Preliminary report of seismic observation in Wakayama District, (read at the meeting of Seism. Soc., Japan, Nov. 1954.)
23. S. Miyamura, On seismic activities in the Kii-Peninsula, (read at the meeting of Seism. Soc., Japan, Nov. 1956)
24. T. Yoshizawa, (read at the meeting of Soc. Expl. Geophys., Japan, Apr. 1955.)
25. Y. Kishimoto, Seismometric investigation of the earth's interior, Part 1., 2.
Part 1. On the structure of the earth's upper layer
Part 2. On the structure of the earth's crust
Mem. Coll. Science, Kyoto Univ., A, **27** (1954), 125; A, **27**. (1954), 243.
26. Y. Miyayama, On the accuracy of determination of hypocentre, (in Japanese) Journ. Meteorol. Soc., Japan, Ser. 2, Vol. 9 (1931), 23.
27. S. Asano, On the accuracy of hypocentre determination, 1., 2., Bull. Earthq. Res. Inst., **32** (1954), 371; **33** (1955), 199.
28. W. Inouye, Notes on the origins of earthquakes, Bull. Earthq. Res. Inst., **14** (1936), 572.
29. K. E. Bullen, Introduction to the Theory of Seismology, p. 237, p. 75.
30. R. Yoshiyama, On a dimension of seismic focus, (in Japanese), Journ. Seism. Soc., Japan, **14** (1942), 120.
31. R. Yoshiyama, On the hypocentral region of earthquakes, 1, 2., Bull. Seism. Soc. Amer., **39** (1949), 187; **43** (1953), 153.
32. S. Takagi, On the origin of earthquake (the 13th paper), Quarterly Journ. Seism., C. M. O., **19**, No. 1 (1954), 1.
33. B. Gutenberg and C. F. Richter, Apparent origin time of S., Bull. Seism. Soc. Amer., **33** (1943), 269.
34. H. Kawasumi, Study on the propagation of seismic waves (2nd paper), Bull. Earthq. Res. Inst., **11** (1933), 403; **12** (1934), 660.

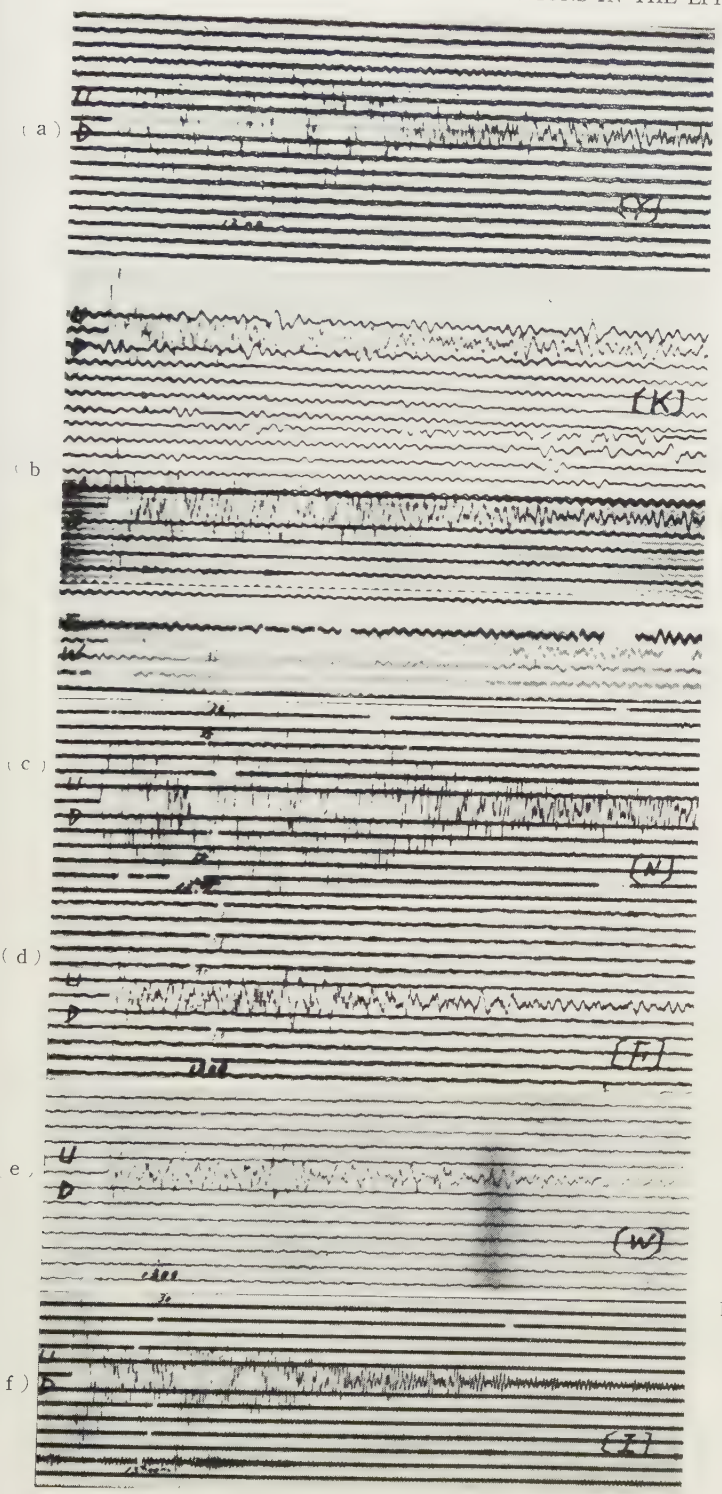

Fig. 11. Examples of seismograms obtained at six stations; No. 247, Apri 21, 1956, 12h 45m. (a) Yoro, (b) Kainan, (c) Nokami, (d) Fuyuno, (e) Wakanoura, (f) Idakiso.

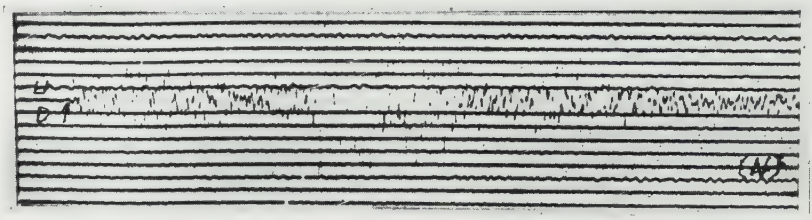

Fig. 12. Seismogram recorded at Nokami-station ; No. 240, April 21, 1956, 19h 26m, near Kyoto.

APPENDIX

Notes on Seismometers of Variable Reluctance Type

The electromechanical transducer of variable reluctance type or changing-flux type has the remarkable feature that the magnetic flux density varies with the change in the length of working air gaps between two magnetic poles due to a pendulum motion, while in the transducer of moving-coil type a coil moves within a constant magnetic field. In the former type a high magnification can be obtained, and it is suitable for measurement of vibrations of short period. The first seismographs with variable reluctance type transducer were designed by H. Benioff (**2**) in 1932. His vertical seismographs and the Bullard's seismometer are representative of transducers of this type.

In the study on the crustal structure from the seismometric observation of local shocks and artificial explosions, the sensitive seismometer without amplifier has gradually been required with a view to investigate, in particular, the seismic waveforms, and therefore variable reluctance seismometers with short period and high magnification were designed and constructed in the present case. The properties of these seismometers designated R_2-type will be described in an appendix in this paper through the theoretical calculations regarding the transducer and the determination of constants by experimental measurements.

1. Electromechanical transducer

The theory of this type of electromechanical transducer has been developed by E.C. Bullard (**5**), T.T. Devlin (**6**) and others since its first study by Benioff, and recently seems to have been completed for the greater part by K. Tajime (**13**～**18**).

Of this type of transducer, however, there are some limitations to efficiency. For stability of a pendulum motion, the suspension must be controlled to overcome the negative stiffness due to magnetic force with an adequate factor of safety. And it is said (**12**) that the linearity between the displacement of the pendulum and the voltage output does not always remain constant, and the theoretical calculation of various constants of the transducer is more complex than with a moving-coil type transducer.

In the present study, several types of variable reluctance transducers were designed taking the foregoing disadvantages into account. The complete calculations on these types seem not to have been previously made, and hence, the theoretical and experimental considerations on the detailed properties, comparing each with the other, will be made in this paper.

(A)-type

A-1 : This type is the "moving armature geophone" designed by S.A. Scherbatskoy and J. Neufeld (**3**). It consists of two parmanent magnets elastically supported by

two springs attached to the case, and of an armature placed in the air gap between the magnets and rigidly connected to the case. Two connected magnets move vertically as a suspended mass.

A-2: With this type the armature is connected to a pendulum and moves horizontally with a vertical or horizontal motion of the pendulum in the air gap between two fixed magnets opposite each other.

A-3: The armature moves vertically with a vertical pendulum motion in the air gap between two fixed magnets placed one upon the other.

(B)-type In this new type, two magnets are placed facing each other with an adequate interval, and the armature moves vertically in the air gaps between two poles of the respective magnets, with a vertical motion of the dendulum.

The rough sketches of these types of transducer are shown in Fig. 1.

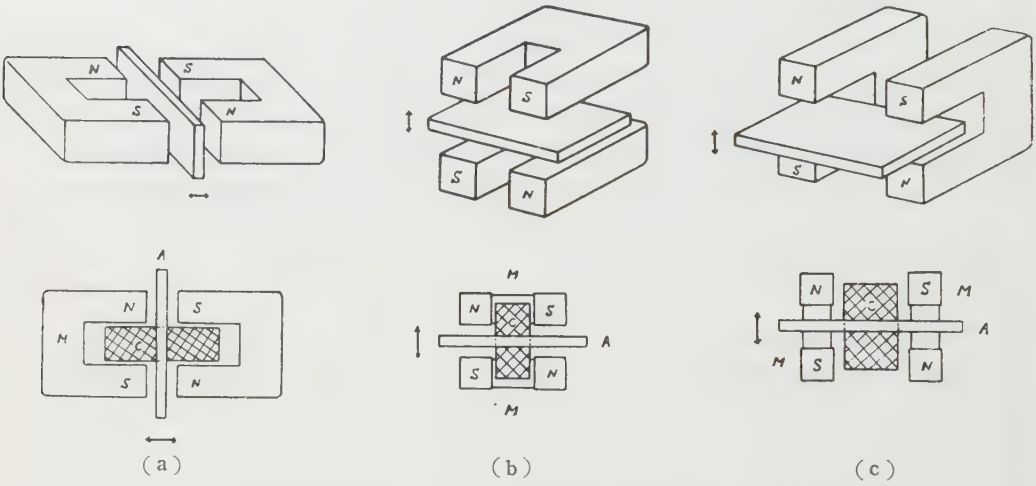

Fig. 1. Sketches of three types of variable reluctance transducer.
(a) A-1, A-2, (b) A-3, (c) B
M; magnet, *A*; armature, *C*; coil.

(1) *Electromotive force and voltage sensitivity*

The displacement of the armature caused by movements of the inertia reactor relative to the fixed system of the seismometer varies the length of working air-gaps and hence reluctance of them, and this in turn varies the magnetic flux through the gaps. The changes in flux thus induce the electromotive force in the coil surrounding the armature and the resulting currents are lead to the circuits.

The variation of flux through the moving armature due to the pendulum motion and the electromotive force induced in the coil were here calculated. In this case the effects such as magnetic hysteresis, eddy currents and viscosity inside, or in the vicinity of the magnetic poles were neglected. The changes in magnetic flux caused

by displacement of the reactor are found with a phase lag to the displacement. This is considered to be owing to the eddy currents and other effects (**15**).

Now, let the length of air-gap when the armature is in the position of equilibrium be x_0, let each length of both sides in the case of displacement of x_0 from the position be x_1 and x_2, let the reluctances corresponding to the respective lengths $R_A/2$, $R_1/2$ and $R_2/2$, respectively; and let the cross section of magnet A.

Then,
$$R_A = 2x_0/A, \quad R_1 = 2x_1/A, \quad R_2 = 2x_2/A$$
and
$$x_1 = x_0 - x, \quad x_2 = x_0 + x \qquad (x_2 > x_1) \qquad (2.1)$$

The idealized magnetic circuits on the (A)- and (B)-types of transducers are schematically represented as shown in Fig. 2.

Here, let:

F be the magnetomotive force of each magnet.
R be the reluctance of armature. $R = l/\mu A$
R_M be the reluctance of each magnet. $R_M = L/\mu' A$
R_1, R_2 be the reluctance of each working air gap.
R_S, R_L be the reluctance of leakage circuits.
l be the length of armature.
L be the length of magnet.
μ be the permeability of armature consisting of iron piece.
μ' be the apparent permeability of magnet.

Let the flux through the armature caused by its displacement be ϕ, and ϕ_i be the fluxes respectively indicated in Fig. 2.

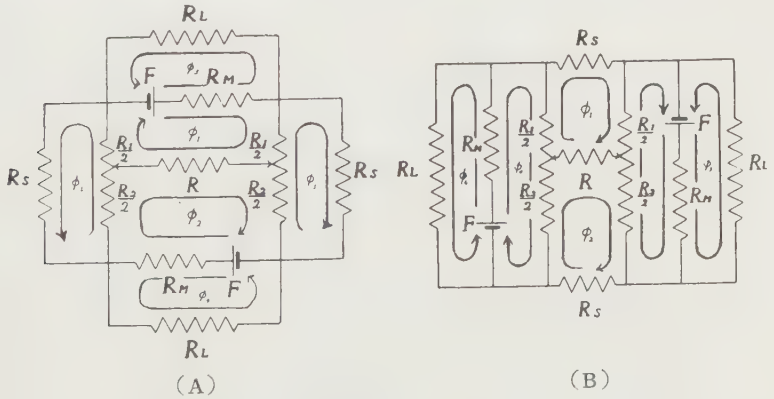

Fig. 2. Schematic representations of the magnetic circuits of variable reluctance transducers.
(A), (B): Magnetic circuits of (A)- and (B)-type respectively.

And then applying the Kirchhoff's law to the above magnetic circuits, we have,

(A)
$$\left.\begin{aligned}
&\phi=\phi_1-\phi_2 && \text{i)}\\
&\phi_1(R_1+R_M+R)-\phi_2R+\phi_3R_M-\phi_5R_1/2+\phi_6R_1/2=F && \text{ii)}\\
&\phi_2(R_2+R_M+R)-\phi_1R+\phi_4R_M-\phi_5R_2/2+\phi_6R_2/2=F && \text{iii)}\\
&\phi_3(R_M+R_L)+\phi_1R=F && \text{iv)}\\
&\phi_4(R_M+R_L)+\phi_2R=F && \text{v)}\\
&\phi_5\{(R_1+R_2)/2+R_S\}-\phi_1R_1/2-\phi_2R_2/2=0 && \text{vi)}\\
&\phi_6\{(R_1+R_2)/2+R_S\}+\phi_1R_1/2+\phi_2R_2/2=0 && \text{vii)}\\
&R_1+R_2=4x_0/A=2R_A && \text{viii)}
\end{aligned}\right\} \quad (2.2.a)$$

Solving these simultanaeous equations;

$$D\phi=4FR_SR_L(R_A+R_S)(R_M+R_L)(R_2-R_1)$$

where
$$\begin{aligned}
D=&[2(R_1+R+R_M)(R_M+R_L)(R_A+R_S)-2R_M^2(R_A+R_S)-R_1^2(R_M+R_L)]\\
&\times[2(R_2+R+R_M)(R_M+R_L)(R_A+R_S)-2R_M^2(R_A+R_S)-R_2^2(R_M+R_L)]\\
&-(R_M+R_L)^2[2R(R_A+R_S)+R_1R_2]^2
\end{aligned}$$

Now, let the flux through each magnet when the armature is in equilibrium, ie. when $x=0$, be ϕ_0, that is; $(\phi_1)_{x=0}=(\phi_2)_{x=0}\equiv\phi_0$

we get;
$$D_0\phi_0=4FR_L(R_A+R_S)^2\{(R_A+2R)(R_M+R_L)+R_MR_L\}$$

where
$$\begin{aligned}
D_0\equiv(D)_{x=0}=&4(R_A+R_S)\{(R_A+2R)(R_M+R_L)+R_MR_L\}\\
&\times\{R_AR_S(R_M+R_L)+R_MR_L(R_A+R_S)\}
\end{aligned}$$

then;
$$\frac{D\phi}{D_0\phi_0}=\frac{R_S(R_M+R_L)(R_2-R_1)}{(R_A+R_S)\{(R_A+2R)(R_M+R_L)+R_MR_L\}}$$

Therefore, the flux ϕ can be written in the form;

$$\left.\begin{aligned}
&\phi=2c_a\frac{\phi_0}{x_0}x[1+\alpha_a(x/x_0)^2+\cdots]\\
&\text{where}\quad c_a=\frac{R_AR_S}{(R_A+R_S)(R_A+2R+R'_M)}<1\\
&\alpha_a=\frac{R_A{}^2(R_S+R'_M)}{(R_A+2R+R'_M)\{R_AR_S+R'_M(R_A+R_S)\}}<1,\\
&\frac{1}{R'_M}=\frac{1}{R_M}+\frac{1}{R_L}
\end{aligned}\right\} \quad (2.3.a)$$

(B)
$$\left.\begin{aligned}
&\phi=\phi_2-\phi_1 && \text{i)}\\
&\phi_1(R_1+R+R_S)-\phi_2R-\phi_3R_1/2-\phi_4R_1/2=0 && \text{ii)}\\
&\phi_2(R_2+R+R_S)-\phi_1R-\phi_3R_2/2-\phi_4R_2/2=0 && \text{iii)}\\
&\phi_3\{(R_1+R_2)/2+R_M\}-\phi_1R_1/2-\phi_2R_2/2+\phi_5R_M=F && \text{iv)}\\
&\phi_4\{(R_1+R_2)/2+R_M\}-\phi_1R_1/2-\phi_2R_2/2+\phi_6R_M=F && \text{v)}\\
&\phi_5(R_M+R_L)+\phi_3R_M=F && \text{vi)}\\
&\phi_6(R_M+R_L)+\phi_4R_M=F && \text{vii)}
\end{aligned}\right\} \quad (2.2.b)$$

Solving the above equations by the same approach in the case of (A)-type,

we have;

$$\phi = 2c_b \frac{\phi_0}{x_0} x[1+\alpha_b(x/x_0)^2+\cdots]$$

where,

$$\left.\begin{aligned}
\phi_0 &= (\phi_3)_{x=0} = (\phi_4)_{x=0} \\
&= \frac{FR_L(R_A+R_S)}{R_AR_S(R_M+R_L)+R_MR_L(R_A+R_S)} \\
c_b &= \frac{R_AR_S}{(R_A+R_S)(R_A+2R+R_S)} < 1 \\
\alpha_b &= \frac{R_A^2(R_S+R'_M)}{(R_A+2R+R_S)\{R_AR_S+R'_M(R_A+R_S)\}} < 1
\end{aligned}\right\} \quad (2.3.b)$$

In both cases, ϕ_0, c and α are related with the gap width x_0, but are the constants having nothing to do with the displacement x, so far as the gap width is constant.

The variation of ϕ with gap-width change can be found from $c\phi_0/x_0$.

$$c\phi_0/x_0 = \frac{2F}{A} \cdot \frac{R_SR'_M/R_M}{(R_A+2R+R'_M)[R_AR_S+R'_M(R_A+R_S)]} \quad \text{(A)}$$

$$= \frac{2F}{A} \cdot \frac{R_SR'_M/R_M}{(R_A+2R+R_S)[R_AR_S+R'_M(R_A+R_S)]} \quad \text{(B)} \qquad (2.3')$$

If the reluctance R_A of air gaps are much larger than that of circuits, it is in nearly inverse proportion to the square of x_0. That is, the obtained flux increases rapidly with decreasing x_0, but there is a limitation on decreasing x_0. It is by reason that the pendulum motion becomes unstable owing to the increasing of magnetic stiffness as subsequently mentioned, and the linearity of flux in relation to x results unfavourably due to the increase of x/x_0. In the (B)-type ϕ has a maximum value when $R_S^2 = \frac{R_AR'_M(R_A-2R)}{R_A+R'_M}$, which are found out by a reluctance matching. Namely the maximum value of ϕ can be obtained by an adequate adjustment of the interval between two magnets.

The flux through the armature, in both cases, can formally be represented as follows:

$$\phi = 2c \frac{\phi_0}{x_0} x[1+(x/x_0)^2+\cdots] \qquad (2.3)$$

when the phase lag to displacement is omitted.

Hence, the electromotive force or open circuit voltage induced in the coil is,

$$E_0 = -N\frac{d\phi}{dt} = -N(d\phi/dx)(dx/dt)$$

$$= -2cN\frac{\phi_0}{x_0}[1+3\alpha(x/x_0)^2+\cdots]\frac{dx}{dt} \qquad (2.4)$$

where N is the number of turns of the coil.

If $x/x_0 < 1/10$, the second and its following terms in bracket in the above equation can be disregarded, because $\alpha < 1$, and we get;

$$\phi = 2c\phi_0 x/x_0, \quad E_0 = -Gx, \quad G = 2cN\phi_0/x_0 \tag{2.5}$$

where G is designated the voltage sensitivity.

In the types of transducer designed here, it was also ascertained that the induced flux is approximately proportional to the armature's displacement, and the electromotive force to the velocity of the armature's motion.

(2) *Secondarily induced magnetic flux*

When the electric current i is induced into closed circuits including the coil due to the armature's displacement, a secondary magnetic flux is caused by this induction current in the sense to prevent the motion of armature. This flux has a phase lag to the current.

The counter-magnetomotive force is expressed as $F' = 4\pi N\, i$. Provisionally separating the total flux Φ induced by the displacement of armature into two parts; ϕ directly due to the displacement, and ϕ' due to the induction current, and then Φ can be written; $\Phi = \phi + \phi' = \Phi_1 - \Phi_2$. When the magnetomotive force F' is induced into the circuit R indicated in Fig. 2(A), ϕ_1' streams in the same sense with ϕ_1, and ϕ_2' in the opposite one with ϕ_2, because $R_1 < R_2$ and $\phi_1 > \phi_2$.

Therefore,

$$\left.\begin{aligned} &\Phi_1 = \phi_1 + \phi_1', \quad \Phi_2 = \phi_2 - \phi_2' \\ &\Phi = \Phi_1 - \Phi_2 = (\phi_1 - \phi_2) + (\phi_1' + \phi_2') = \phi + \phi' \\ &\phi' = \phi_1' + \phi_2' \end{aligned}\right\} \tag{2.6}$$

ϕ' can be calculated from the ensuing equations. A dash in the shoulder denotes the quantities relating to the induction current.

(A)

$$\left.\begin{aligned} &\phi' = \phi_1' + \phi_2' && \text{i)} \\ &\phi_1'(R_1 + R_M + R) + \phi_2' R + \phi_3' R_M - \phi_5' R_1/2 + \phi_6' R_1/2 = F' && \text{ii)} \\ &\phi_2'(R_2 + R_M + R) + \phi_1' R - \phi_4' R_M + \phi_5' R_2/2 - \phi_6' R_2/2 = F' && \text{iii)} \\ &\phi_3'(R_M + R_L) + \phi_1' R_M = 0 && \text{iv)} \\ &\phi_4'(R_M + R_L) - \phi_2' R_M = 0 && \text{v)} \\ &\phi_5'\{(R_1 + R_2)/2 + R_S\} - \phi_1' R_1/2 + \phi_2' R_2/2 = 0 && \text{vi)} \\ &\phi_6'\{(R_1 + R_2)/2 + R_S\} + \phi_1' R_1/2 - \phi_2' R_2/2 = 0 && \text{vii)} \end{aligned}\right\} \tag{2.6.a}$$

From these equations,

$$\phi' = \frac{8\pi Ni}{R_A + 2R + R_M'}[1 + \beta_a(x/x_0)^2 + \cdots]$$

where

$$\beta_a = \frac{R_A^2(R_S + R_M')}{(R_A + 2R + R_M')\{R_A R_S + R_M'(R_A + R_S)\}} = \alpha_a < 1 \tag{2.7.a}$$

(B) In this case, $\phi_2 > \phi_1$ when $R_1 < R_2$, and then

$$\left.\begin{aligned} &\phi' = \phi_1' + \phi_2' && \text{i)} \\ &\phi_1'(R_1 + R + R_S) + \phi_2' R + \phi_3' R_1/2 + \phi_4' R_1/2 = F' && \text{ii)} \\ &\phi_2'(R_2 + R + R_S) + \phi_1' R - \phi_3' R_2/2 - \phi_4' R_2/2 = F' && \text{iii)} \\ &\phi_3'\{(R_1 + R_2)/2 + R_M'\} + \phi_1' R_1/2 - \phi_2' R_2/2 = 0 && \text{iv)} \\ &\phi_4'\{(R_1 + R_2)/2 + R_M'\} + \phi_1' R_1/2 - \phi_2' R_2/2 = 0 && \text{v)} \end{aligned}\right\} \tag{2.6.b}$$

$$\left.\begin{aligned} 1/R_M' &= 1/R_M + 1/R_L \\ \phi' &= \frac{8\pi Ni}{R_A+2R+R_S}[1+\beta_b(x/x_0)^2+\cdots] \\ \text{where} \quad \beta_b &= \alpha_b < 1 \end{aligned}\right\} \tag{2.7}$$

Hence, the secondarily induced flux ϕ' caused by the induction current can be expressed in the following form, in both cases of (A) and (B),

$$\left.\begin{aligned} \phi' &= \frac{F'}{R_0'}[1+\alpha(x/x_0)^2+\cdots] \\ \text{where} \quad F' &= 4\pi Ni, \quad R_0' = \frac{1}{2}(R_A+2R+R_M') \ \text{(A)}, \quad R_0' = \frac{1}{2}(R_A+2R+R_S) \ \text{(B)}, \end{aligned}\right\} \tag{2.7}$$

The induced electromotive force E is expressed as follows, neglecting the higher order terms following $(x/x_0)^2$ in comparison with unity and omitting the phase lags.

$$\begin{aligned} E &= -N(d\Phi/dt) = -N(d\phi/dx)(dx/dt) - N(d\phi'/dt) \\ &= -Gx - \frac{4\pi N^2}{R_0'}\frac{di}{dt} \end{aligned}$$

where $4\pi N^2/R_0' \equiv L$ is equivalent to the self-inductance of coil.
Hence, Φ and E can be written,

$$\left.\begin{aligned} \Phi &= Gx/N + Li/N \\ E &= -Gx - L\,di/dt \end{aligned}\right\} \tag{2.8}$$

(3) *Magnetic stiffness*

In the variable reluctance type transducer, the restitutive force of the moving system must overcome the negative stiffness due to magnetic force, because the magnetic force pulls the armature to an unbalanced position. The magnetic force acting between two poles at intervals in the air gap is expressed in the following formula in general, provided that the flux density B through the air gap is uniform, $f = B^2A/8\pi$, where A is the cross section of the air gap.

In our case, the armature is placed between two magnets with an equal length of air gap on both sides, and therefore, the magnetic pulls from both sides are balanced so far as the armature does not displace from the position of equilibrium.

When the armature moves x from the original position, the magnetic force is

$$f = f_1 - f_2 = \frac{\Phi_1^2 - \Phi_2^2}{4\pi A} \tag{2.9}$$

And then it becomes, taking the relations (2.6) into consideration, $f = \frac{[(\phi_1+\phi_2)+(\phi_1'-\phi_2')]\Phi}{4\pi A}$. Substituting the calculated values from the afore mentioned circuits for $(\phi_1+\phi_2)$, $(\phi_1'-\phi_2')$ and Φ, assuming that

$$R'_M\left(\frac{1}{R_A}+\frac{1}{R_S}\right)\ll 1,\quad \frac{x/2\phi_0 x_0}{R_A R_S+R'_M(R_A+R_S)}\ll 1,\quad \frac{R'_M/2+R}{R_A}\ll 1 \quad \text{and} \quad (x/x_0)^2\ll 1,$$

it becomes

$$f=\frac{c^2\phi_0^2}{\pi x_0 A}x+\frac{2cN\phi_0}{x_0}i=s''x+Gi$$

where

$$s''=c^2\phi_0^2/\pi x_0 A \tag{2.10}$$

The first term represents the negative stiffness which results from the distribution of the flux in the air gaps even when no current is flowing in the seismometer's coil and lengthens the natural period of the pendulum. The second term represents the force resulting from the change in the flux due to the current. It acts as an electromagnetic damping.

2. Seismometers

The electromagnetic seismometers designed here have a variable reluctance type transducer. The armature connected with the pendulum moves in the air gap between two magnets with vertical or horizontal surface movements. The vertical and horizontal seismometers were constructed so as to be convertible from one to the other.

In the following discussions the under-mentioned notations were used.

M: the mass of the moving system in the seismometer.
K: the moment of inertia of pendulum about the rotation axis.
H: the distance between the centre of gravity of the pendulum and its rotation axis.
L_1: the distance between the centre of the armature and the rotation axis.
L_2: the distance between the supporting point of the helical spring and the rotation axis.
l: the equivalent length of the pendulum.
c: the restitutive force of the leaf spring for a unit rotation angle.
f: the magnetic stiffness.
D: the coefficient of the fluid friction.
$\bar{R}$: the total resistance of the circuit.
L: the self-inductance of the seismometer's coil.
θ: the angular displacement.
x: the displacement of the armature's centre from a position of equilibrium.
ξ: the displacement of the ground surface.

(1) *Horizontal seismometer*

This consists of a vertical pendulum with the inertia mass and the armature, supported by two sets of crossed leaf springs in the upper part. Fig. 3 shows a horizontal seismometer. The equation of motion of the horizontal motion pendulum treated here is,

$$K\ddot{\theta} = -D\dot{\theta} - c\theta - MgH\sin\theta - L_1 f - MH\ddot{\xi}$$

Provided θ is not too great, $\sin\theta \approx \theta$ and $x \approx L_1\theta$

Hence, the equation about the armature's displacement x is as follows, considering f $s''x$ Gi,

$$Kx + Dx + (c + MgH - L_1^2 s'')\, x = -ML_1 H - L_1^2 Gi \qquad (3.1)$$

The natural period without damping in an open circuit is,

$$T_H = 2\pi\sqrt{K/(c + MgH - L_1^2 s'')} \qquad (3.2)$$

where $c/2 = Eab^3/9r$, E is the Ycung's modulus of the leaf spring, r the length, a the width and b the thickness.

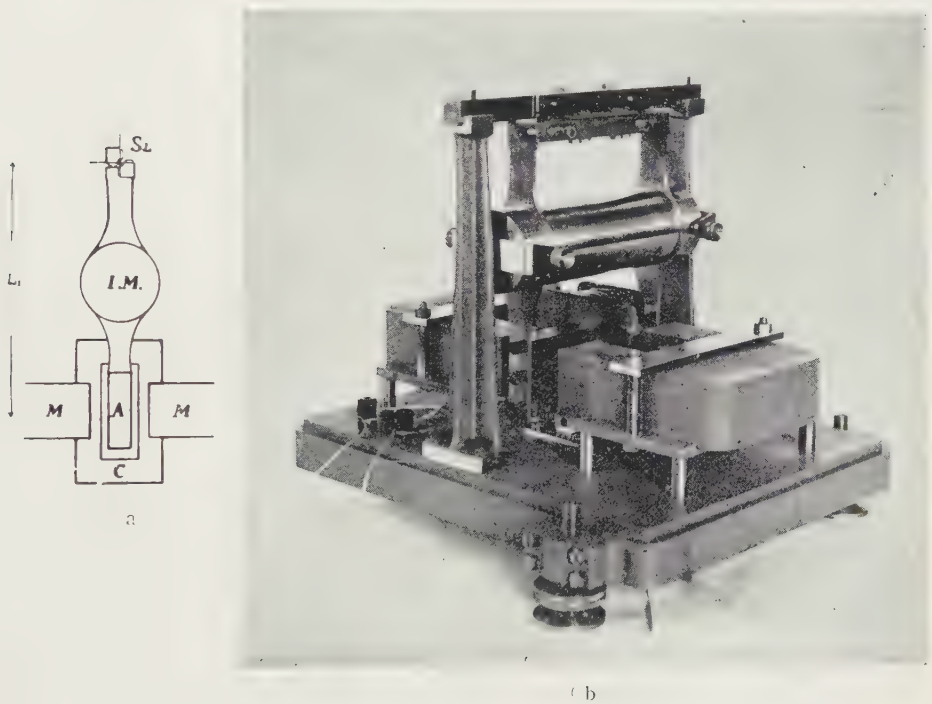

(a) (b)

Fig. 3. (a), (b) Horizontal seismometer of A 2 (R_2)-type.
I.M.; inertia mass, M; magnet, A; armature, C; coil, S_L; leaf springs, S_H; helical spring.

(2) *Vertical seismometers*

i) A-1: Two connected magnets supported by a helical spring and two leaf springs move themselves as a suspended mass. The armature is fixed to the case. (Fig. 6)

ii) A-2: The inertia mass is supported by a close-coiled helical spring, and two sets of crossed leaf springs, and the mass and the armature being rigidly connected

with a L-shaped frame form the pendulum. The armature moves horizontally with a vertical motion of mass. In this type, however, the seismometer was constructed so that the moment of inertia of the armature about the rotation axis may be far smaller than that of the mass. (Fig. 4)

iii) A-3: The inertia mass and the armature are connected with a frame corresponding the horizontal seismometer, and supported by a helical spring and crossed springs. (Fig. 5)

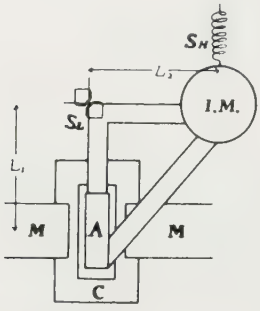

Fig. 4 (a)

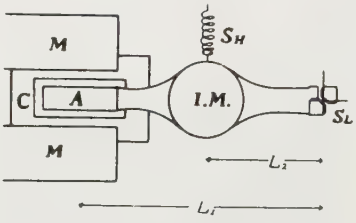

Fig. 5

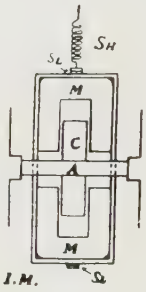

Fig. 6

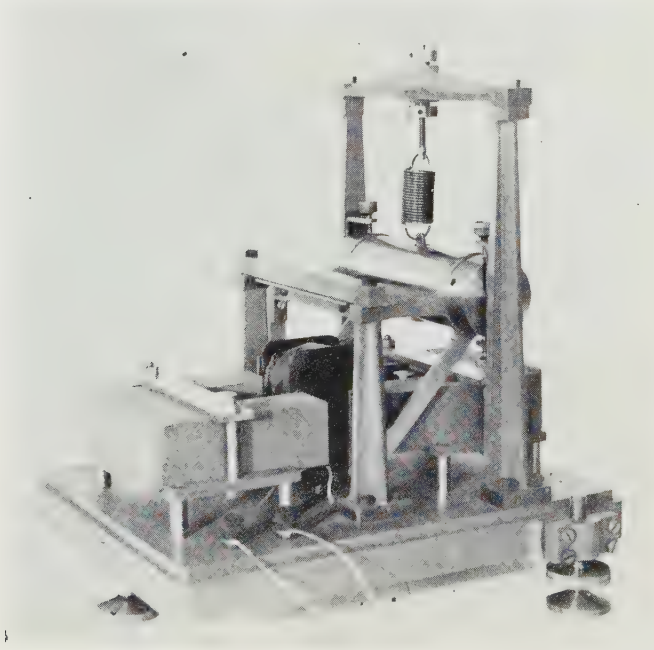

Fig. 4 (b)

Fig. 4. (a), (b) Vertical seismometer of A-2 (R_1)-type.
Fig. 5. Vertical seismometer of A-3 (R_2)-type.
Fig. 6. Vertical seismometer of A-1 type.

The equation of motion of all types of vertical seismometers mentioned here can be expressed in the ensuing symbol, provided that θ is negligibly small,

$$K\ddot{\theta}+D\dot{\theta}+(c+L_2^2k)\,\theta=-MH\ddot{\xi}-L_1f$$

or

$$K\ddot{x}+D\dot{x}+(c+L_2^2k-L_1^2s'')\,x=-ML_1H\ddot{\xi}+L_1^2Gi \tag{3.3}$$

The free period is,

$$T_V=2\pi\sqrt{K/(c+L_2^2k-L_1^2s'')} \tag{3.4}$$

where k is the spring constant of the helical spring or the restitutive force for unit elongation and can be written as follows from the balance condition in equilibrium, $k=MgH/L_2\Delta l$. Then, the equation of motion both on the vertical and horizontal seismometers of the variable reluctance type designed here can be written in the general form:

$$K\ddot{x}+D\dot{x}+(S-S'')\,x=-ML_1H\ddot{\xi}-L_1^2Gi$$

or

$$\ddot{x}+2\varepsilon_f\dot{x}+n^2x=L_1^2Gi/K-L_1\ddot{\xi}/l \tag{3.5}$$

where

$$\left.\begin{aligned}&2\varepsilon_f=D/K,\quad n^2=(S-S'')/K,\quad l=K/MH\\&S=c+L_2^2k\ \text{(Vert.)},\quad S=c+MgH\ \text{(Hor.)}\\&S''=L_1^2s'',\quad s''=c^2\phi_0^2/\pi x_0A\end{aligned}\right\} \tag{3.6}$$

The free period is related with the negative magnetic stiffness. It becomes longer than in the case without a magnet. And the period varies with the change in length of the air gaps on account of the close relation between the negative stiffness and the gap width.

The various constants on our seismometers are shown in Table 1.

Table 1. Constants of seismometers.

	H	V	
	A-2 (R_2)	A-2 (R_1)	A-3 (R_2)
M	3.66×10^3 gr.	3.68×10^3 gr.	3.68×10^3 gr.
K	3.51×10^5 c.g.s.	2.49×10^5 c.g.s.	6.12×10^5 c.g.c.
H	8.81 cm	6.20 cm	12.0 cm
l	10.8 cm	9.18 cm	13.8 cm
L_1	15.5 cm	7.90 cm	19.3 cm
L_2	—	8.40 cm	10.7 cm
c	3.96×10^8 c.g.s.	1.17×10^8 c.g.s.	3.96×10^8 c.g.s.
k	—	2.76×10^5 c.g.s.	2.76×10^5 c.g.s.
T	0.447 sec.	0.455 sec.	0.45 sec.
(X_0)	15.0 mm	14.0 mm	7.0 mm

(3) *Electromagnetic damping and the effect of self-inductance*

In the seismometers designed here the damping relies only upon an electromagnetic one. Matsuzawa (**10**) and Tajime (**14**) had already studied the effects of self-inductance on the electromagnetic damping, and Sparks, Hawleg (**8**) and Silverman (**9**) investigated them especially in conjunction with the reluctance type seismometer.

In this paper the more detailed study of the conditions for critical damping in free oscillation of reluctance seismometers will be made, taking the effects of self-inductance into consideration.

When the effects of self-inductance are taken into account, the voltage difference $\bar{E}$ in both terminals of the seismometer's coil induced by the motion of pendulum is; $\bar{E}=G\dot{x}+Ldi/dt+i\bar{R}$. In a closed circuit, $\bar{E}=0$, and hence $-G\dot{x}=Ldi/dt+i\bar{R}$. Now combining the preceding expression on $\dot{x}$ with the equation (3.6), we obtain the linear differential equations of third order with respect to x. That is,

$$\dddot{x}+(2\varepsilon_f+\nu)\ddot{x}+(2\nu\varepsilon_e+2\nu\varepsilon_f+n^2)\dot{x}+\nu n^2 x=-\nu L_1\ddot{\xi}/l$$

where $$1/\nu=L/\bar{R},\quad 2\varepsilon_e=L_1^2G^2/K\bar{R} \tag{3.7}$$

This is equivalent to the equation derived by Washburn (**4**) and Matsuzawa. When the damping depends only upon the electromagnetic one, the above equation in free oscillation becomes,

$$\dddot{x}+\nu\ddot{x}+(2\nu\varepsilon_e+n^2)+\dot{x}\nu n^2 x=0 \tag{3.8}$$

According to Sparks' method (**8**), assuming the general solution of equation (3.8) to be the form $x=x_0e^{pt}$, we get the third order equation of p. This equation at least has a real root. Let the other two roots of conjugate and complex be $p=h\pm ik$, and the two equations $f(h,k)=0$, and $g(h,k)=0$ are obtained. With a view to find out the values of h and k to realize the state of maximum damping by adjustment of the terminal resistance, the following procedures are pursued. Eliminating k from the above two equations, we obtain $F(h)=0$, and the condition for maximum damping is $dF(h)/d\nu=0$. From these two equations we get the values to give a maximum damping, that is,

$$\left.\begin{aligned} h_m &= -\tau^2/2n \\ k_m &= n[1+(\tau^2/n^2)-(\tau^2/2n^2)^2]^{1/2} \\ \nu_m &= \bar{R}_m/L=(n^2+\tau^2)/n \end{aligned}\right\} \tag{3.9}$$

where $$\tau^2=\nu\varepsilon_e$$

For critical damping which is greater than a maximum one, the motion must be non-oscillatory, ie. $k_m=0$, that is, $1+(\tau^2/n^2)-(\tau^2/2n^2)^2=0$

therefore, $$\tau^2/n^2=2(\sqrt{2}+1)\equiv C_{\tau n} \tag{3.10}$$

While, from the following formula, the equation (3.11) is obtained;

that is, $G=2cN\phi_0/x_0$, $L=4\pi N^2/R_0$, $R_0\approx x_0/A$ and $s''=c^2\phi_0{}^2/\pi x_0 A$

therefore, $$G^2=Ls'' \quad\text{and}\quad L_1G^2=LS'' \tag{3.11}$$

Hence, $\tau^2=S''/2K$, $n^2=(S-S'')/K$, and we get,

$$S''/S=4(3-\sqrt{2})/7=0.906\equiv C_s \tag{3.10'}$$

That is to say, Sparks and others suggested that damping depends on the ratio S''/S and the coefficient of negative stiffness must be greater than 91% of the constant of

the total restitutive force before the reluctance seismometer can be critically damped only owing to electromagnetic damping (**8**).

However, the condition for critical damping suggested by them is not complete, because the relation between the resistance and self-inductance was omitted from consideration. This relation can be expressed in the ensuing form by means of the constants $C_{\tau n}$ or C_s in critical damping.

$$\nu_m = \bar{R}_m/L = (1+C_{\tau n})n = (2-C_s)n/2(1-C_s) \tag{3.12}$$

because $\tau^2 = \nu\varepsilon_e = \nu_m n - n^2 = C_{\tau n} n^2$.

Substituting the values indicated by (3.10) or (3.11) for the above expression,

$$\bar{R}_m/nL = 3+2\sqrt{2} \tag{3.13}$$

This is one of the conditions for critical damping.

Namely, in order to obtain critical damping, total resistance in the circuit must be adjusted to satisfy the equation (3.13) for the known value of self-inductance, and S''/S must be selected so as to be $0.91 < S''/S < 1$. The condition derived by the above authors is one of the necessary conditions for critical damping, but not complete by itself.

In addition, when S''/S tends to unity in (3.12), $\bar{R}_m$ tends to increase to infinitive, that is, it has no objective however much one may select the values of resistance for critical damping. In this case, however, the pendulum motion becomes unstable and the armature finally sticks to the magnet. S''/S is required to be as small as possible only for stability sake.

Moreover, the damping factor can be written with the constants $C_{\tau n}$ or C_s,

$$\varepsilon_e/n = C_{\tau n}/(1+C_{\tau n}) = C_s/(2-C_s) \tag{3.14}$$

Substituting $C_{\tau n} = 2(\sqrt{2}+1)$ for the above expression, we get,

$$(\varepsilon_e/n)_m = 2(\sqrt{2}-1) = 0.83 < 1 \tag{3.15}$$

ε_e/n is formally equivalent to the damping factor h in the case of no self-inductance. The condition for critical damping is, of course, $h=1$ when the effect of self-inductance is not taken into account, and so it can be said that the self-inductance increases the damping. That is, it acts favourably to damping in the range $0 < nL/\bar{R} < 3-2\sqrt{2}$, but when this condition does not hold even by adjustment of $\bar{R}$, owing to the largeness of L, it acts disadvantageously. This result suggests the same sense with that derived by Matsuzawa (**10**).

The general effect of self-inductance on the electromagnetic damping in the case of external forced-vibrations were investigated in detail by K. Tajime (**14**).

According to his study, the damping factor with self-inductance can be expressed,

$$h_L = h/[(1+\alpha^2)\sqrt{1-\{2\lambda/(1+\alpha^2)\}}] \tag{3.16}$$

where $\lambda = \varepsilon_e/\nu = hnL/\bar{R}$, and $\alpha = \omega/\nu = \omega L/\bar{R}$

ω is the angular frequency of external force.

The above formula indicates that the larger the natural frequency of the seismometer's pendulum in comparison with the external one is, the larger the effect of self-inductance on the admping. In the case of no external force or free oscillation, $\alpha = 0$, and then, $(h_L)_{\alpha=0} = h/\sqrt{1-2\lambda}$. Especially in the critical damping, $h_L = 1$. Combining the condition for critical damping $nL/\bar{R} = 3-2\sqrt{2}$ and the above expression, h agrees with the values shown in (3.15). In our seismometers, $L = 1.62$ henries, $\bar{R} =$ 350 ohms, $n = 14$, $\omega < 60$, and hence $\alpha = 0.25 < 1$, $\lambda = 0.06 < 1$, impedance $Z = \bar{R} + j\omega L \approx \bar{R}$, $0 < nL/\bar{R} = 0.06 < 3-2\sqrt{2}$. From the above conditions, S''/S must be larger than 0.97 in order that our seismometer may be critically damped only by electromagnetic damping. As mentioned above, this is difficult to realize in respect to stability.

The equation of motion is as follows, when $1/\nu = L/\bar{R} = 0$, that is, the self-inductance may be ignored when compared with resistance.

$$x + 2\varepsilon_f x + n^2 x = L_1^2 Gi/K - L_1\ddot{\xi}/l \quad \text{and} \quad i = E/\bar{R} = -Gx/\bar{R}$$

or $$x + 2\varepsilon_e x + n^2 x = -L_1\ddot{\xi}/l$$

where $$2\varepsilon = 2\varepsilon_f + 2\varepsilon_e, \quad 2\varepsilon_f = D/K, \quad 2\varepsilon_e = L_1^2 G^2/K\bar{R} \tag{3.18}$$

If another damper is equipped, $2\varepsilon = 2(\varepsilon_f + \varepsilon_e + \varepsilon')$.

It is usual for the purpose of increasing the electromagnetic damping to equip a shunt-coil. In the present case it is wound around the outside of an ordinary coil.

When the armature moves, the electromotive force $E' = -G'x$, $(G' = 2cN'\phi_0/x_0)$ is induced and the current $i' = E'/R'$ streams in the shunt-coil. The counter-magnetomotive force $F' = 4\pi N'i'$ and hence the secondary flux are caused by this induction current. Therefore, the magnetic stiffness increases to $f' = s''x + Gi + G'i'$. Hence, the new electromagnetic damping whose factor is expressed with $2\varepsilon' = L_1^2 G'^2/KR'$ is added. The method for using the conductive bobbin with coil for increasing the damping is the same in its principle as that of the shunt-coil. The vertical seismometer of A-1 type is equipped with a copper bobbin. But this method is not so good on account of many reasons as pointed out by Tajime (**14**).

3. Experimental determination of constants

In this paragraph, the voltage sensitivity will be determined from an experimental measurement and the linearity between the voltage output and the displacement will be examined. And the variations of the voltage sensitivity, period, magnetic stiffness,

and damping factor with the changes in the length of air gap are measured, and the magnification was calculated here.

(1) *Determination of voltage sensitivity*

The voltage sensitivity was determined from the damping factor h by means of galvanometric registration of free oscillation of the seismometer's pendulum.
The damping factor can be written,

$$h = \frac{\varepsilon}{n} = \frac{T_0}{2\pi} \cdot \frac{1}{2K}\left(D + f_d + \frac{L_1^2 G^2}{\bar{R}}\right) \tag{4.1}$$

where $2\varepsilon' = f_d/K$, and f_d is the coefficient of damping force other than the electromagnetic damping. As D is usually far smaller than the coefficient of electromagnetic damping, G can immediately be obtained from h on the record of free oscillation, omitting D, if there is no damping force besides the electromagnetic one (**13**).
Otherwise, the damping factor must be measured in each case of varied values of the external resistance r_i. That is,

$$h_i = \frac{T_0}{2\pi} \cdot \frac{1}{2K}\left(D + f_d + \frac{L_1^2 G^2}{\bar{R}_i}\right), \quad \bar{R}_i = R + \frac{rS_i}{r + S_i} + r_i$$

Hence,

$$\left.\begin{aligned} G &= \frac{2}{L_1}\sqrt{\frac{\pi K}{T_0} \cdot \frac{R_1 R_2}{R_2 - R_1}(h_1 - h_2)} \\ D + f_d &= \frac{4\pi K}{T_0} \cdot \frac{R_1 h_2 - R_2 h_1}{R_1 - R_2} \end{aligned}\right\} \tag{4.2}$$

G can also be obtained from the following relationship. Combining the equation (3.13), $L_1 G^2 = LS''$, and the free period $T_0 = 2\pi\sqrt{K/(S - S'')}$, we get, $G = \sqrt{\frac{L}{L_1}\left(S + \frac{4\pi^2 K}{T_0^2}\right)}$. That is, G can be calculated by the value of S'' from measurement of the natural period.
From the experimental measurements in the present case, G was calculated as follows;

$$G = \frac{1.71}{1.79} \times 10^8 \text{ e.m.u. when } \begin{cases} x_0 = 13.0 \text{ mm (Vert.)} \\ x_0 = 15.0 \text{ mm (Hor.)} \end{cases}$$

The generalized voltage sensitivity is defined as $\bar{G} = GL_1/l$. The value of $\bar{G}$ of horizontal seismometer is 2.57 volt/kine. Comparing with the theory described in the first section, the value of c was estimated to be 0.342 at $x_0 = 15.0$ mm, because $N =$ 4,000 turns and $\phi_0 = 115{,}000$ maxwells. And for $D + f_d$, it was found $D + f_d = 1.18 \times 10^6 < \frac{L_1^2 G^2}{R} = 1.74 \times 10^7$. The coefficient f_d of damping force due to a supplementary damper (copper plate) takes charge of about 10% of total damping. Moreover, it is found from the equation (4.1) that $\bar{R}$ must be adjusted to be 240 ohms in vertical and 700 ohms in horizontal seismometer, in order to realize the critical damping.

In these types of variable reluctance seismometers the voltage output is proportional to the velocity of the pendulum's motion, if the oscillation amplitudes are not much larger than the length of the air gap, consequently expressed, $(x/x_0)^2 \ll 1$. Whether or not this linearity holds even in larger amplitudes was examined by the ensuing method. The equation of motion on the seismometer's pendulum in free oscillation is expressed in the following form, if the coupling motion with the galvanometer's coil can be ignored.

$$\ddot{x}+2\varepsilon_f x+n^2\dot{x}=L_1^2Gi/K \qquad \text{i)}$$

or

$$\ddot{x}+2\varepsilon x+n^2\dot{x}=0 \qquad \text{ii)}$$

When a displacement x_1 is given to the pendulum by sending a weak current i_1 to the seismometer's coil, x is estimated from the above equation i),

$$n^2x_1=L_1^2Gi_1/K \tag{4.3}$$

Then, making the pendulum free oscillation by cutting off the current, the motion can be expressed in the formula derived from solving the equation ii) with the initial conditions: $x=x_1$ and $\dot{x}=0$, when $t=0$,

$$x=x_1e^{-\varepsilon t}\left(\cos\gamma t+\frac{\varepsilon}{\gamma}\sin\gamma t\right), \quad \text{where} \quad \gamma^2=n^2-\varepsilon^2 \tag{4.4}$$

Hence, the equation of motion on a galvanometer's coil is,

$$\ddot{\varphi}+2\varepsilon_g\dot{\varphi}+n_g^2\varphi=\beta x=-(\beta\dot{x}_1n^2e^{-\varepsilon t}/\gamma)\sin\gamma t \tag{4.5}$$

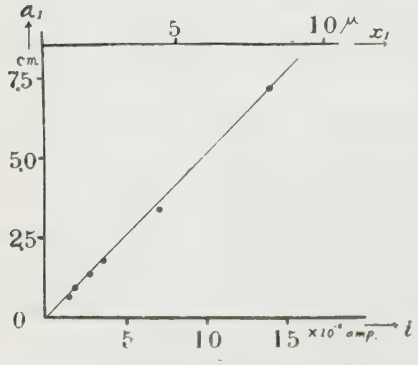

Fig. 7. Linearity between displacement and voltage output.

a_1 ; initial maximum amplitude on record,
x_1 ; initial given displacement of armature,
i_1 ; initial current to give the displacement x_1.

where β is the transmission constant or "die Übertragungsfaktor".

The particular solution of (4.5) is as follows when $\varepsilon_g=n_g$, neglecting the free oscillation of the galvanometer's coil by means of strong damping.

$$\left.\begin{aligned}\varphi&=\frac{-\beta x_1n^2/\gamma}{\sqrt{(\varepsilon-n_g)^2+\gamma^2}}e^{-\varepsilon t}\sin(\gamma t-\delta),\\ \text{where}\quad \tan\delta&=\frac{2(\varepsilon-n_g)\gamma}{\gamma^2-(\varepsilon-n_g)^2}\end{aligned}\right\} \tag{4.6}$$

The deflection of the galvanometer's coil is proportional to the initial given displacement of the seismometer's pendulum. Let the first maximum amplitude on the record be a_1, and then a_1 can be estimated from the equation

(4.6) and from the condition for its maximum or $d\varphi/dt=0$. Substituting the equation for x_1 in the modified equation of (4.6), we get,

$$a_1=2A\varphi=\frac{2\beta AL_1^2Gi/K}{n\sqrt{(\varepsilon-n_g)^2+\gamma^2}}\exp\left[-\frac{\varepsilon}{\gamma}\left\{\tan^{-1}\left(\frac{\gamma}{\varepsilon}\right)+\delta\right\}\right] \tag{4.7}$$

That is, a_1 is found to be proportional to i_1, and therefore, the linearity can be examined when a_1 is plotted against various values of i_1 and against x/x_0. The relation between a_1 and i_1 or x_1 is shown in Fig. 7. Generally speaking, the linearity holds good in the range of $x<10\mu$.

(2) *Variation of voltage sensitivity, period, magnetic stiffness, and damping factor with the change in the gap width*

As described from the afore-mentioned theoretical calculation,

$$G=2cN\phi_0/x_0,\quad T=2\pi\sqrt{K/(S-S'')},\quad h\approx L_1^2G^2T_0/4\pi K\bar{R}\quad\text{and}\quad S''=L_1^2c^2\phi_0^2/\pi x_0A \tag{4.8}$$

All of these factors vary with the change in the gap width. C also changes with the change of the air gap because it is a function of x_0, but has no relation to displacement. It is an advantageous in these types of variable reluctance seismometers that the above factors can be adjusted by variation of the gap width, but unfavourable because they are not independent of each other. From the records of free oscillation of the seismometer's pendulum, the damping factor $h(x_0)$, and the natural period without damping $T(x_0)$ can easily be obtained. The coefficient of negative stiffness $S(x_0)$ is then calculated after the spring constant S was known from the period T in the case of $x=\infty$. The voltage sensitivity $G(x_0)$ can be estimated from $h(x_0)$ and $T(x_0)$ by the above described method. The general appearance of variation of G with the gap-width change will also be learned from the recorded initial amplitudes in free oscillation of pendulum. These factors were plotted against the length of air-gap as shown in Fig. 8.

The voltage sensitivity increases, theoretically, in inverse proportion to the square of the gap width and the negative stiffness in inverse proportion to its cube, because the factor c has an order of $1/x_0^2$ provided that the reluctance of the air gap is much larger than that of other magnetic circuits. The measured values of these factor in experiment shows a comparatively good accordance with this theory. For comparison with the theory of electromagnetic damping and self-inductance, the relationship between h and S''/S was supplementarily investigated.

(3) *Magnification*

The equations of motion of the seismometer's pendulum and the galvanometer's coil, when directly connected, are usually expressed in the following form, when the

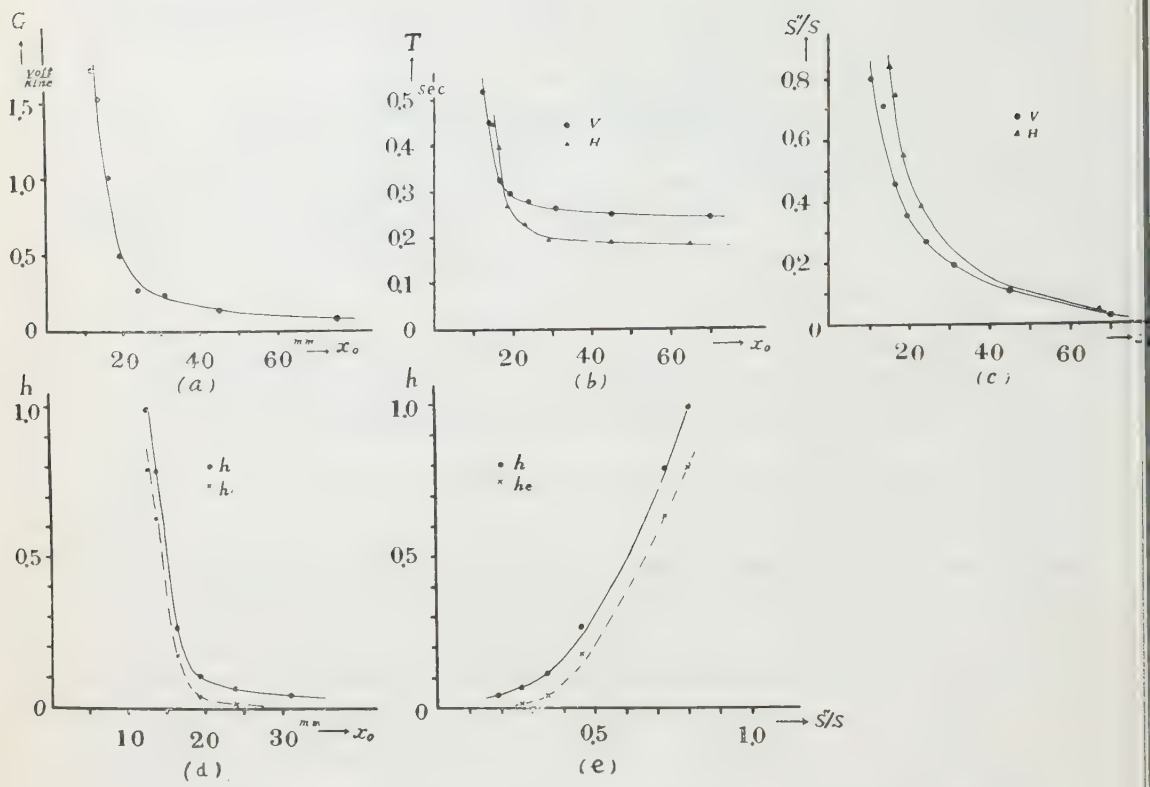

Fig. 8. Variation of various factors with the change in the gap-width.
(a) voltage sensitivity, (b) period, (c) magnetic stiffness,
(d) damping factor, (e) damping factor-magnetic stiffness relation.

self-inductance is omitted in comparison with the resistance. That is,

$$\left.\begin{aligned} &\ddot{x}+2\varepsilon\dot{x}+n^2x=-L_1\ddot{\xi}/l+\gamma\dot{\varphi} \\ &\ddot{\varphi}+2\varepsilon_g\dot{\varphi}+n_g^2\varphi=\beta\dot{x} \end{aligned}\right\} \qquad (4.9)$$

where $2\varepsilon_g=(d+g^2/\bar{R})/k$, $n^2=u/k$, $\gamma=L_1^2Gg/K\bar{R}$ and $\beta=Gg/k\bar{R}$

Now, if the effect of counter-electromotive force caused by the reaction of galvanometer's coil, as represented by the second term on the right-hand side of the former equation, is negligible, the motion of the seismometer's pendulum can be expressed with a linear differential equation of second order. According to the Tajime's study (**17**), it was found that the coupling effect between the two systems is avoidable without respect to the motional characteristics of them, if an adequate combination of values of resistances has only to be obtained by means of a shunt circuit. In the present case, $R=360$ ohms, $r=35$ ohms and the shunt resistance $S=40$ ohms, and hence σ

in his paper becomes 0.05. The coupling effect, therefore, seems permissible to neglect.

The magnification can be expressed as follows, from the steady part of the solution for the above equations of motion, assuming the ground motion to be a simple harmonic motion (**1**).

$$V = \frac{2AL_1}{l} \cdot \frac{Gg}{k\bar{R}} \cdot \frac{1}{p} \cdot \frac{1}{\sqrt{(u_1^2-1)^2+4h_1^2u_1^2}} \cdot \frac{1}{\sqrt{(u_2^2-1)^2+4h_2^2u_2^2}} \tag{4.10}$$

$$= \frac{2\pi\bar{G}}{S_g T_2^2 \bar{R}} \cdot \frac{1}{\sqrt{(u_1^2-1)^2+4h_1^2u_1^2}} \cdot \frac{1}{\sqrt{(u_2^2-1)^2+4h_2^2u_2^2}} \tag{4.11}$$

where $\bar{G} = GL_1/l$, $l = K/MH$, $S_g = u/2Ag$, $\bar{R} = R + r + Rr/S$

$$u_1 = T_p/T_1, \quad u_2 = T_p/T_2$$

S_g is the sensitivity of the galvanometer and T_p, T_1 and T_2 are the periods of ground motion, seismometer's pendulum and galvanometer's coil, respectively. In this special case $h_1 = h_2 = 1$, that is, when the two moving systems are critically damped,

$$V = \frac{2\pi\bar{G}}{S_g T_2 \bar{R}} \frac{u_2}{(1+u_1^2)(1+u_2^2)} \tag{4.12}$$

Recently, a new formula on the magnification with simple expression was derived by Tajime (**18**). According to his study,

$$V = \frac{a}{\xi} = \frac{2A}{l} \sigma^{1/2} \left(\frac{K}{k}\right)^{1/2} \sqrt{\frac{2h_1u_1}{(u_1^2-1)^2+4h_1^2u_1^2}} \sqrt{\frac{2h_2u_2}{(u_2^2-1)^2+4h_2^2u_2^2}} \tag{4.13}$$

That is, the static magnication depends only upon the ratio of the moments of inertia involving two moving systems, the geometrical magnification, and the combination of resistances. The upper limit of magnification can be estimated from $V < 2AK^{1/2}/lk^{1/2}$ without determining the voltage sensitivity. But the voltage sensitivity is implicitly included in the damping factor. Namely, the formula (4.13) is reduced to the equation (4.10), when h_1 and h_2 are re-written. The two formulae imply the same result in spite of the apparent difference of the motional characteristics and other factors.

In our seismometers the various constants related to magnification are,

	(V)	(H)	
G	1.71	1.79	volt/kine
K	2.49×10^5	3.51×10^5	c.g.s.
L	7.90	15.5	cm
l	9.18	10.8	cm
$\bar{R}$	386 ($R=353$) ($r=33$)	736 ($R=335$) ($r=33$) ($S=33$)	ohms
σ	1	0.05	
T_1	0.455	0.447	sec

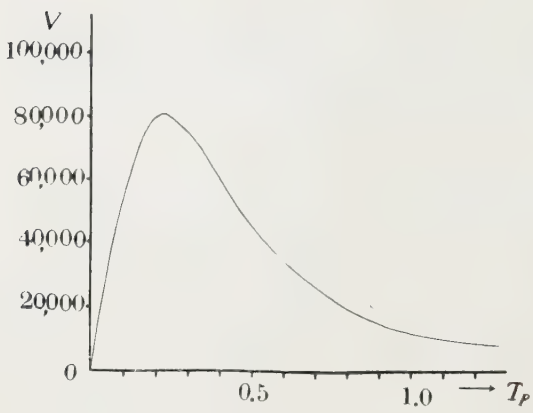

Fig. 9. Magnification curve.

and $A = 1$ m, $S_g = 3.11 \times 10^{-8}$ amp/mm, $T_2 = 0.35$ sec., $k = 7.64 \times 10^{-4}$ c.g.s. and $h_1 = h_2 = 1$.

The maximum magnification is 80,300 when $T_p = 0.227$ sec.

Fig. 9 shows the calculated magnification curve.

To recapitulate, the properties of variable reluctance seismometers designed were investigated. There are some defects in respect of linearity, stability and frequency characteristics, but other charac-

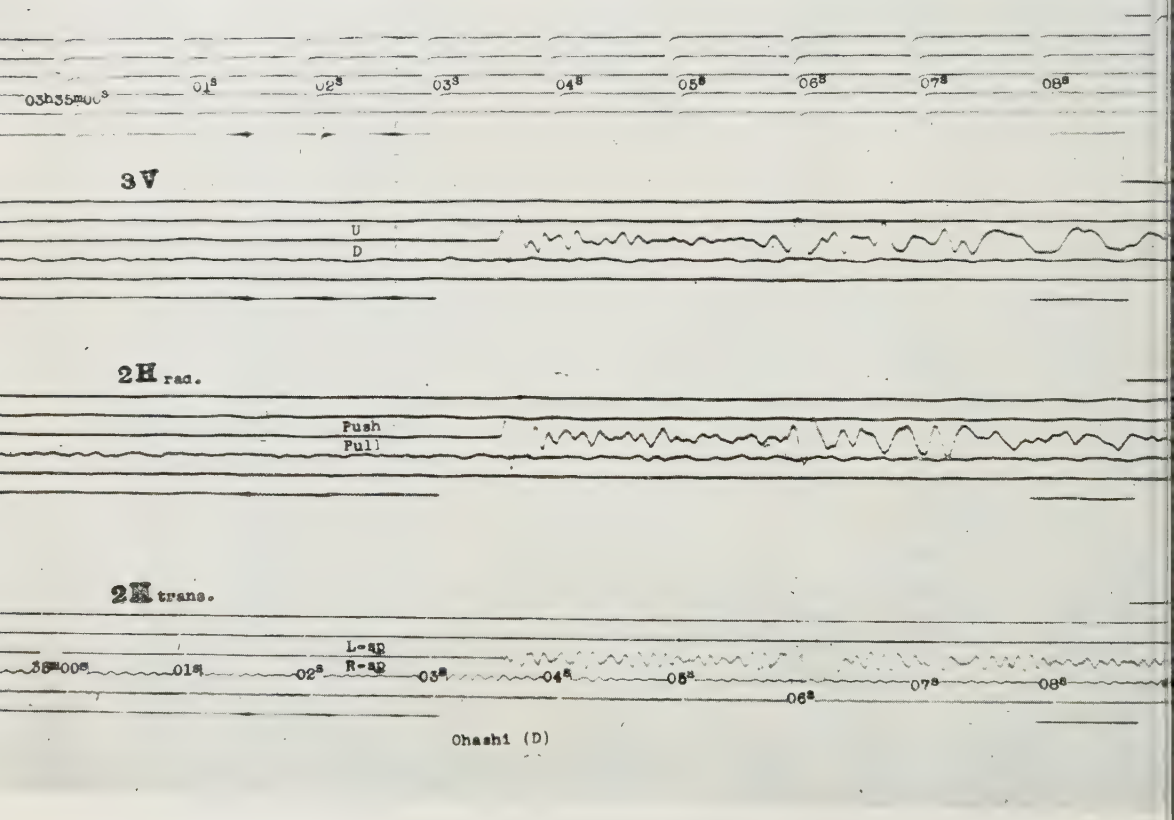

Fig. 10. Seismogram recorded by the R_2- seismometers in an explosion seismic observation. (at Ohashi-station, May, 3rd, 1954, 03h35m, Kamaishi-explosion.)

teristics seem to be satisfactory for the greater part. These seismometers were already successfully used in the observations of local earthquakes and artificial explosions. The examples of seismograms obtained are shown in Fig. 10. Moreover, a grouping observation with four vertical seismometers of this type was made in explosion for the purpose of recording the reflected waves.

The writer expresses his heartfelt thanks to Dr. E. Nishimura and Mr. A. Kamitsuki for their kind advices and to Messrs. M. Ōtsuka and Y. Tanaka for their considerate help in these experimental works and for their valuable suggestions. He is also indebted to Mr. Y. Satō for his laborious calculations.

REFERENCES TO THE APPENDIX

1. F. B. Galitzin, Vorlesungen über Seismometrie, B. G. Teubner (1914)
2. H. Benioff, A new vertical seismograph, Bull. Seism. Soc. Amer., **22** (1932), 155.
3. S. A. Scherbatskoy and J. Neufeld, Fundamental relations in seismometry, Geophys., **2** (1937), 188.
4. H. W. Washburn, Experimental determination of the transient characteristics of seismograph apparatus, Geophys., **2** (1937), 243.
5. E. C. Bullard, The theory of Benioff seismograph, Mon. Not. Roy. Astr. Soc., Geophy. Suppl., **4** (1938), 336.
6. T. T. Devlin, The electromechanical transducer in the new Benioff seismograph, Bull. Seism. Soc. Amer., **28** (1938), 255.
7. E. C. Bullard and C. K. Grant, The design and testing of geophones and their amplifiers, Mon. Not. Roy. Astr. Soc., Geophys. Suppl., **4** (1938), 341.
8. N. R. Sparks and P. F. Hawleg, Maximum electromagnetic damping of reluctance seismometer, Geophys., **4** (1939), 1.
9. D. Silverman, The frequency response of electromagnetically damped dynamic and reluctance seismometers., Geophys., **4** (1939), 53.
10. T. Matuzawa, Effect of self-inductance on the electromagnetic damping, (in Japanese), Journ. Seism. Soc., Japan, **12** (1940), 339.
11. T. Asada, On a changing-flux type transducer, (in Japanese), Geophysical Notes, Tokyo Univ., **1** (1947), 1.
12. P. L. Willmore, The theory and design of two types of portable seismograph, Mon. Not. Roy. Astr. Soc., Geophys. Suppl., **6** (1950), 129.
13. K. Tajime, A simple method for measuring the voltage-sensitivity of an electromagnetic transducer, (in Japanese), Journ. Seism, Soc., Japan, Ser. 2, Vol. 3, No. 2, (1950), 26.
14. K. Tajime, On the motion of the moving coil influenced by the self-inductance, (in Japanese), Rep. Mining Inst., Akita Univ., **9** (1953), 7.
15. K. Tajime, Equation of motion of changing-flux type transducers, (in Japanese), Rep. Mining Inst., Akita Univ., **10** (1953), 1.
16. K. Tajime, Transformations between electrical and mechanical quantities in electrodynamical seismometer, (in Japanese), Journ. Seism. Soc., Japan, Ser. 2, Vol. 7, No. 2 (1954), 96.
17. K. Tajime, Coupling effect of the galvanometer connected directly to the electrodynamical seismometer, (in Japanese), Jorun. Seism. Soc., Japan, Ser. 2, Vol. 8, No. 1 (1955), 23.
18. K. Tajime, Some notices on the design of the electromagnetic recorder having no amplifier, (in Japanese), Journ. Seism. Soc., Japan, Ser. 2, Vol. 8, No. 3 (1956), 138.
19. T. Hagiwara, Shindô-Sokutei (measurement of vibration) (in Japanese), Hôbun-kan (1948).
20. S. K. Charabarty, Response characteristics of electromagnetic seismograph and their dependence on the instrumental constants, Bull. Seism. Soc. Amer. **39** (1949), 205.

CONTENTS

Time Variation of the Atmospheric Radon Content Near the Ground Surface with Relation to Some Geophysical Phenomena

By Sigeru Okabe 99

Seismometric Investigation of the Earth's Interior (III)

By Yoshimichi Kishimoto 117

On the Seismic Waves Reflected at the Mohorovičić Discontinuity (I)

By Akira Kamitsuki 143

Precise Seismometric Observations in the Epicentral Region of Local Shocks

By Takeshi Mikumo 161

Printed by NIPPON INSATSU SHUPPAN

Fukushima, Osaka